UNIVERSITAT POLITÈCNICA DE VALÈNCIA

School of Industrial Engineering

Evaluating electrolyser setups for hydrogen production from offshore wind power: A case study in the Baltic Sea

Master's Thesis

Master's Degree in Energy Technologies for Sustainable Development

AUTHOR: Franzén, Kenzo

Tutor: Sánchez Díaz, Carlos

ACADEMIC YEAR: 2022/2023

Abstract

As part of the transition towards a fully sustainable energy system, green hydrogen shows great potential to decarbonise several hard-to-abate sectors. To provide the fossil-free electricity required for electrolysis, offshore wind power has emerged as a suggested option. In this report, four scenarios using different electrolyser placements and technologies are compared and applied in a 30-year case study considering a 1 GW offshore wind farm in the Baltic Sea. The scenarios are evaluated through the optimisation of electrolyser capacities, full system modelling and simulation, a techno-economic assessment, as well as a literature review of technological readiness, safety aspects and operational considerations.

It is shown that a range of installed capacities offers only slight differences in levelised costs and that the optimal sizes to a large part depend on future electrolyser cost developments. A 1:1 sizing ratio between electrolyser capacity and maximum available power is not suggested for any of the studied configurations. Further, the simulations indicate that electrolyser inefficiencies constitute 63.2–68.5% of the total energy losses. Power transmission losses are relatively small due to the short transmission distance, while the power demands of several subsystems are nearly insignificant. Onshore H_2 production using an alkaline electrolyser system is highlighted, offering the highest system efficiency and largest hydrogen production, at 55.93% and 2.23 Mton, respectively. This setup is further shown to be the most cost-efficient, offering a levelised cost of hydrogen at 3.15 €/kgH_2. However, obstacles in the form of social and environmental concerns and regulations are seemingly larger compared to the scenarios using offshore electrolysis. Further, rapid future cost developments for electrolysers are likely to strengthen the case for offshore and PEM electrolyser configurations. A range of research opportunities are highlighted to fill the identified knowledge gaps and enable further insights.

Keywords: electrolysis; energy systems modelling; green hydrogen; offshore wind power; power-to-x

Resumen

Como parte de la transición hacia un sistema energético totalmente sostenible, el hidrógeno verde muestra un gran potencial para descarbonizar varios sectores en los que es difíciles de conseguir. La energía eólica marina ha surgido como una opción para suministrar la electricidad libre de fósiles necesaria para la electrólisis. En este informe se comparan y aplican cuatro escenarios que utilizan diferentes ubicaciones y tecnologías de electrolizadores en un estudio de caso a 30 años que considera un parque eólico marino de 1 GW en el Mar Báltico. Los escenarios se evalúan mediante una optimización de la capacidad de los electrolizadores, la modelización y simulación de todo el sistema, una revisión bibliográfica de la disponibilidad tecnológica, teniendo en cuenta los aspectos de seguridad y las consideraciones operativas.

Se demuestra que una gama de capacidades instaladas ofrece sólo ligeras diferencias en los costes nivelados y que los tamaños óptimos dependen en gran medida de la evolución futura de los costes de los electrolizadores. No se recomienda una relación de tamaño de 1:1 entre entre la capacidad del electrolizador y la potencia máxima disponible. Además, las simulaciones indican que las ineficiencias del electrolizador constituyen entre el 63,2% y el 68,5% de las pérdidas totales de energía. Las pérdidas de transmisión de energía son relativamente pequeñas debido a la corta distancia de transmisión, mientras que las demandas de energía de varios subsistemas son casi insignificantes. Destaca la producción de H_2 en tierra utilizando un sistema de electrolizador alcalino, que ofrece la mayor eficiencia del sistema y la mayor producción de hidrógeno, con un 55,93% y 2,23 Mton respectivamente. Además, este sistema es el más rentable, con un coste nivelado del hidrógeno de 3,15 €/kgH_2. Sin embargo, los obstáculos sociales, medioambientales y normativos parecen ser mayores que en el caso de la electrólisis en alta mar. Además, es probable que la rápida evolución de los costes de los electrolizadores refuerce las configuraciones de electrolizadores marinos y PEM. Se destacan en el documento una serie de oportunidades de investigación con el fin de completar el estado del arte identificado.

Palavras clave: electrólisis; energía eólica marina; hidrógeno verde; modelado de sistemas de energía; power-to-x

Resum

Com a part de la transició cap a un sistema energètic totalment sostenible, l'hidrogen verd mostra un gran potencial per a descarbonitzar diversos sectors en els quals és difícils d'aconseguir. L'energia eòlica marina ha sorgit com una opció per a subministrar l'electricitat lliure de fòssils necessària per a l'electròlisi. En aquest informe es comparen i apliquen quatre escenaris que utilitzen diferents ubicacions i tecnologies de electrolizadors en un estudi de cas a 30 anys que considera un parc eòlic marí d'1 GW en la Mar Bàltica. Els escenaris s'avaluen mitjançant una optimització de la capacitat dels electrolizadors, la modelització i simulació de tot el sistema, una revisió bibliogràfica de la disponibilitat tecnològica, tenint en compte els aspectes de seguretat i les consideracions operatives.

Es demostra que una gamma de capacitats instal·lades ofereix només lleugeres diferències en els costos anivellats i que les grandàries òptimes depenen en gran manera de l'evolució futura dels costos dels electrolizadors. No es recomana una relació de grandària de 1:1 entre entre la capacitat de l'electrolizador i la potència màxima disponible. A més, les simulacions indiquen que les ineficiències de l'electrolizador constitueixen entre el 63,2% i el 68,5% de les pèrdues totals d'energia. Les pèrdues de transmissió d'energia són relativament xicotetes a causa de la curta distància de transmissió, mentre que les demandes d'energia de diversos subsistemes són quasi insignificants. Destaca la producció d'H_2 en terra utilitzant un sistema de electrolizador alcalí, que ofereix la major eficiència del sistema i la major producció d'hidrogen, amb un 55,93% i 2,23 Mton respectivament. A més, aquest sistema és el més rendible, amb un cost anivellat de l'hidrogen de 3,15 €/kgH_2. No obstant això, els obstacles socials, mediambientals i normatius semblen ser majors que en el cas de l'electròlisi en alta mar. A més, és probable que la ràpida evolució dels costos dels electrolizadors reforce les configuracions d'electrolizadores marins i PEM. Es destaquen en el document una sèrie d'oportunitats d'investigació amb la finalitat de completar l'estat de l'art identificat.

Paraules clau: electròlisi; energia eòlica marina; hidrogen verd; modelització de sistemes energètics; power-to-x

Acknowledgements

I wish to express my immense gratitude to all the people who have supported and assisted me throughout the writing of this thesis. I consider myself fortunate to have received so much valuable input from experts from many of the subjects I have studied in the report. Navigating through the wide range of technical systems involved, as well as the many uncertainties with regard to their practical application, would have been significantly more difficult without their contributions. I wish to thank many of the helpful and knowledgeable people at AFRY for answering my questions and offering their insights while being incredibly friendly and including along the way. The positive work culture at AFRY has been an essential factor in making the thesis process both fun and rewarding.

I wish to give a special thanks to Greta Blomstrand, who offered valuable guidance at AFRY in the early stages, helping considerably with developing the scope of the work. I also want to express my gratitude to my tutor at UPV, Dr. Carlos Sánchez Díaz, who has contributed with important feedback, experience and support throughout the process. My deepest thanks to Emil Lillieblad and Pedro Raposo, my supervisors at AFRY, who have dedicated a significant part of their time to support me from start to finish. Our weekly meetings were a recurrent source of inspiration and knowledge, always leaving me with new ideas and directions to explore.

Contents

List of Figures

List of Tables

Acronyms

AEM anion exchange membrane. 13, 17, 31, 61, 62

ALK alkaline. 13–17, 21, 24, 25, 27, 31, 32, 49, 51, 52, 54, 57, 59–63

ATR autothermal reforming. 8

BOL beginning-of-life. 31, 42

BOP balance of plant. 14, 21, 35

CAPEX capital expenditures. 17, 28, 35, 36, 61

CCUS carbon capture, utilization and storage. 4, 6, 9

COFF-P centralised offshore – PEM. 36, 37, 40–42, 53, 54, 58, 60, 80, 81

CON-A centralised onshore – ALK. 36, 37, 50–54, 58–60, 80

CON-P centralised onshore – PEM. 36, 37, 47–49, 53, 54, 58–60, 80

DOFF-P decentralised offshore – PEM. 36, 37, 43–46, 53, 54, 58, 59, 61, 80

DR-HVDC diode rectifier based HVDC. 19

EIA environmental impact assessment. 22

EOL end-of-life. 42, 52

EU European Union. 6, 17, 19, 20

GHG greenhouse gas. 1, 3, 4, 12

GRP glass reinforced plastic. 33

HHV higher heating value. 3

HVAC high voltage alternating current. 18, 19, 23, 27, 36

HVDC high voltage direct current. 18, 19, 23, 27, 60

ICE internal combustion engine. 3

LCC-HVDC line commutated converter HVDC. 19

LCOE levelized cost of electricity. 17

LCOH levelised cost of hydrogen. 2, 8, 9, 28, 29, 54, 58, 61, 63

LFAC low-frequency alternating current. 18

LHV lower heating value. 3, 43, 44, 48, 80

LNG liquified natural gas. 11

LOHC liquid organic hydrogen carrier. 9, 10, 12

OPEX operating expenditures. 28, 35–37, 61

OWF offshore wind farm. 18–21, 23, 24, 30, 31, 39, 40, 43

PEM proton-exchange membrane. 1–3, 13–17, 21, 24–27, 31, 32, 37, 39, 42, 43, 45, 46, 48, 51, 52, 54–57, 59, 61–63

POX partial oxidation. 8

PSU power supply unit. 35, 42, 45, 48, 51, 53, 60

PV photovoltaic. 17

SMR steam methane reforming. 4–9

SOEC solid oxide electrolyzer cell. 13, 16, 17, 21, 31, 61, 62

TRL technology readiness level. 17

UPS uninterruptible power supply. 25, 60, 62

VSC-HVDC voltage source converter HVDC. 19

1 Introduction

The energy situation of today is not like any other in history. Human society has certainly seen energy crises before, though not with the same complexities as today. Now, several challenges exist in parallel, ranging from the increasingly looming threats of climate change and resource scarcity to geopolitical energy conflicts and a rapidly growing population. Additionally, though human civilisation has previously undergone multiple society-wide energy transitions, it has never happened on the same scale or breadth as what is currently being developed, proposed and considered necessary. Solutions are and will continue to have to be found and implemented for a wide range of energy services, to the point where the main goal lies rather in transforming the very nature of the energy system itself. [1]

Reaching a fully sustainable energy system, however, involves balancing overarching goals where synergy is not always present. Energy security refers to the capacity to reliably and resiliently meet the energy demands of today as well as in the future. Energy equity reflects the capability to supply not only sufficient but also affordable and fairly priced energy for residential and commercial purposes. Lastly, environmental sustainability relates to the mitigation of climate change impacts as well as other environmental damages occurring due to our energy systems. This is reached mainly by decarbonising and increasing energy efficiencies within the sectors. Together they constitute an energy trilemma, where a successful balancing of the goals would guide towards long-term energy prosperity. [2]

An often proposed way towards this future is through the electrification of sectors and industries while simultaneously modernizing the grids and using clean electricity to cover the increased power demands. Decisive and immediate electrification efforts could offer a significant leap towards true energy sustainability [1]. It is estimated that the electrification of society could cover up to 70% of the final energy demand by the year 2050, as compared to approximately 20% today, considering a five-fold increase in the size of the global power system [3]. However, for a range of industries, electrification is still considered an infeasible option. Increasingly, efforts are being made into instead utilising hydrogen to cover the demands of these hard-to-abate industries, mainly due to its ability to be stored, combusted and used as a chemical component in ways similar to how fossil fuels are currently being used, with the potential benefit of having low or no direct GHG emissions. Additionally, hydrogen has the potential to be used as a reducing agent, for example, in steel-making and chemical industries as a substitute for natural gas [4] [5].

1.1 Purpose

This report aims to evaluate the technological and techno-economic prospects of feasible and sustainable production of hydrogen through electrolysis from large-scale offshore wind power, applied to a case study in the Gulf of Bothnia in the northern Baltic Sea, located in the Swedish economic zone. Three electrolyser system configurations, (i) centralised offshore, (ii) decentralised offshore and (iii) centralised onshore H_2 production, will be compared and evaluated using suitable electrolyser types. By modelling and simulating the system setups, quantitative results are obtained, in the form of H_2 production, energy losses and efficiencies, among other factors. To achieve this, an optimisation will be performed to find a reasonable electrolyser size for each configuration. A brief techno-economic assessment is performed, using available cost specifications to obtain LCOH values and enable comparisons between scenarios. Additionally, a comparative qualitative study will investigate factors such as technological maturity, environmental risks, operation and management, as well as safety considerations.

Based on these factors, a comprehensive analysis of different design alternatives of hydrogen production systems connected to offshore wind power is made to contribute to knowledge that can be applied to future electrolyser system design choices and placements. The report can additionally be seen as a concept study for an actor wishing to invest in the green hydrogen industry.

1.2 Scope and objectives

To reach the aims set for the report, the scope will be narrowed down to the aspects considered the most important for the study. Apart from the evaluation of electrolyser configurations, comparisons of electrolyser types and adjacent subsystems will constitute parts of the work. Due to the many possible combinations of electrolyser types and setups available, the report will focus on the options identified as the most promising.

Meanwhile, several parts of the relevant systems will be excluded from the investigation without downplaying their importance, as seen from a larger perspective. The system begins with the wind turbine output and ends with the hydrogen output on shore, meaning that the study will not go in-depth into either the storage or downstream integration of hydrogen into land-based systems or applications. For the same reason, wind turbine technologies will not be compared, although the wind power setup should be well-defined to match the studied electrolyser systems. Further, any results from the case study may not be fully applicable to other geographical contexts. In-depth regulatory aspects and profitability considerations are also outside the scope of this report.

2 Background

This chapter aims to give a brief introduction to hydrogen as an energy vector, through history and up until today, where the current hydrogen value chain and its technologies are presented. Additionally, it aims to give a introduction to offshore wind power and some of its challenges with regard to technological and legal aspects, followed by an overview of previous research and state-of-the-art of the applications specifically studied in this report.

2.1 Hydrogen — the second decarbonisation vector

More than 90% of the atoms in the universe are hydrogen, being the simplest atom with only one proton and one electron. Other rarer isotopes exists, such as deuterium which has an additional neutron and the more unstable tritium having two neutrons. Having one valence electron, hydrogen easily reacts to form molecules like hydrogen gas (H_2), water (H_2O) as well as many other organic and inorganic compounds. Despite its universal abundancy, finding hydrogen in its pure form is very rare, so to obtain it, a separation from its compounds is necessary. At normal conditions, hydrogen is a non-toxic, colorless and odorless gas. Its low melting and boiling points give hydrogen the property of being a gas except for in cases where conditions are extreme. [6]

There are several attributes that makes hydrogen interesting from a energy sustainability perspective. The element is reactive, possible to store and can be produced from non-carbon energy sources [5]. Further, the possibility to combust hydrogen in ICEs without significant GHG emissions or air pollutants, as well as its use in fuel cells, add to its potential. The ideal combustion of hydrogen occurs according to:

$$H_2 + \frac{1}{2}O_2 \longrightarrow H_2O \tag{1}$$

The gravimetric calorific value of hydrogen is also higher than any other fuel, with a LHV of 33.33 kWh kg^{-1} where the water remains in gaseous state, and a HHV of 39.44 kWh kg^{-1} where the water is condensed [6]. Similar to electricity, hydrogen is considered a promising energy vector due to its versatile characteristics with potential to cover many different types of demands. Meanwhile, it is important to note that by itself, hydrogen is not an energy source [7].

2.1.1 Historical pursuits and uses

The idea of hydrogen as an energy vector is not new. As early as in the 19th century, water electrolysis and fuel cells became known techniques. The earliest combustion engines as well as the space rockets in the 1960s were fueled by hydrogen, while balloons and airships have been utilising its lifting power [5]. Later, during the early 20th century, the gas became used for industrial purposes like ammonia synthesis as well as for cooking, heating and lighting purposes [7].

Throughout history, several attempts have been made to push for a larger transition into hydrogen technologies. In the 1970s, growing interest in hydrogen for the transport sector followed the oil crises and increasing worries of pollution. At that time, the proposed electricity sources were coal and nuclear. The interest then subsided as nuclear power started facing public resistance, oil prices decreased, new oil reserves were discovered and other solutions were found to the air pollution problem. During the 1990s, the interest was reawakened due to growing concerns about climate change and a lot of investments were made, mainly within the transport sector. However, hydrogen could not compete with the low oil prices and the interest faded. A third wave of excitement about hydrogen occurred in the early 2000s, following climate policy developments and investments, also here mainly for the transport sector. This time, it was the complexities of hydrogen infrastructure and the rise of battery electric vehicles that stopped the hydrogen momentum. [5]

Although hydrogen has not yet managed to reach its suggested potential as a widespread and versatile energy carrier, the fuel is currently an important component in a range of applications. The next chapter will offer an overview of the current applications and long-term prospects of hydrogen technologies through the value chain.

2.2 The hydrogen value chain

The hydrogen value chain can generally be seen, in order from upstream to downstream, as consisting of production methods, conversion, transport and distribution, storage, and end-use applications [8].

2.2.1 Production methods

Since hydrogen is not an energy source, the advantages and disadvantages of hydrogen are highly dependent on how it is produced, similar to electricity [7]. A range of technologies and methods exist, each with their own costs and environmental impacts, some of which with significant GHG emissions and others without [9].

Of the hydrogen produced globally, the major part is currently from carbon-intensive processes. Steam methane reforming (SMR) of natural gas without the use of carbon capture, utilization and storage (CCUS) constitutes 71% and coal gasification 27% of the total production, leaving only about 2% to production methods like SMR with CCUS and electrolysis [4]. However, there are growing incentives and interests in rapidly increasing these types of low-carbon installations [5]. Further, alternative production methods show promise for the future, although most of which are not yet demonstrating a technological readiness sufficient for commercial implementation [10]. The production methods of hydrogen are often categorized into different colors, utilising a range of technologies each with their own costs and environmental impacts. However, it is important to note that the exact classifications can differ. Figure 1 gives a brief overview of some of the most commonly suggested hydrogen production methods.

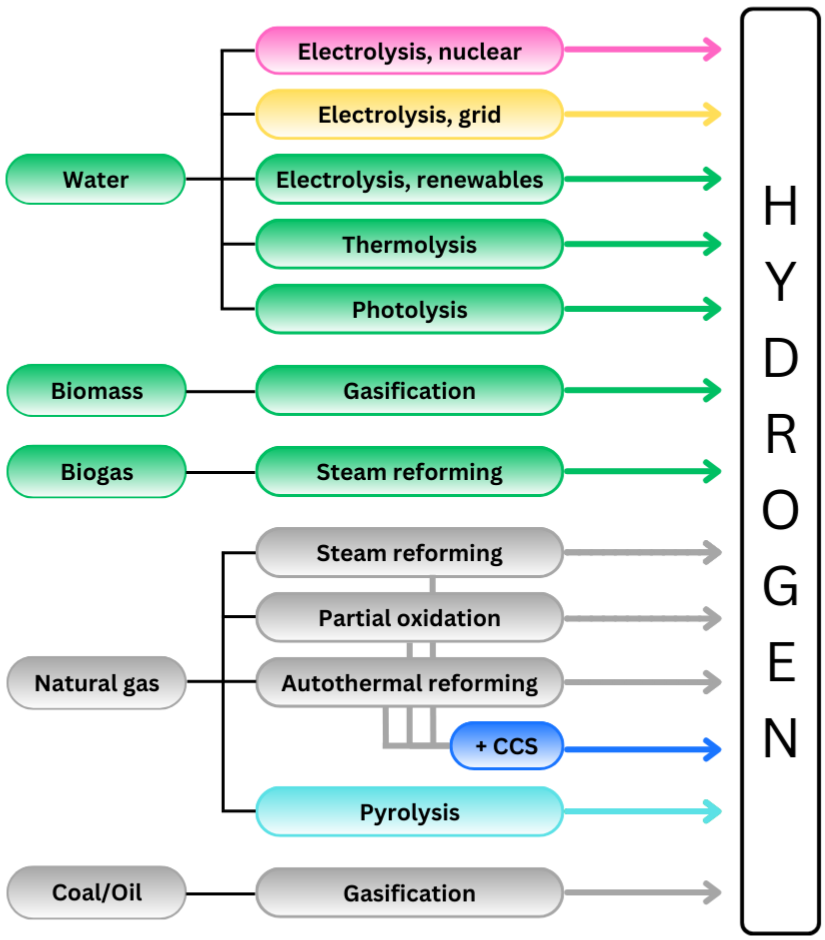

Figure 1: Hydrogen production methods by energy source (source: author)

Steam methane reforming

It is estimated that 205 billion cubic meters, or 6%, of the global use of natural gas is dedicated to this most common method for producing hydrogen today, with an annual production of roughly 70 Mton H_2 [5]. SMR refers to the process in which natural gas is first pre-treated and then split up into syngas (CO and H_2) using steam in a reformer (Eq. 2). The conversion into CO_2 and H_2 is then performed in a water gas shift reaction (Eq. 3), followed by a separation and purification process. [9]

$$CH_4 + H_2O \longleftrightarrow CO + 3\,H_2 \tag{2}$$

$$CO + H_2O \longleftrightarrow CO_2 + H_2 \tag{3}$$

This method without a carbon capture, utilization and storage (CCUS) system is commonly classified, as a fossil-based and carbon-intensive process, as **gray** hydrogen and offers among the lowest costs of today between 0.83–1.61 €/kgH_2 depending on location [11]. It is also an established technology, likely to remain dominant in the near future [5]. However, a major disadvantage is the significant carbon emissions, with estimates ranging from 7.5 to 12 ton CO_2 per ton H_2 produced [12].

However, the carbon emissions can be limited by including a carbon capture, utilization and storage (CCUS) system. CCUS mainly refers to technologies that captures CO_2 from large point sources, such as industrial or power generation facilities. The captured CO_2 is then used in certain applications or permanently stored in geological formations [13]. By installing a CCUS system, around 60% of the CO_2 can be captured with some additional costs and around 90% with significant costs due to large retrofitting requirements, during the production of what is commonly called **blue** hydrogen. To be considered a low-carbon production method according to European Union (EU) policy, a 90% capture rate is necessary, corresponding to a maximum of 2.26 kg CO_2 per kg H_2 produced [4]. Since an additional system needs to be added, as compared to SMR without CCUS, the cost is roughly 1.33–2.19 €/kgH_2 [11]. Costs are likely to decrease slightly during the upcoming decades, although volatile natural gas prices lead to projection uncertainties [4]. With the use of CCUS, SMR is often considered to be an important technology to use during the transition to green hydrogen production methods, due to its decent technological maturity and the possibility to retrofit old facilities. However, questions remain with regard to system-wide emission reduction potential as well as carbon storage methods [9].

Coal gasification

The second most used production method around the world, and specifically in China, is coal gasification due to the large and commonly existing coal reserves. 107 Mton of coal, an estimated 2% of the global use, are being used for producing hydrogen [5]. Dried coal is pulverized and reacts with oxygen and water steam under high temperatures via two steps. Parts of the coal is first oxidised into CO_2 (Eq. 4) by feeding air into a gasifier, followed by H_2 being produced when steam is injected and reacts with the coal in a shift conversion reaction similar to SMR (Eq. 5) [9].

$$C + O_2 \longrightarrow CO_2 \tag{4}$$

$$C + H_2O \longrightarrow CO_2 + H_2 \tag{5}$$

This process is a mature and well-established technology, mainly for coal but to a lesser extent also oil, and the low costs are considered to be similar to other grey hydrogen technologies like SMR [9]. However, significant CO_2 emissions occurs with this method, making it fall into the **gray** hydrogen category. 19 ton CO_2 is estimated to be emitted per ton H_2 produced [5]. Considering the need for low-carbon hydrogen, as well as the projected lack of technological development, coal (and oil) gasification is likely to be replaced with other production methods during the coming decades [4] [5].

Electrolysis

While not playing a significant role in the current energy system, electrolysis — the splitting of water molecules into hydrogen and oxygen gas by a direct electric current — is a well-proven technology expected to have a considerable importance for the sustainable energy system of the future [4]. A rapid scale-up of the global installed capacity is projected, from 300 MW in 2019 to 134-240 GW in 2030, considering the realisation of all currently planned projects [14]. A general advantage compared to other production methods is the high output hydrogen purity of more than 99.95% [9]. However, most of its advantages and disadvantages will largely depend on the investment costs and how the electricity is sourced. For example, the electrolytic CO_2 emissions are directly related to the CO_2 intensity of the electricity used, whereas by increasing the share of renewables in the grid, the corresponding emissions will decrease [7]. Producing hydrogen through electrolysis from grid electricity is commonly referred to as **yellow** hydrogen. Meanwhile, the flexibility of electrolytic hydrogen production further allows for using dedicated electricity sources as its sole energy input, where **green** hydrogen refers to the use of electricity from renewable sources and **pink** hydrogen considers as an input electricity from nuclear power [9].

Apart from electricity, water is needed as input for the electrolysis. Considering the need for water with high purity, due to impurities being detrimental to the electrolysers, it is important to take into account the need for freshwater supply or installation of desalination plants [15]. Desalination offers the possibility of electrolysis in regions with freshwater scarcity with additional costs of less than 0.02 €/kgH_2. Further, considering the much larger water demands of fossil fuel extraction and processing activities, the water use of electrolysers is unlikely to be a significant issue from a global perspective [4]. Deionisation plants require additional investments and maintenance, although the increased water purity supports electrolyser function and health [16].

Moreover, there is growing interest in the ability of electrolysers to react quickly to input and demand variations, where low start-up and ramp-up times add important flexibility, especially considering hydrogen production from intermittent electricity sources. Apart from making electrolysers more suitable for renewables, fast response times offer economic opportunities through ancillary services and demand response [17]. Additional key technological parameters include the load ranges of the electrolysers in relation to the nominal load, the footprints or area requirements of the systems, operational output pressures as well as current densities [18].

Compared to methods like SMR, electrolysis is small-scale by nature mainly due to electrode limitations. In order to scale up the electrolysers to enable coupling to electricity sources, since their capacities needs to be within the same order of magnitude, a typical solution is thus to use multi-stack module systems with up to 100 cells per stack. Beyond that, there are increased risks for electrical shorts and gas collection issues. The multi-stack systems can then be placed in parallel to further increase the capacity while decreasing costs [17].

At its current state, electrolytic hydrogen is significantly more expensive than previously mentioned methods, ranging from 2.76–11 €/kgH_2 [11]. However, the costs of producing green hydrogen are projected to decrease rapidly due to cheaper renewable electricity as well as falling electrolyser costs, possibly reaching prices even below 1 €/kgH_2 until 2050 [4]. If the LCOH through electrolysis can reach the 2030 target of 2 €/kgH_2, by then it would already make green hydrogen competitive with gray hydrogen [19]. An introduction to the main electrolyser technologies is shown in section 2.3.

Additional methods

Apart from the more established production pathways, other methods are being proposed within certain contexts and applications, while others show long-term potential although their technological maturity is currently low. Some, but not nearly all of them, are introduced below.

Similar to SMR, partial oxidation (POX) and autothermal reforming (ATR) are methods for producing hydrogen from natural gas. While SMR uses water as oxidant and hydrogen source, POX instead uses oxygen as its oxidant. Meanwhile, ATR can be viewed as a combination of both methods, with the main difference to POX being the performance at lower temperatures and the use of a catalyst [5] [4]. The main advantage of these alternatives is due to their ability to allow for higher carbon capture rates at significantly lower costs, making them a better choice for new blue hydrogen projects [4].

Methane pyrolysis is another suggested production pathway where methane is heated to above 750 °C without oxygen, forming solid carbon and what is commonly called **turquoise** hydrogen. This method could require significantly less electricity as compared to electrolysis while being free from CO_2 emissions. While its technological maturity is improving, technical challenges regarding process efficiency and hydrogen purity remain. [4]

Some methods instead focus on using biomass as feedstock, with the most prominent and mature processes being biomass gasification [9] and biomass reforming [10]. The main advantages are the low-carbon properties and relatively high technological maturity, although several challenges remain with regard to efficiencies and feedstock availability [10], the latter being important due to the risk of competing with other biomass use cases [7]. Other biological production processes such as microbial electrolysis and dark fermentation are being researched [9].

Further, photonic production methods exist in the form of photobiological and photoelectrochemical systems, where light is used to split H_2O into H_2 and O_2. These methods show significant long-term potential for zero-carbon hydrogen production, although still in early research stages [10].

Another way of splitting H_2O to obtain hydrogen is by heating it in a process called thermolysis, typically at temperatures above 2500 K, or thermochemical water splitting, a modification of the thermolysis process which lowers the temperature requirement significantly. By using a sulphur–iodine thermochemical cycle, there is improvement and commercialisation potential, although the high complexity of the process remains a barrier [20]. Table 1 shows the commercially available hydrogen production methods as well as their respective costs and CO_2 emissions. It is important to note that they refer to the emissions during their use and do not consider their full lifecycle global warming potential [15].

Table 1: Commercially available H_2 production methods

Method		LCOH	Cost development	Emissions (per kgH_2)
SMR without CCUS		0.83–1.61 €/kgH_2	Insignificant	7.5–12 kg CO_2
SMR with CCUS		1.33–2.19 €/kgH_2	Slight decrease	0–2.26 kg CO_2
Coal gasification		0.83–1.61 €/kgH_2	Insignificant	19 kg CO_2
Electrolysis (grid)		2.76–11 €/kgH_2	Strong decrease	$\geq$ 0 kg CO_2
Electrolysis (renewable)		2.76–11 €/kgH_2	Strong decrease	0 kg CO_2
Electrolysis (nuclear)		2.76–11 €/kgH_2	Strong decrease	0 kg CO_2

2.2.2 Conversion, transport and distribution systems

Hydrogen can be transported either as compressed gas (<1000 bar), a liquid ($-253\,^{\circ}$C) or chemically stored in more easily manageable carrier molecules, such as ammonia or liquid organic hydrogen carriers (LOHCs) [4]. Among the LCOHs, toluene is mainly considered, with dibenzyltoluene, methanol and formic acid being some of the proposed alternatives [5]. Since most of the hydrogen used today is produced and used on-site, the distribution networks are very limited in scale. The processes involved in hydrogen transport each add to the costs and energy losses, but to increase hydrogen use in the suggested sectors, the systems for transport and distribution will need to be significantly upscaled. Meanwhile, the geographical flexibility and scalability of green hydrogen production systems have some potential to offset the need for large distribution systems [4].

Conversion

For each form hydrogen is transported as, an energy-demanding conversion process is required. This is in contrast with direct electrification, which is generally more efficient. The necessary compression and decompression of hydrogen gas creates energy losses of 0.5–11% [4]. In the case of pipelines with compressed hydrogen gas, different levels of compression are needed depending on the operating pressure of the electrolyser, hydrogen flow, transport distance, the pressure drop in the pipeline and end-use requirements [21].

The liquefaction of hydrogen, meaning to cool the gas to ($-253\,^{\circ}$C), currently requires 25–35% of the energy content in the hydrogen itself. However, there is potential to reduce the energy losses to 18% in the future. Further, the conversion to and reconversion from ammonia each results in energy losses of 7–18%, depending on the system location and size. For conversion to LOHCs, the losses can be as high as 35–40% [5].

Transport and distribution

To make hydrogen technologies competitive, limiting transportation costs are of great importance since long-distance transportation could lead to costs up to three times higher than the hydrogen production. Several methods are suggested, where the advantages and disadvantages of each will to some part depend on sector, region, distance and scale [5].

Ships are considered the most economically viable hydrogen transmission option considering large volumes and long distances, above 10 ton H_2/day and longer than 5 000 km, where the currently most mature methods include chemically storing the hydrogen in carrier molecules, such as LOHCs or ammonia [5] [4]. The high storage and conversion costs involved in the process generally make ships an unsuitable mode of transportation for any small volumes or short distances with total transportation costs of above 2 €/kgH_2. However, ship transport could be viable for shorter distances in some exceptions, such as when transporting ammonia for end use as ammonia [4].

Trucks are often suggested for volumes lower than 10 ton H_2/day, with the most economical choice being to transport the hydrogen in its pure form. For distances below 300–400 km, compressed gaseous hydrogen is cheaper (0.50–0.69 €/kgH_2 depending on the distance) since the conversion costs are lower, while for longer distances, liquid hydrogen is the most viable option (0.69–2.41 €/kgH_2) due to lower volume requirements [4].

Pipelines are the preferred choice for volumes above 10 ton H_2/day for distances ranging from a few to several thousands of kilometres. While the infrastructure costs are significant, the low transmission costs (0.05–0.08 €/kgH_2 for distances up to 100 km, 0.08–1.8 €/kgH_2 for distances up to 5 000 km) offer promising economic opportunities [4]. The transmission losses from high-pressure gas pipelines are notably small, at 0.02–0.05%/1000 km [21] [22]. Further, the type of pipeline can vary, using dedicated distribution pipelines to handle lower capacities and ultra-high-capacity transmission lines to transport thousands of tons of H_2 daily in its pure, gaseous form. Notably, such large capacity pipelines are likely to be the most cost-efficient option in the future, although it would require a rapidly growing hydrogen use to rationalise their implementation. Currently, only 4 500 km of hydrogen pipelines are in use, most of which are just a few kilometres long, illustrating the need to develop new pipeline networks to cover future demands. Instead of constructing new pipelines, retrofitting natural gas pipelines offer the potential to reduce construction costs by 40–65% [4].

2.2.3 Storage technologies

To find suitable storage technologies for the produced H_2, several challenges connected to the characteristics of hydrogen have to be overcome. Many types of storage methods have been suggested, from storing the hydrogen in its pure form to the use of chemical and physical adsorption [23].

Gaseous storage

There are strong similarities between storing hydrogen gas and natural gas, where the two main methods of storage are inside metal tanks and in natural underground structures. However, there are several important differences. Contrary to natural gas, leakages can be significant due to the small hydrogen molecules, especially when using natural structures for storage. Material degradation in metals due to hydrogen embrittlement is also a significant difference, adding to storage risks and costs. Meanwhile, the existence of hydrogen-decomposing bacteria can negatively impact the purity of certain storage types. The almost linear relation between hydrogen density and pressure indicates the benefits of increasing pressures to reduce required storage volumes, although beyond 100 bar, corresponding to a density of 7.8 kg/m^3, the operating costs and material properties become limiting factors [21].

Currently, the most practical and cost-efficient way of storing large amounts of gaseous hydrogen is inside underground salt caverns, where leakage rates are low, construction is cheap, withdrawal and injection rates are high and where bacteria do not thrive. This approach is already in use and shows no remarkable differences when compared to storing natural gas in the same structures [21].

While pipelines are considered transmission systems, they also have the potential to function as storage systems through line packing. Injecting and withdrawing hydrogen from a pipeline can be compared to storage charge and discharge, although the energy content of storage by line packing for hydrogen gas is about 20% of that of natural gas [24].

Liquid storage

The storage of hydrogen in liquid form is in many ways similar to storing LNG in metal tanks. Liquid hydrogen has a significantly higher density (70 kg/m^3) than gas at 100 bar pressure, although the electricity needed to liquefy the hydrogen is somewhere between 6–10 kWh/kgH$_2$. For this reason, and considering the large capital costs required, global liquefaction capacity remains very low [21]. Boil-off management and production plant efficiency remain the main technological and scale-up challenges. However, the technological maturity and supply chain integration of liquid hydrogen storage is high [5].

Chemical storage

Instead of storing hydrogen in its pure form, carrier molecules can be used, where the hydrogen is converted to be chemically stored in a molecule. One candidate for both mobile and stationary storage applications is the use of metal hydrides, where hydrogen–metal interactions allow for the storage of hydrogen in certain host metals. A metal (M) will form a metal hydride and heat (Q) when exposed to hydrogen, as seen in Eq. 6 [25]. Metal hydrides offer cheap, simple, compact and reliable designs while being safe and easy to use. However, their reactions are slow and in many cases irreversible while requiring high pressures and temperatures [20].

$$\mathrm{M} + \frac{\mathrm{x}}{2}\mathrm{H}_2 \rightleftharpoons \mathrm{MH}_x + \mathrm{Q} \tag{6}$$

Complex metal hydrides, alanates and borohydrides are other proposed types of host materials currently being researched [20]. Storing the hydrogen as ammonia or LOHCs is considered a reasonable option in cases where they are directly used in end-use sectors, though they may face challenges connected to safety and public acceptance [5].

Physical storage

Physical adsorption processes refer to the interaction of hydrogen with surface atoms of certain materials, creating weak bonds between the substances. These materials include, among others, graphite, carbon nanotubes and metal organic frameworks, most of which offering inexpensive and simplistic designs. However, they generally have a low hydrogen density and require maintaining low temperatures and high pressures [20].

2.2.4 End-use applications

Many uses for hydrogen have been tried and suggested, while the two main groups of applications can be distinguished between (i) existing uses, with large potentials for a switch to clean hydrogen, and (ii) long-term uses, where the future demand of hydrogen is highly likely [4].

Existing applications

Currently, the main use of hydrogen is within industrial applications such as oil refining (33% of global use), ammonia production (27%) and methanol production (11%), almost all of which are produced by fossil fuels [5]. The manufacturing of ammonia and methanol are currently the main GHG emitters within the chemicals industry, as natural gas is used as a common feedstock [26]. As part of the oil refining process, hydrogen is used for the upgrading of heavy residual oils, although due to the transition from fossil fuels, this use category is projected to decline in the coming decades. Meanwhile, the role of hydrogen in ammonia and methanol production will remain important and aligned with the aims of long-term decarbonisation efforts. 80% of ammonia produced is used for fertiliser production, and the demand is expected to grow slightly, while methanol produced from hydrogen is expected to grow as part of decarbonising the production of commodities such as plastics, paints and explosives [4].

Long-term applications

Looking further into the future, hydrogen is suggested to play an important role in the decarbonisation of several industries, although technological readiness is currently lower and costs higher compared to existing hydrogen end-use technologies [4].

Primary steel production is a carbon-intensive industry, currently adding 3 Gt of CO_2 into the atmosphere annually, 7% of total global CO_2 emissions. Several of the largest steel production companies have committed to net-zero emissions until 2050, for which hydrogen technologies are suggested as the main components to enable the substitution of coking coal in the process of reducing iron ore [4]. Just by using fossil-free hydrogen as a reducing agent, up to 70% of steelmaking emissions can be avoided [26]. The key challenges are not mainly technological but rather connected to the great demand for low-carbon electricity that would require policy support and low electricity prices to be reasonable from an economic perspective [5].

Long-distance shipping has the potential to utilise hydrogen-based fuels in marine power systems, where existing engines can be adapted to fuels such as ammonia or methanol [4]. Fuel cell passenger ferries and floating barge electrolysis are currently being developed. Opportunities exist to substitute fossil fuels with hydrogen or hydrogen carriers not only within ships but also for ports, and other maritime infrastructure [26].

Long-distance aviation is an industry where electrification is considered difficult due to the low energy density of batteries. Instead, synthetic hydrogen-based fuels are suggested to substitute conventional jet fuels for longer distances, while for shorter distances, hydrogen in pure forms could be used [4]. Although challenges remain with regard to the storage density of hydrogen, several projects with direct use of hydrogen have been demonstrated in smaller aircraft applications. Both fuel cells and hydrogen combustion systems are being considered [26].

Power system balancing is an application with the potential to contribute to dispatchable generation and seasonal balance in electricity grids with a large share of intermittent renewables, which are becoming increasingly common. Whenever there is surplus electricity being generated, hydrogen can be produced through electrolysis and later converted back to electricity via combustion when demand again exceeds supply [4]. The energy storage capabilities offer several benefits with regard to time shifting, limiting transmission line buildout, as well as other ancillary grid services. Additionally, fuel cells have the potential to replace generators as a backup power source for critical services and microgrids [26].

Other applications for hydrogen are also suggested for the future. Industrial applications that require high temperatures, such as refining, cement and glass manufacturing, could benefit from the combustion of hydrogen or hydrogen blends. Meanwhile, replacing fossil fuels with hydrogen, in particular medium- and heavy-duty vehicles, could significantly reduce emissions. Similarly, hydrogen can play a complementary role in decarbonising the passenger and freight rail sectors [26].

2.3 Electrolyser technologies

The three main types of electrolysers, each with its specific advantages within different applications and contexts, are (i) alkaline (ALK), (ii) proton-exchange membrane (PEM) and (iii) solid oxide electrolyzer cell (SOEC) electrolysers [4]. The general setup of an electrolyser requires an anode, a cathode, an electrolytic membrane and a power supply. The ALK and PEM electrolysers make use of electrolytes, a liquid alkaline solution and a solid polymer, respectively, where a current causes the formation of hydrogen ions that become positively charged in the anode. When passing through the electrolyte, they merge with the electrons, forming hydrogen gas (Eq. 7–10). In SOEC electrolysers, water is split into hydrogen and negatively charged oxygen in the cathode when merging with electrons, with the oxygen giving away its electrons in the anode after passing through the solid electrolyte, forming oxygen gas (Eq. 11 & 12) [9]. A fourth type of electrolyser, anion exchange membrane (AEM), is on the cusp of becoming commercially available [14]. Roughly half of the electrolyser system costs are due to the electrolyser stacks, costs that are likely to decrease in the future following technological innovation and increased economies of scale within manufacturing processes [5].

Apart from the electrolyser stacks, several other components are required as part of the electrolyser balance of plant (BOP) and its adjacent subsystems. Units for gas-liquid separation are needed to separate both hydrogen and oxygen from the recirculating liquids. Additional hydrogen treatment is required in the form of driers, which remove any remaining water, and oxidisers, which remove excess oxygen. Demineralisation units are implemented to obtain the necessary ultrapure water for electrolysis, while compressors are used to adapt the hydrogen pressure to the output requirements. Cooling units and heat exchangers constitute an additional subsystem, as do the power electronics, such as rectifiers and transformers. Further, piping and power connections between the components are required. [27]

With regards to electrolyser stack costs, learning rates of 9% for ALK and 13% for PEM electrolyser systems are considered [28], with some studies suggesting electrolyser learning rates of up to 16–21% [15]. However, electrolyser costs are subjected to large uncertainties, as further introduced below.

2.3.1 ALK

ALK electrolysers are a highly mature technology (TRL 9) since long used within the chloralkali industry, the currently largest user of electrolyser technologies, while also being projected to keep the largest market share for hydrogen production for the short-term future [14]. Despite already having been used for a century, some progress is expected, though not as much as for other electrolysers [21]. The electrical efficiencies of ALK electrolysers currently range between 63–70%, with projected efficiencies of 65–71% in 2030 and 70–80% for the longer term [5]. The operating pressures of ALK electrolysers range from atmospheric, for older generation electrolysers, up to 30 bar for newer ones. Higher output pressures lower the compression requirements and thus the investment costs [21]. A combination of pressurised and unpressurised ALK systems might improve the flexibility and performance [29].

$$Cathodic: 2\,H_2O + 2\,e^- \longrightarrow H_2 + 2\,OH^- \tag{7}$$

$$Anodic: 2\,OH^- \longrightarrow H_2O + \frac{1}{2}O_2 + 2\,e^- \tag{8}$$

Apart from the technological maturity, low capital costs (460–1 300 €/kW [14]) and long operational lives are the main advantages, with the main disadvantage being the need for continuous use to avoid damaging the system [18]. For these reasons, ALK electrolysers today need to maintain a load of at least 20–30%, which is especially significant in the context of using intermittent renewable power as input, although the compatibility of using ALK electrolysers with fluctuating currents is being improved. Part of the challenge is the slow dynamic response, having start-up and shutdown times of 1–10 minutes as well as ramp-up and ramp-down rates of 0.2–20 %/second [30]. Other concerns regard corrosion and the difficulty in handling low current densities [9]. A general overview of the hydrogen production process using an alkaline electrolyser is shown in Figure 2.

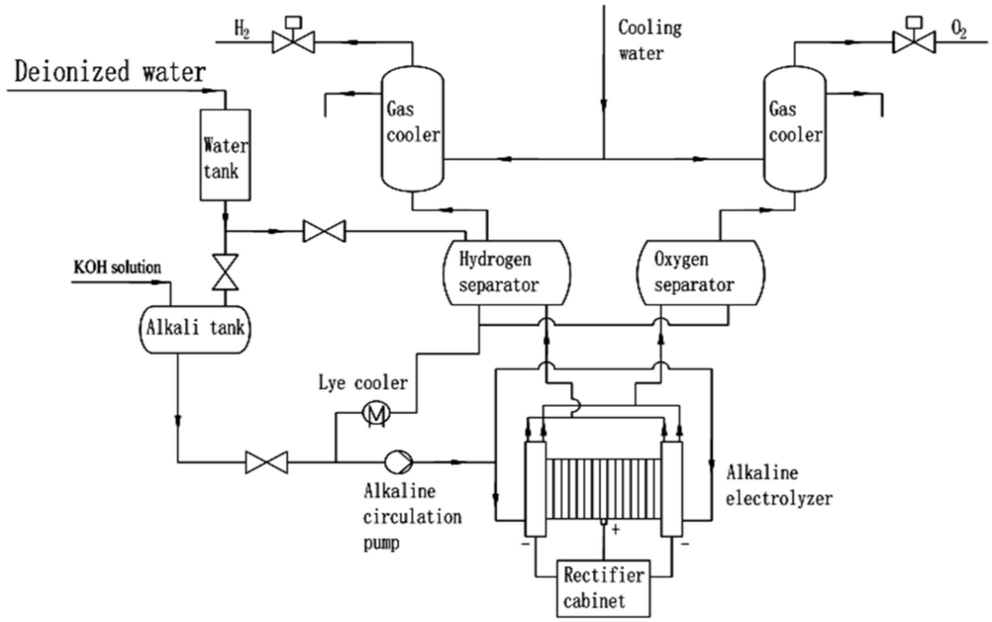

Figure 2: ALK process flow chart [31]

2.3.2 PEM

PEM electrolysers are considered to be an equally mature technology as ALK electrolysers for hydrogen production, with high commercial availability as well as rapid cost reductions [14]. However, the mature technology and supply chains are complemented by a rapid increase in demand, with risks of delays due to bottlenecks [32]. The operating pressure of commercial PEM electrolysers is typically around 30-40 bar, although due to their use of a solid polymer electrolyte, much larger pressures are possible. Electrolysis at 80, 200, and even 350 bar is likely to be economically viable, considering that the eliminated need for post-electrolysis compression is suggested to compensate for the increase in electrolyser investment cost [33].

$$Cathodic : 2\,H^+ + 2\,e^- \longrightarrow H_2 \tag{9}$$

$$Anodic : H_2O \longrightarrow 2\,H^+ + \frac{1}{2}\,O_2 + 2\,e^- \tag{10}$$

Contrary to ALK electrolysers, PEM electrolysers are a good fit in contexts with intermittent electricity supply due to their fast dynamic response, with start-up and shutdown times of only seconds as well as full ramp-up and ramp-down in a second [30]. This makes them suitable for applications such as power system balancing [4]. Further, the plant footprints are about half that of ALK systems, a significant advantage when considering applications with space and weight limitations [34]. Current disadvantages include higher capital costs (1 000–1 700 €/kW [14]) and issues due to geographical supply conditions of the reserves for the required catalysts and membrane material. To scale the technology, looking into materials other than the commonly used iridium and platinum is suggested [4]. The operational lifetimes of PEM electrolysers are shorter than ALK electrolysers and are likely to remain so for the near future [30]. They also currently offer lower electrical efficiencies, usually ranging from 56–60%, than other electrolyser technologies [9], but with projected efficiencies of 63–68% in 2030 and 67–74% for the long term [5]. Hybrid configurations combining PEM and ALK systems could prove useful for certain applications [29]. The hydrogen production process using a PEM electrolyser is exemplified in Figure 3.

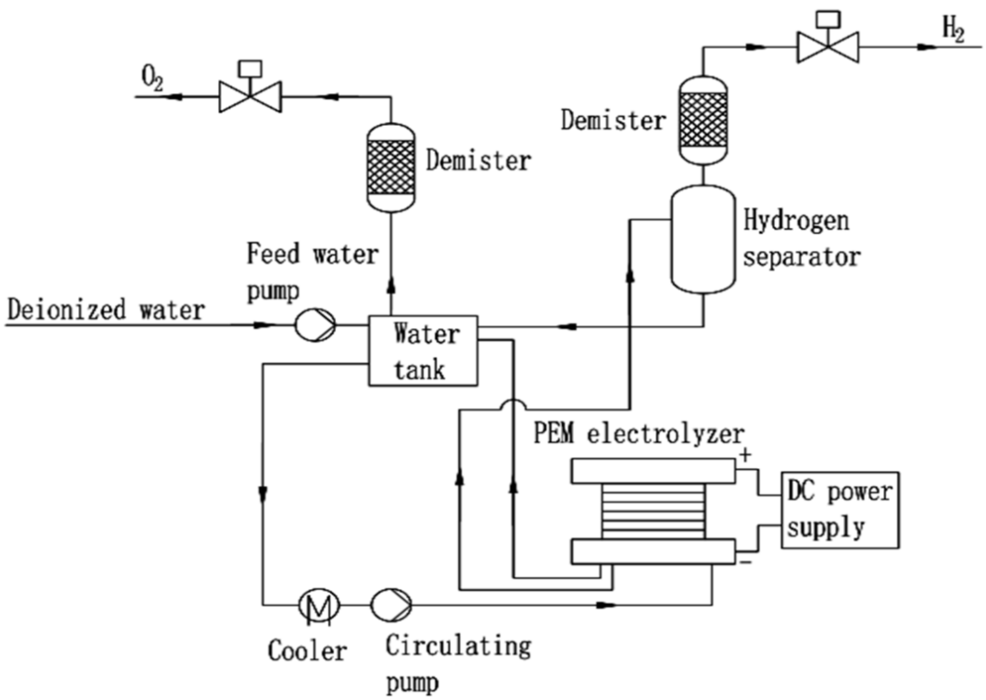

Figure 3: PEM process flow chart [31]

2.3.3 SOEC

SOEC electrolysers are a more immature technology (TRL 7 [14]), recently becoming commercially available. However, they are showing great promise with regard to expected costs and system efficiencies currently ranging between 74–81% [9], with stated efficiencies of up to 84% [35] as well as projected efficiencies of 77–84% in 2030 and potentially 77–90% in the longer term [5]. Currently, capital costs are high (2 600–5 200 €/kW) and policy support is required to make SOEC suitable for commercial purposes [14]. Unlike ALK and PEM, they operate at high temperatures [30] and the main challenges involve ensuring material stability under these conditions [36].

$$Cathodic: H_2O + 2\,e^- \longrightarrow H_2 + O^{2-} \tag{11}$$

$$Anodic: O^{2-} \longrightarrow \frac{1}{2}O_2 + 2\,e^- \tag{12}$$

2.3.4 AEM

Anion exchange membrane (AEM) is another electrolyser technology undergoing rapid developments with several projects in the pipeline, although still being a more immature technology (TRL 6) not yet proven at a market scale [14]. The potential benefits are significant, combining the characteristics of low-cost catalysts with a solid polymer electrolyte structure suitable for intermittent electricity supplies, with recorded efficiencies of up to 74% [37]. For AEM electrolysers to reach commercialisation, policy support is required [14]. Table 2 gives an overview of a few main characteristics for the mentioned electrolyser types.

Table 2: Main characteristics of electrolyser technologies

Electrolyser	CAPEX (per kW)	Cost development	η_{el} (current)	η_{el} (long-term)	TRL
ALK	460–1 300 €	Slight decrease	63–70%	70–80%	9
PEM	1 000–1 700 €	Strong decrease	56–60%	67–74%	9
SOEC	2 600–5 200 €	Requires support	74–84%	77–90%	7
AEM	Not commercial	Requires support	<74%	–	6

2.4 Offshore wind power

During the past decade, the world has seen significant declines in the costs of renewable electricity, becoming progressively more competitive with electricity from fossil fuels with each passing year. Looking at LCOE estimates, costs for solar PVs have decreased with more than 80% and wind power with 55% since 2010 [3]. The global deployment of these two technologies is expected to be rapidly scaled up, with solar PVs being the leading technology in regions with high solar potential, while onshore and offshore wind power offering to be the main generation technology in other regions. In the EU, wind power is projected to contribute with 40–50% of all electricity generation in 2050 [1]. Meanwhile, it is also suggested that until then, 45% of the Swedish electricity demand could be covered by offshore wind power alone, illustrating its significant technological and geographical potential [38].

The interest and investments in offshore wind power have grown in parallel with the decreasing costs, mostly in Europe, where the investments are currently larger than for onshore wind. There are several arguments to be made in favor of offshore wind power, as compared to onshore wind power, mainly due to (i) higher and less variable wind speeds, (ii) less noise and visual pollution and (iii) the possibility to install larger turbines [39]. The case for offshore wind power further strengthens when considering the expected reductions in capital costs, with estimates suggesting a 80% decrease until 2050. The main reasons for this include an increase in turbine sizes, product improvements and growing economies of scale [3]. Turbines between 3.5–

8.8 MW were used for European offshore wind projects commissioned in 2018, while until 2030, turbine sizes of 15–20 MW are expected with rotor diameters of more than 230 m. In less than two decades, the average turbine size for offshore wind projects has more than tripled [40]. As offshore turbine sizes increase beyond 15-20 MW, the higher currents and their associated losses become a problem, leading to medium voltage converters becoming a more cost-efficient choice than the low voltage systems currently in use [41].

The power in the wind can be expressed by $P = \frac{1}{2}\rho AV^3$, where ρ is the air density (kg/m^3), A the cross-sectional area normal to the wind direction (m^2) and V the wind speed (m/s). Betz's law indicates that the maximum theoretical extraction of the wind power is 59.3%, due to the reduction of wind speed by the wind turbine itself [42]. Together with the increase in turbulence when the wind passes a wind turbine, this creates a wake effect, where adjacent turbines have their performance negatively impacted by the energy losses in the incoming wind. Thus, a minimum distance of 7 rotor diameters is recommended [43], avoiding power losses of approximately 10–20% [44]. The rated wind speed is a key design parameter defining the speed where the turbine reach its rated power output, while the cut-in and cut-off wind speeds indicate when the wind turbines start and stop their power generation to avoid damage [42].

Typically, wind turbines can be categorised into fixed and variable speed wind turbines, with the difference being if the rotational speed varies according to the wind speed or not. The variable speed wind turbines are more efficient and are thus the most commonly installed wind turbine. Among the variable wind speed turbines, the preferred type is using a full-converter wind turbine, whose synchronous generator is excited by permanent magnets or a DC source. The generator uses a power converter to connect to the grid and enable power regulation. This turbine type offers insignificant rotor losses and cheap maintenance. [39]

An offshore wind farm (OWF) can consist of fixed bottom wind turbines or floating turbines, with the first being the most commonly used technology with 25 GW installed capacity compared to the 62 MW for the latter. However, the rapidly decreasing costs for floating wind farms enable the installation in waters more than 60 meters deep, where fixed installations are infeasible but which account for 80% of offshore wind resources [21] [18]. Currently, several OWF projects are being planned and tried for permits within the Swedish economic zone in the Gulf of Bothnia located in the northern Baltic Sea. Each of these OWFs are planned to generate 1000s of GWh yearly, with the largest being Eystrasalt with a projected 13 800 GWh annual generation from its 286 wind turbines [45].

2.4.1 Integration into onshore grids

To connect a large OWF to the onshore grids, three main types of transmission are suggested: (i) high voltage alternating current (HVAC), (ii) high voltage direct current (HVDC) and (iii) low-frequency alternating current (LFAC). All of these are considered reasonable choices as transmission technologies, the latter being more technologically immature, with transmission distance being the main factor deciding which is the most desirable for a specific context. The maturity and reliability of HVAC technology, as well as lower converter station costs and footprints, makes it a reasonable choice for many larger OWFs [46]. The extra conversion steps required for HVDC transmission leads to losses between 0.6–1% of the delivered power [47]. However, capacitive charging effects on the cables limit the viability of HVAC for longer transmission distances.

HVDC losses average at 3.5% per 1000 km compared to roughly 6.7% for HVAC lines [22]. Thus, for subsea transmission distances longer than 60–75 km, HVDC is generally a more desirable choice [39].

In short, a HVAC transmission system consists of (i) an offshore substation to raise voltage levels, (ii) three-core HVAC submarine cables, (iii) reactive compensation units as well as (iv) an onshore substation to match grid voltages. Meanwhile, a HVDC connection requires apart from (i) an offshore and (ii) onshore substation, also (iii) an AC/DC rectifier, (iv) AC and DC filters, (v) HVDC submarine cables and (vi) a DC/AC converter. [39]

Among the HVDC systems, two technologies are currently implemented for OWFs, using a line commutated converter HVDC (LCC-HVDC) or a voltage source converter HVDC (VSC-HVDC) [39]. The former is the main technology for onshore, long-distance transmission with low costs and losses, although their large converter stations are not optimal for offshore applications. Meanwhile, VSC-HVDC is the most common for large OWFs, offering the possibilities of black starts — the ability to restore power within a system — as well as the interconnection of passive networks, contributing to the targets of global power interconnection [46]. Another HVDC technology proposed lately is diode rectifier based HVDC (DR-HVDC) consisting of diodes, a transformer and a smoothing reactor, a system that would require significantly less weight and volume while offering reductions in costs and power losses. However, barriers remain before the successful large-scale implementation of DR-HVDC for OWFs [39].

2.4.2 Technical challenges

While many benefits of the use of offshore wind power have been identified, there are notable challenges. Its intermittent properties are due to the heavy dependence on weather conditions, leading to an uncontrollable and non-dispatchable electricity generation. When replacing conventional, dispatchable electricity sources, the stability of the grid frequency is negatively impacted following the reduction of rotational inertia. Among the proposed solutions are (i) a range of frequency control strategies, (ii) the complementation of different intermittent sources, such as wind and solar, and (iii) the use of energy storage systems, including flywheels, batteries and hydrogen. [39]

Another challenge regards the electricity transmission to shore, where neither of the proposed transmission systems fulfil the criteria of both low costs and power losses while at the same time being a mature enough technology to be implemented on a large scale. Considering the utilisation of OWF power for electrolytic hydrogen production, there is a case to be made for placing the hydrogen production offshore, transporting the gas to shore in subsea pipelines. That way, costs and losses can be reduced simultaneously. [21]

2.4.3 Regulations

An important geographical aspect for the techno-economic assessment of power station projects in a Swedish context is the concept of bidding zones, which were created in 2011 to fulfil EU competition policy requirements. The use of four bidding zones, from SE1 and SE2 in the north to SE3 and SE4 in the south, is supposed to ensure a fairer and more reliable trade system seen from an EU perspective. Due to the northern parts of the country often having surplus electricity, while southern Sweden stands for the major part of the demand, there are notable bottlenecks with limited transmission capacity. While the bidding zones are implemented as a market solution to include transmission limitations, there can be significant price differences between the zones. [48]

In 2022, the Swedish government requested an expansion (Government Decision I2021/02682) of the transmission grid into areas of high potential for additional offshore electricity production. The costs for connection are suggested to be partly covered by the state-owned enterprise Svenska Kraftnät and partly by the connecting actor, with a new customer model compatible with EU state aid regulations [49].

Following the Swedish Environmental Code (1998:808), the construction of an OWF in Swedish territorial waters (<22.2 km from shore) or economic zone (22.2–370.4 km) requires permits for environmentally hazardous activities and water operations. A permit is also required according to the Act on the Continental Shelf (1966:314) while a registration of the project activity is required according to the Planning and Building Act (2011:338). Further, if the OWF is planned outside of Sweden's territorial waters, in the economic zone, a permit is mandatory following the Swedish Exclusive Economic Zone Act (1992:1140). Typically, these permits are tried by the Swedish Land and Environment Court. [50]

2.5 Electrolytic hydrogen production from offshore wind power

Many sectors and industries have been identified to have potential to be transformed by substituting fossil fuels with hydrogen. For this purpose, as well as for existing process industry needs, it is estimated that just in Sweden, up to 130 TWh of electricity per year could be required to produce the needed hydrogen using electrolysis. Since that is roughly equal to the current electricity use of the whole country, increased offshore wind capacity is suggested in order to keep electrolysis costs at low levels, enabling not only sufficient amounts of green hydrogen for domestic purposes but also international market and climate support opportunities [38].

Meanwhile, the planned integration of offshore wind in the scale of hundreds of GW within the coming decades into the EU power system creates significant grid-related challenges. The intermittency of wind power output creates power system imbalances which not only add risk but also require large investments for reinforcements to improve grid stability. By producing hydrogen, either from all of or just the surplus electricity, the grid stability can be improved and reduce the need for grid reinforcements [34].

The dedication of offshore wind power to produce green hydrogen has large potential for low-cost electrolytic production, compared to activities where grid electricity is used, due to the reduced or eliminated costs associated with transmission. EU projections for 2030 shows a cost range of offshore wind of 35.02–61.28 €/MWh with transmission while only 26.27–43.78 €/MWh without transmission. Lately, a growing interest in producing green hydrogen from offshore wind has been observed within the energy industry [18]. In the Baltic Sea alone, several large offshore wind-to-hydrogen projects have been suggested from actors such as Siemens [51], Eolus [52], ABB, Lhyfe and Skyborn [53].

2.5.1 System configuration

Three main types of electrolyser system configurations are suggested: offshore hydrogen production (i) either on a central platform or (ii) connected to each turbine in the OWF, or (iii) in an onshore facility. The electrolyser system can be connected to both fixed and floating wind farm structures, with the latter including simpler designs like spar buoys or as more complex semi-submersible platforms [21]. There are also possibilities to co-generate hydrogen and electricity for all configurations, where a hydrogen-driven system prioritises to maximise electrolyser capacity and an electricity-driven system prioritises the power demand while using only the surplus electricity as input to the electrolyser [34].

2.5.2 Electrolyser system

Considered the central process in the system, the electrolyser setup may be optimized differently for each specific context. Due to the variable power outputs of the wind turbines, the limited response capabilities of current ALK electrolysers generally make them unfit for the purpose, although they are likely to become better adapted in the future. Meanwhile, the fast response capacity as well as the compact designs of PEM electrolysers generally make them a suitable choice, while it should also be noted that the necessary catalysts are expensive. While showing great promise, especially considering system efficiency, SOEC electrolysis is a technology requiring high temperatures. In offshore setups however, this adds to leakage and fire risks in environments where maintenance is difficult and vulnerabilities with regard to safety and equipment are high. Instead, PEM and ALK electrolysers are suggested as the main candidates [18].

There are several arguments to be made for PEM electrolysers to be the technology of choice for offshore production, especially in decentralised configurations. Maintenance, generally being more complicated offshore, is both easier and not needed as often as for other electrolysers [21]. Performing electrolysis in connection to each turbine creates a greater need for compactness which PEM electrolysers can offer, while the maintenance dynamic performance, being even more important for decentralised production, further strengthens their case. They can also remove the need for a distinct compression system for the hydrogen buffer tank, due to the possibility of already reaching 80 bars of pressure during the PEM electrolysis process [18]. However, many PEM electrolysers currently have output pressures closer to 30 bar which could indicate a need for additional compression when delivering the hydrogen to shore [21].

Considering that volume and weight requirements are significantly less important in onshore configurations, ALK electrolysers are considered to be feasible for this type of setup [18]. Due to onshore environments offering easier access to the electrolyser, the increased need of maintenance for ALK electrolysers is not a significant barrier. Further, onshore configurations offer better sheltering for electrolysers and other sensitive equipment [21]. For the offshore environments, platforms or artificial islands to accomodate the electrolyser, balance of plant (BOP) and power electronics systems are required [34]. Large economic uncertainties remain for these offshore facilities, while the technical feasibility is considered high due to similarities to offshore gas and oil platforms [54].

2.5.3 Water supply

In all electrolyser configurations, a supply of demineralised water is required [4]. Theoretically, 9 kg of water is required for the electrolysis process, although in reality, it can be as much as 18–24 kg required for each kg of hydrogen produced [15]. This additional need is due to low recovery values during the pretreatment of raw water as well as treatment to ultrapure water quality, especially in the case of seawater desalination, due to its large osmotic pressures. The use of ultrapure water, instead of freshwater that contains problematic ions and molecules, is an affordable way to limit degradation and irreversible damage to the electrolyser stacks [55]. For offshore configurations, a desalination unit, which can be powered directly from the AC output of the wind turbines, is required together with a reservoir for desalinated water [21]. Desalination through standardised reverse osmosis is considered sufficient [55]. These desalination units are suggested and tried with pilot projects, but remain to be manufactured on an industrial scale where bottlenecks are likely to occur in the supply chain [32]. Other methods such as thermal desalination using heat pumps have been proposed for offshore environments, enabling the utilisation of excess heat from the electrolyser, while reducing the electricity demand by half [56].

A seawater pump is required for the reverse osmosis desalination, requiring energy in the range of 2–4 kWh/m^3, depending on factors such as pump efficiency and seawater salinity. However, the total cost of desalination is only slightly increasing the hydrogen production costs by roughly 0.01 €/kgH$_2$, when getting the electricity input directly from the wind turbines [18]. Using the middle estimates of the above-mentioned energy and water requirements, the resulting energy needed for the desalination of the water supplied to the electrolyser is roughly 0.06 kWh/kgH$_2$. Meanwhile, environmental considerations are required due to the adverse effects of brine discharge on marine ecosystems, with proven risks of damaging plants and animals through an increased salinity of the rejected water. Adopting EIA strategies are suggested together with a range of technological solutions, among them by diluting the brine with cooling water or utilising other methods of diffusion [57].

Desalination units can be built not only offshore, but also on onshore environments such as coasts and islands [32]. However, for onshore configurations there is also an option to connect the electrolyser system to the freshwater grid, a solution that might be preferred in regions with surplus freshwater [21]. However, while electrolytic water consumption is large, it would constitute only 1.3% of the total water use in the global energy sector, even if all hydrogen today was produced through electrolysis [5].

After obtaining freshwater from the grid or from the desalination unit, several measures can be taken in order to make the water ultrapure and even more suitable for the electrolysers. Free chlorine can be removed using active carbon, while a double reverse osmosis system can be used to remove the majority of ions, molecules and particles. Additionally, by using a softener or antiscalant, issues of hardness due to the presence of Ca or Mg ions can be solved, while a membrane degasser can be used to remove the dissolved gases that passes through the reverse osmosis process. Lastly, a final deionisation using a mixed bed filter or an electrodeionisation unit will handle the remaining ions. This process requires 3.3 m^3 of seawater to obtain 1 m^3 of ultrapure water. [55]

A seawater pump is required also for providing the water required to keep the electrolyser stacks within a desired temperature range. Large-scale electrolysers can not be cooled externally, leaving two main options for internal cooling: either by using excess amounts of process water or by implementing a dedicated circuit using a cooling fluid. The main advantage of the excess process water method is its high heat transfer efficiency, while contamination is observed as a downside. Meanwhile, the use of a separate cooling circuit avoids contamination risks and has no direct effect on cell performance, although a challenge is the limited space between the cells, where the cooling channels would need to be located. [56]

2.5.4 Transmission vector

Among the largest costs for an OWF is the equipment to transport the electricity to shore, which involves power electronics, cables and transformers. In the offshore electrolyser setups, hydrogen pipelines instead connect the OWF with the onshore systems, with lower transmission losses and cheaper investment costs than in cases where subsea power cables are used [21].

The requirements for hydrogen compression depend on several factors. As mentioned previously, the compressor is sized depending on the operating pressure of the electrolyser, hydrogen flow, transport distance and the pressure drop in the pipeline. Required pipeline pressures of up to 100 bar have been identified for hydrogen pipelines in offshore environments. For offshore configurations, the hydrogen compressor runs on AC power directly from the wind turbines or central platform [21]. The subsea pipeline transportation of large volumes of hydrogen over large distances remains a subject where little research has been done, both with regards to costs and technical performance. However, the characteristics of hydrogen gas and the general performance of gas pipelines are well understood [58].

The onshore configuration transports the energy as high voltage electricity to shore, where it is then converted into hydrogen. This technology can be seen as the traditional transmission setup for a large OWF, where both HVDC and HVAC are considered reasonable options, with the main deciding factor being the distance from shore [18] [39].

2.5.5 Back-up and buffer systems

When coupled to an intermittent power source, a backup power source is required to ensure that there is sufficient energy during periods of shutdown, when small amounts of power are required to remain in standby mode. For offshore configurations, the rectified DC output power from the turbines or central platform is used [21]. A battery system is suggested for this purpose, ensuring the fulfilment of minimum requirements for operating conditions during varying wind output yields [18]. For onshore configurations where the electrolyser system is connected to the onshore grid, the back-up power could be supplied by the grid.

Due to the fluctuating characteristics of hydrogen, a buffer is required before pipeline transmission to the off-taker, generally in the form of a hydrogen storage tank [18]. However, space limitations might present an issue due to large-scale electrolyser systems requiring large hydrogen storage volumes, above 55 000 m^3/day for a 1 GW electrolyser [21].

3 Methodology

This model-based study aims to analyse the system setup for hydrogen production from offshore wind power in a geographical context considered suitable and relevant for the project activity. The OWF in this study is dedicated to hydrogen production as an off-grid setup using either hydrogen pipelines or power lines for transmission from the hub to shore, but not both. Further, this chapter aims to give an overview of the software tools and processes used to obtain the results, followed by the defined assumptions and limitations of the study.

3.1 Site

The systems studied in the report are assumed to be located in the Gulf of Bothnia in the Baltic Sea, outside of the Swedish territorial zone but within its economic zone, at coordinates 61.4460378, 18.1222082. The distance from the hub to shore is 50 km, which is the value that will be used in the study, with the closest point on shore located between the cities of Söderhamn and Hudiksvall as seen in Figure 4. The location of the offshore hub is marked, and the areas in blue signify offshore wind farms currently being planned [45].

The area surrounding the location has available depths of less than 60 metres, which has previously been identified as feasible for fixed-bottom wind turbines. This has been validated with the use of the Baltic Sea Bathymetry Database [59]. Further, the wind data of the location is assumed to be the same for the whole project area and is gathered from the MERRA-2 dataset for 2019 at the height of 210 m [60].

3.2 Activity

In the study, the project is assumed to be up and running in 2030, with a lifetime of 30 years. The electrolyser system, either PEM or ALK, gets its power supply from 40 offshore wind turbines, each with a rated power of 25 MW, totalling an installed capacity of 1 GW. A central, bottom-fixed platform is used for the placement of several of the necessary system components before transmission to shore. A more detailed system setup follows for each case.

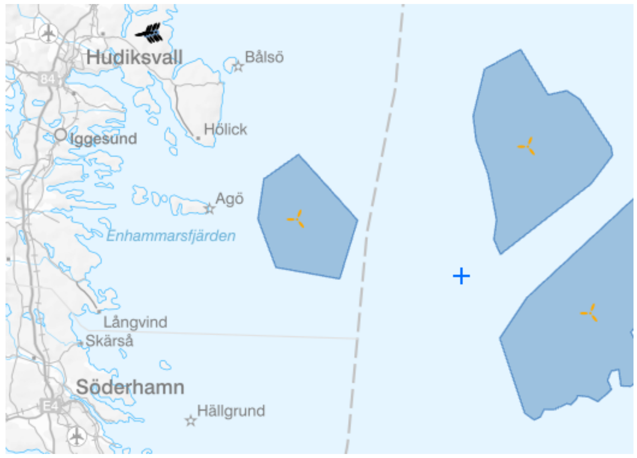

Figure 4: Project location [45]

3.3 Typologies

To clarify the model designs, the system components considered are described below, together with definitions of the general setups for the three electrolyser system typologies (Fig. 5–7).

3.3.1 Centralised offshore

This setup is defined as the hydrogen being produced on a central platform offshore and then transported to the shore in a pipeline. Smaller dynamic cables are used for outputting the power from each wind turbine [18], creating a 66kV AC underwater inter-array transmission grid [61] connected to the substation, seawater pumps and compressor on the central platform [21]. The offshore substation is used to integrate, rectify and convert the wind power output to meet electrolyser requirements. A larger dynamic power cable for DC transmission then connects the substation with the electrolyser [18]. Due to the short transmission distances on the central platform, any power transmission losses are assumed to be negligible.

The central platform is used for the placement of the electrolyser, desalination unit, cooling units, backup power system and compressor if needed [18]. For offshore setups, PEM electrolyser systems are considered, but not ALK systems due to larger maintenance requirements and footprints [21][34]. Further, there are difficulties in supplying backup power and handling lye in harsh, offshore environments [29]. A reverse osmosis system is considered for the desalination of the pumped seawater needed for the electrolyser, with further purification through softening, demineralisation, degassing and polishing EDI/mixed-bed [55]. The cooling is done by pumping seawater through heat exchangers to move the heat generated from the electrolysis process using a separate circuit. Since only pressurised PEM electrolyser systems are considered for this setup, no compressor is included. Lastly, a UPS system, charged by excess wind power output, is placed to ensure that there is a backup power source for heating the electrolyser and safety systems in standby mode.

A pipeline is considered for hydrogen transmission to shore and offers further benefits as a gas buffer due to the pipe volume. No dedicated hydrogen buffer, such as tanks, is considered. Figure 5 shows the centralised offshore (COFF) system setup and boundaries.

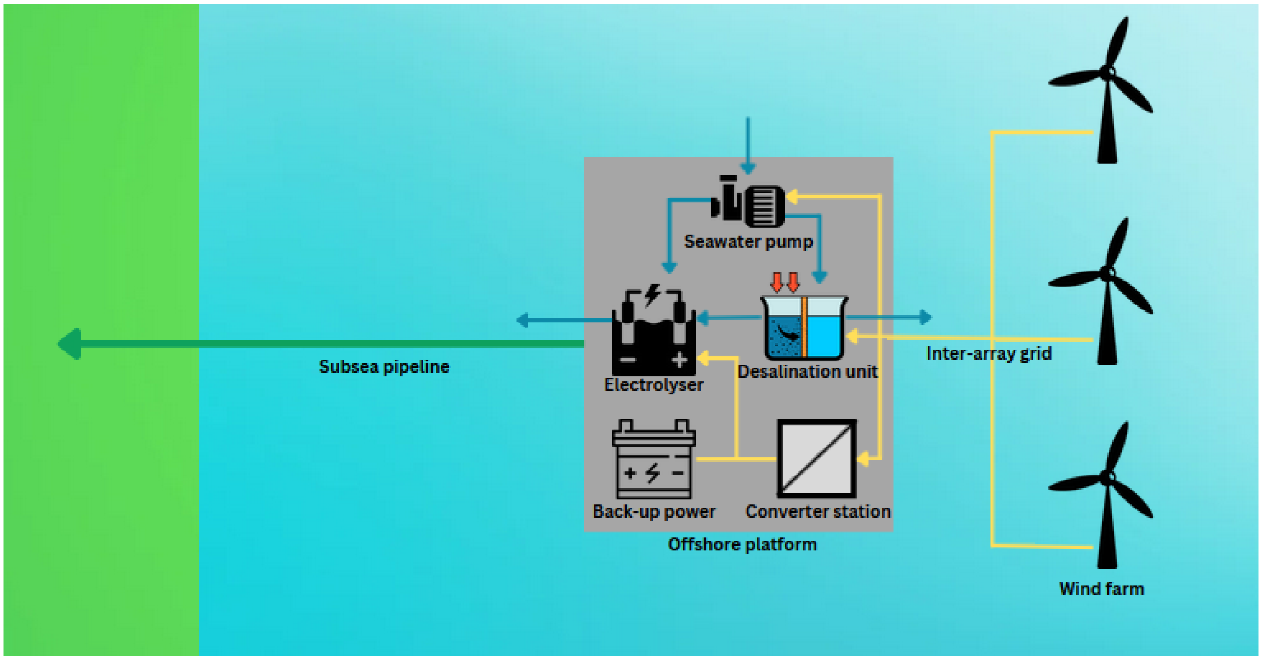

Figure 5: Centralised offshore electrolyser setup (source: author)

3.3.2 Decentralised offshore

In this configuration, the hydrogen is produced on a transition piece in connection to each turbine and then transported to the shore in a pipeline. The wind power output is rectified and converted to meet electrolyser requirements, apart from the power needed for the desalination and compression processes [21]. Since only pressurised PEM electrolyser systems are considered for this setup, no compressor is included.

On the transition piece, a PEM electrolyser module is placed together with similar configurations for water purification, cooling and backup power systems as in the centralised offshore typology. The main difference is that each wind turbine has its setup rather than one large setup on the central platform, making it a decentralised system.

Static pipelines transport the hydrogen to the hub, where the gas is compressed if required and then transmitted to shore in a larger pipeline [18]. As in the centralised offshore setup, no dedicated gas buffer is considered apart from the pipeline. Figure 6 illustrates the decentralised offshore (DOFF) system design.

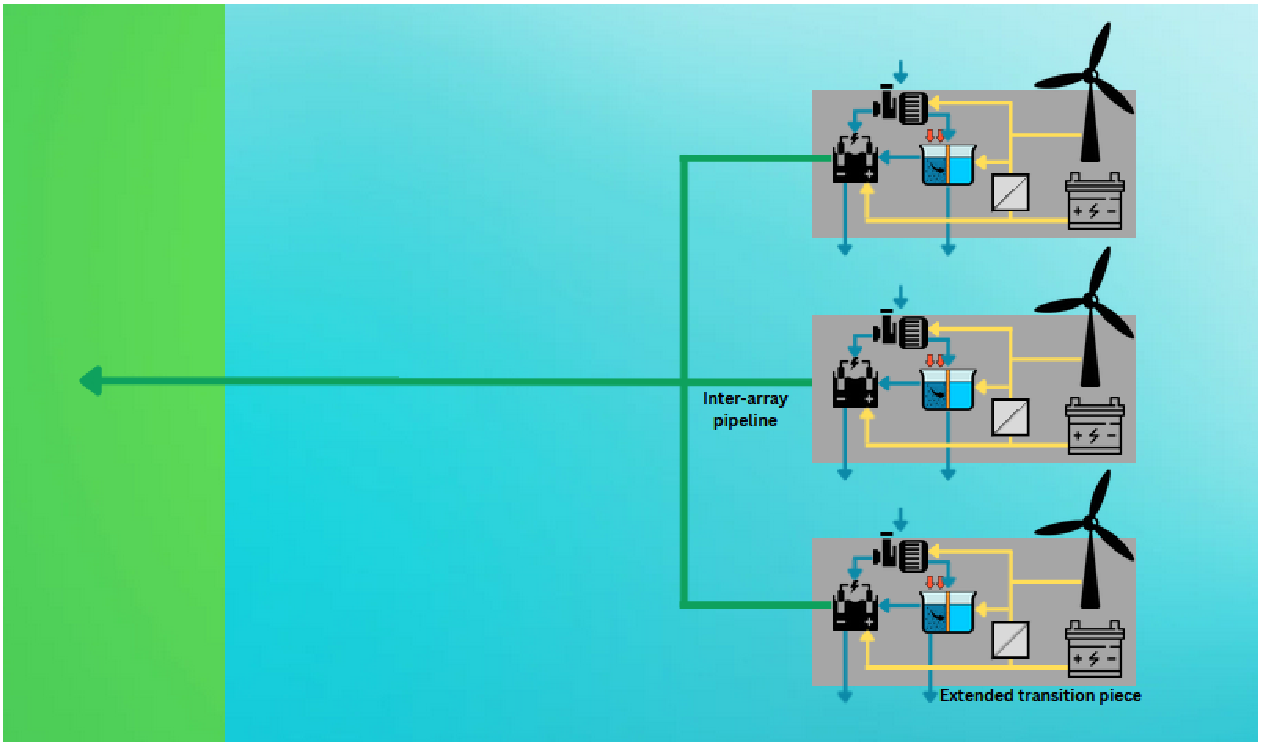

Figure 6: Decentralised offshore electrolyser setup (source: author)

3.3.3 Centralised onshore

The setup is defined by the hydrogen being produced on land from wind power directly transmitted to shore. As for the centralised offshore setup, smaller dynamic cables are used for outputting the power from each wind turbine to a 66kV AC underwater inter-array transmission grid connected to the substation located on the central platform. In the offshore substation, the voltage is stepped up, and the power is transmitted as HVAC to shore, as the distance is likely not long enough for HVDC to offer a better system performance, considering a breakeven distance of 50–80 km. [39].

On shore, the power is rectified and converted into low voltage DC to fulfil electrolyser requirements, apart from the power needed for the cooling pumps and compressor. A PEM or ALK electrolyser system is placed in a facility together with water purification, cooling and backup power systems. Desalination is not considered due to the assumed freshwater access, although further water purification processes are still required to fulfil purity requirements. If required, a compressor is used to fulfil the minimum outlet pressure requirements. In Figure 7, the centralised onshore (CON) system is visualised.

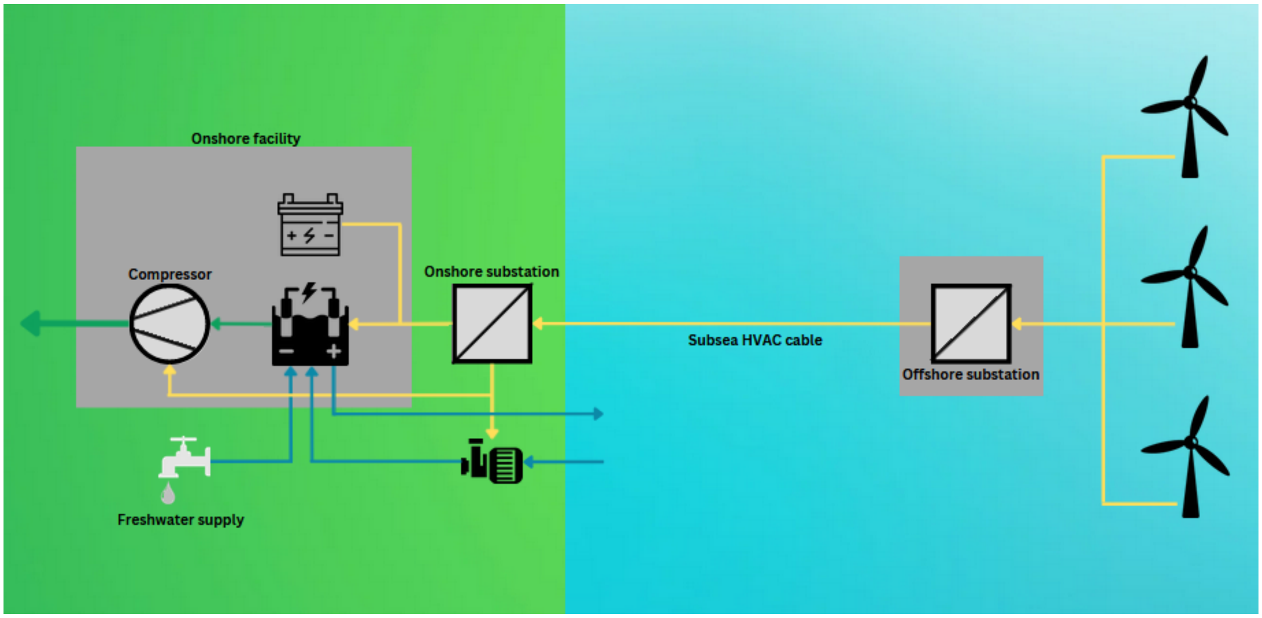

Figure 7: Centralised onshore electrolyser setup (source: author)

3.4 Tools and methodology

Below, the tools used for gathering and analysing the results are introduced, together with a main outline of the processes and steps followed.

3.4.1 Electrolyser capacity optimisation

The choice of electrolyser system capacity is based on which system size offers the cheapest hydrogen production, determined in €/kgH_2. The load duration curve of electrolyser power inputs that is obtained from the simulations is fitted with a 9th degree equation curve in MATLAB, and thus, the load factor for any capacity can be obtained through integration, getting an approximation of the total H_2 produced (as shown in section A.2). Using Excel, the full CAPEX and OPEX costs are then combined to obtain the full, non-discounted costs for all studied capacities. Thus, the hydrogen cost can be calculated according to Eq. 13.

$$LCOH = \frac{\sum_{t=1}^{n} C_{sys} + C_{el} \cdot P_{el}}{\frac{P_{el} \cdot \eta_{tot} \cdot LF \cdot 525600 \cdot 10^3}{LHV}} \tag{13}$$

where C_{sys} represents the non-electrolyser costs in €; C_{el} the electrolyser cost in €/MW; P_{el} the total electrolyser capacity; η_{tot} the full system efficiency; LF the load factor and LHV the lower heating value, 33.33 kWh/kg. The capacities with the lowest obtained levelised cost of hydrogen (LCOH) are then further investigated through modelling and an expanded techno-economic assessment.

3.4.2 System modelling

MATLAB and Simulink, a MATLAB-based graphical programming tool, are the main tools used to design, model and simulate the electrolyser setups. The input specifications are defined in a main MATLAB script, which calls several functions where:

- Hourly wind data is imported from the MERRA-2 2019 dataset via renewables.ninja [60] and interpolated to obtain estimations of minute-by-minute wind speeds.
- A wind turbine power curve is designed, and a Savitsky-Golay filter which smooths according to a quadratic polynomial, is applied to the power output, taking into account the levelling impacts of different wind power potentials due to weather differences between the turbine locations. This is used only for the centralised setups, which at some point integrate the turbine outputs.
- The electrolyser function is calculated. The electrolyser degradation and efficiency, operating hours, replacements and necessary backup power are obtained, together with the gas conditions required for the simulations.
- Compressor energy demand is determined using Eq. 22 to fulfil transmission requirements for pressures and velocities.
- A water pumping system configuration is chosen based on the typology.

The obtained values are then used as input in the Simulink models, where simulations are performed using time steps of 1 minute, totalling 525 600 minutes for 1-year and 15 768 000 minutes for 30-year simulations. Three models are constructed, one for each configuration, based on the components and flows introduced in Figure 5–7. From the simulation output, a MATLAB script then determines the surplus energy produced. A third MATLAB script is then used to plot the relevant, simulated data points in graphs.

3.4.3 Techno-economic assessment

With the obtained system efficiencies and H_2 productions, a more thorough economic assessment is performed. Using Excel, the LCOH for the different cases are calculated with Eq. 14 [62].

$$LCOH = \frac{\sum_{t=1}^{n} \frac{CAPEX_t + OPEX_t}{(1+r)^t}}{\sum_{t=1}^{n} \frac{m_{H2,t}}{(1+r)^t}} \tag{14}$$

where n signifies the project lifetime in years, t the year of operation, $m_{H2,t}$ the sum of hydrogen produced in kg and r the discount rate.

3.4.4 Qualitative study

After determining the modelling results and costs, a literature study is performed to gather other valuable insights about the different configurations. The gathered information is divided into categories of (i) technological readiness, (ii) safety and regulations, as well as (iii) installation, operation and maintenance. The sources are chosen based on two main indicators: credibility and applicability to the studied case.

3.5 Assumptions

Here, the assumptions made to provide a foundation for the modelling, analysis and interpretation will be outlined. By providing a comprehensive analysis of the assumptions made, the aim is to be able to draw more accurate and meaningful conclusions from the results.

3.5.1 Electrolyser capacity optimisation

The optimisations are done prior to the simulations, although the system efficiency input to the optimisation is obtained through a single iteration after performing one simulation. The possible system sizes range from 25 MW up to the maximum available input power for each respective case, using steps of 25 MW in accordance with the determined module size.

3.5.2 System modelling

To develop the model, assumptions for technical specifications and values are required for a range of parameters. Predicted values for 2030 are used wherever available due to anticipated technological advancements and long project development times. For certain specifications, the aim is for the values to be chosen based on existing or planned industry projects. As mentioned, the model considers a project lifetime of 30 years with a time step of one minute.

Wind power system

The output of the OWF is calculated using the specifications seen in Table 3, many of which are from a suggested concept of a 25 MW offshore wind turbine [63]. The purpose of these is to determine the input into the electrolyser system. Applying a cubic model, a theoretical power curve is used to simulate the wind power output $P_{w,r}$ [64], as seen in Eq. 15.

$$P_w = \begin{cases} 0, & \text{if } v_w < v_{w,min} \\ P_{w,r} \cdot \frac{v_w^3 - v_{w,min}^3}{v_{w,r}^3 - v_{w,min}^3}, & \text{if } v_{w,min} \leq v_w < v_{w,r} \\ P_{w,r}, & \text{if } v_{w,r} \leq v_w < v_{w,max} \\ 0, & \text{if } v_{w,max} < v_w \end{cases} \tag{15}$$

To avoid any significant wake effects that would negatively impact power generation, a distance between the turbines of seven times the rotor diameter is proposed in all directions [43]. The minimum distance of 2.1 km leads to a minimum OWF area of 176.4 km^2 with sides of 16.8 and 10.5 km, considering turbine placement in eight rows and five columns. It is further assumed that the wind speed differences due to these distances between the turbines can be modelled according to the Savitsky-Golay filter introduced in section 3.4.2.

Table 3: OWF specifications

Parameter			Ref
Turbines	n_w	40 pcs	
Rated power	$P_{w,r}$	25 MW	[63]
Hub height	H_w	210 m	[63]
Rotor diameter	d_w	300 m	[63]
Distance from shore	L_{shore}	50 km	
Distance between turbines	L_{turb}	7 d_w	[43]
Air density	ρ_{air}	1.21 kg/m^3	[63]
Cut-in wind speed	$v_{w,min}$	4 m/s	[63]
Rated wind speed	$v_{w,r}$	11.3 m/s	[63]
Cut-out wind speed	$v_{w,max}$	24 m/s	[63]

Electrolyser system

ALK and PEM electrolysers will be modelled and compared with specifications obtained from existing research as shown in Table 4. Neither SOEC or AEM electrolysers will be modelled due to their relative lack of technological maturity. A multi-stack design is assumed due to the large module size [15]. For the centralised configurations, the electrolyser module sizes are assumed as 25 MW, and the number of modules will thus vary depending on the total capacity. However, for the decentralised configuration, a constant amount of modules is required for each turbine to be connected to an individual electrolyser, and accordingly, the module size will depend on the total capacity.

In Table 4, the system energy values are assumed to be beginning-of-life (BOL) values and refer to the electrical efficiency of all necessary system components, such as stacks, electronics, gas separators and electrolyte tanks. They do, however, not include balance of plant [5][19]. The degradation of the electrolyser efficiency is modelled on a minute-by-minute basis based on obtained annual degradation rates [65]. A range of possible operating pressures has been observed, with the chosen values corresponding to state-of-the-art ALK and PEM systems [66].

Additionally, although higher load range percentages are proposed [34], a cut-off limit of 100% of the nominal load is set for load range values, considering an increased stack degradation rate when utilising higher loads [29]. The ramp-up of the electrolysers assumes a linear minute-by-minute increase from 0%, and the specified times indicate when 100% of the nominal electrolyser efficiency is reached.

The electrolyser systems are assumed to always be in hot standby mode during downtime, with a heat demand set to be due to area requirements. Considering 41 kW as the necessary heating demand of a 1 MW module [67], and that electrolyser modules scale as a cube, the corresponding heating demand for the 25 MW PEM or ALK module is determined. It is assumed that the modules used for the decentralised setup, irrespective of the module capacity, share the same area and thus, the same heating demand. For the offshore configurations, excess power is required to supply the backup power source to keep the electrolyser warm during downtime. In the onshore configurations, this requirement is not considered since it is assumed that this power can be supplied by the grid.

Table 4: Electrolyser specifications

Parameter		Unit	ALK	PEM	Ref
Maximum module size	$P_{el,mod}$	MW	25	25	[15]
System energy	E_{el} (η_{el})	kWh_e/kgH_2 (%)	49.0 (68)	50.5 (66)	[5]
Stack lifetime	LT_{el}	h	95 000	75 000	[5]
Degradation rate	DR_{el}	%/year	0.5	1	[65]
Operating pressure	p_{el}	bar	15	35	[66]
Operating temperature	T_{el}	K	353.15	353.15	[5]
Load range	$\psi_{el,min} - \psi_{el,max}$	%	10–100	0–100	[34]
Hot ramp-up	$t_{el,ramp}$	min	10	1	[68]
Hot standby power	$P_{el,mod,standby}$	MW	15.3	15.3	[67]

Power conversion and transmission

The main components of the power system between the wind power output and electrolyser are introduced in Table 5, together with their corresponding efficiencies or voltages. These values are used to simulate the power losses that occur outside of the electrolyser systems.

Table 5: Electric conversion and transmission specifications

Parameter			Ref
Inter-array transmission voltage	$V_{tm,ia}$	66 kV	[61]
Long-distance transmission voltage	V_{tm}	400 kV	[69]
AC step-up transformer efficiency	$\eta_{tf,AC}$	98%	[70]
DC buck converter efficiency	$\eta_{tf,DC}$	92%	[71]
Rectifier efficiency	$\eta_{rect,AC-DC}$	99.6%	[71]
LP filter efficiency	η_{LP}	99.9%	[71]
Inter-array AC transmission efficiency	$\eta_{tm,ia}$	99.45%	[61]
To-shore AC transmission efficiency (50km)	η_{tm}	98.86%	[72]

Water system

From the theoretical background, it can be concluded that the electrolyser has a great demand for water in terms of the electrolysis process as well as cooling systems. Thus, the components needed to fulfil this demand are defined in Table 6 below. The values are used to simulate energy and water demands. For the offshore cases, the water demands for the electrolysis process are obtained as an average value [15], corresponding to a requirement of 2.33 m^3 raw water to supply 1 m^3 ultrapure water. This falls in between the estimated demands for seawater and freshwater, which is assumed to be reasonable due to the brackish quality of the water in the Baltic Sea. In the onshore cases, a value of 1.5 m^3 freshwater is assumed to supply 1 m^3 of ultrapure water, corresponding to 13.5 l/kgH_2 [55]. The cooling is assumed to use pumped seawater to transfer heat from the electrolyser through a cooling medium in a closed circuit, considering that all electrolyser losses become excess heat that needs to be removed. The required mass flow of water ($\dot{m}_w$) to lead away the excess heat ($\dot{Q}_{heat}$) for each time step is determined according to Eq. 16.

$$\dot{m}_w = \frac{\dot{Q}_{heat}}{c_{p,w} \cdot \Delta T} \tag{16}$$

The specifications of the pipes for the pumped water correspond to glass reinforced plastic (GRP) pipe values. The required pipe diameters are calculated to fulfil velocity requirements for a maximum combined water flow ($\dot{V}_{max,\mathrm{H_2O}}$) of 60 000 m^3/h, according to Eq. 17.

$$d_{p,\mathrm{H_2O}} = 2 \cdot \sqrt{\frac{\dot{V}_{max,\mathrm{H_2O}}}{3600 \cdot \pi \cdot v_{max,\mathrm{H_2O}}}} \tag{17}$$

Pump heights and lengths are assumed values. The power requirements for the pumps (in W) are then estimated using Eq. 18.

$$P_{pump} = P_{pump,head} + P_{pump,friction} \tag{18}$$

where the vertical pump power ($P_{pump,head}$) is determined with Eq. 19, g being the gravitational constant at 9.81 m/s^2 and $\dot{V}_{\mathrm{H_2O}}$ being the nominal water flow in m^3/h.

$$P_{pump,head} = \frac{\rho_{\mathrm{H_2O}} \cdot g \cdot H_{pump} \cdot \dot{V}_{\mathrm{H_2O}}}{\eta_{pump}} \tag{19}$$

Using the Moody equation, the Darcy friction factors ($f_{p,\mathrm{H_2O}}$) are obtained using values from Table 6. Then, the pump power required to compensate for the pressure loss can be calculated according to Eq. 20.

$$P_{pump,friction} = \frac{L_{p,\mathrm{H_2O}} \cdot f_{p,\mathrm{H_2O}} \cdot \rho_{\mathrm{H_2O}} \cdot \dot{V}_{\mathrm{H_2O}}{}^3}{3600 \cdot \eta_{pump} \cdot 2D} \tag{20}$$

and thus, the pump energy demands can be simulated. However, this applies to the supply of cooling and electrolyser water towards the electrolyser, and no external cooling is considered for managing the heat losses from power conversion components.

Table 6: Water system specifications

Parameter		Unit	COFF	DOFF	CON	Ref
Electrolysis water demand	Q_{el}	l/kgH_2	21		13.5	[15] [55]
Desalination energy demand	E_{desal}	kWh$_e$/m^3H_2O	3.5		–	[34]
Density, H_2O	ρ_{H_2O}	kg/m^3	1000			
Dynamic viscosity, H_2O	μ_{H_2O}	Pa · s	$1.0 \cdot 10^{-3}$			
Specific heat, H_2O	c_{p,H_2O}	kJ/kgK	4.18			
Cooling medium temp diff	ΔT	K	5			[56]
Pump efficiency	η_{pump}	%	75			[73]
Pipe surface roughness	ε_{p,H_2O}	mm	0.02			[74]
Pipe max velocity	v_{max,H_2O}	m/s	5			[75]
Pump height	H_{pump}	m	25		20	
Pipe diameter	d_{p,H_2O}	m	2.06	0.325	2.06	
Pipe length	L_{p,H_2O}	m	100	10	200	
Friction factor	f_{p,H_2O}		0.0091	0.0122	0.0091	

Hydrogen system

The energy needed for the adiabatic compression of 1 kg of hydrogen gas is calculated for each time step as seen in Eq. 21 [18].

$$E_{comp} = \frac{286.76}{G_{H_2} \cdot \eta_{comp} \cdot 3.6 \cdot 10^6} T_{comp} \left(\frac{\kappa}{\kappa - 1}\right) \left[\left(\frac{p_{2,comp}}{p_{1,comp}}\right)^{\frac{\kappa-1}{\kappa}} - 1\right] \tag{21}$$

where E_{comp} is the required energy for the compressor (kWh/kgH_2); G_{H_2} the gas gravity of hydrogen, 0.0696, assuming ideal gas; η_{comp} the compressor efficiency; T_{comp} the mean temperature (K); κ the ratio ($\frac{c_p}{c_v}$) between the specific heat capacities; $p_{1,comp}$ and $p_{2,comp}$ the compressor inlet and outlet pressures (kPa) [18]. Assumptions include a suction temperature equal to the mean gas temperature of 285.15 K [58], a specific heat ratio of 1.4 [76], and a compressor efficiency of 50% due to load variations [18].

Further assumptions are required concerning the system components, as seen in Table 7. The required minimum pressure on the hydrogen out of the system boundaries is assumed as 24 bars [77], a condition that should be met at all times, although in a practical application, the desired pressure will depend on off-taker requirements. Similarly, the maximum velocity limit of 20 m/s should never be exceeded, corresponding to a 30 cm minimum pipe diameter for the chosen capacity and distance [78]. The required compressor outlet pressures for the offshore configurations will consider the pressure losses through the pipeline that are obtained for each time step using Eq. 22 [79].

$$\dot{V}_{H_2}(T,p) = \frac{1.1494}{24} \cdot 10^{-3} \left(\frac{T}{p}\right) \cdot 2\sqrt{\frac{d^5_{p,H_2}(p^2_{1,p} - p^2_{2,p})}{Z \cdot T_{p,H_2} \cdot G_{H_2} \cdot L_{shore} \cdot \lambda}} \tag{22}$$

where $\dot{V}_{H_2}$ is the flowrate (m^3/h) at standard conditions (T = 288.15 K, p = 1 bar); d the inner diameter (m) of the pipe; $p_{1,p}$ and $p_{2,p}$ the inlet and outlet pressures (kPa) in the pipeline; L_{shore} the pipeline length (km); λ the friction coefficient [34], obtained as 0.0207; and Z the compressibility factor, 1 [80].

Table 7: Hydrogen system specifications

Parameter			Ref
Compressor suction temperature	T_{comp}	285.15 K	
Compressor specific heat ratio	κ_{comp}	1.4	[76]
Compressor efficiency	η_{comp}	50%	[18]
Pipeline diameter	d_{p,H_2}	40 cm	[77]
Pipeline surface roughness	ε_{p,H_2}	0.5 mm	[18][78]
Pipeline max velocity	v_{max,H_2}	20 m/s	[78]
Pipeline mean temperature	T_{p,H_2}	285.15 K	[58]
Minimum outlet H_2 pressure	$p_{2,p_{min}}$	24 bar	[77]

3.5.3 Techno-economic assessment

The assumed costs for each of the key components can be divided into capital expenditures (CAPEX) and operating expenditures (OPEX) and are illustrated in Table 8 and Table 9 below. Non-euro costs are based on currency conversion rates of 1\$ = 0.92€ and 1£ = 1.15€ (as of 12.05.2023). Additionally, apart from the electrolysers, all components are assumed to last throughout the project lifetime, and any necessary replacements fall into the OPEX category. CAPEX occur at the start of the project, while OPEX require annual payments using an assumed real discount rate of 2.9%, a rate considered for a future offshore energy project with a similar size [81]. 2030 is the base year considered for economic calculations.

No real-world data have been observed for wind turbines or their required substructures of this size, so the values are assumed to be linearly scaled based on estimations of costs for 15 MW wind turbines [81]. For the decentralised setup, the transition piece is assumed to cost twice as much due to the increased space requirements for the placement of electrolyser systems.

The inter-array cable costs are adapted to the turbine placement of the report, assuming a total inter-array length of 100.8 km, considering eight rows of dynamic cables with lengths of 10.5 km each connected to one with a length of 16.8 km. Similarly, the costs (in €/km) of the inter-array pipelines are unknown but assumed as half of those of the main pipeline transporting the hydrogen to shore.

Apart from the electrolyser stacks, the electrolyser system cost includes BOP components as well as all required PSU components and electronics for a 1 GW plant. Other direct costs, such as civil, structural and architectural costs, are included, as are the costs for utilities and process automation. Further, indirect costs and owners' costs are included together with contingency [27]. Although electrolyser costs are likely to decrease in the future, the rapid increase in electrolyser demand together with production and supply chain limitations, make significant price decreases unlikely until 2030 [29]. Future stack replacement costs are unknown but assumed to be half of the current replacement costs on average due to the stacks being replaced far beyond 2030. Additionally, the electrolyser systems, stack replacements and desalination units are subjected to increased costs when placed offshore, where the base cost is multiplied by an offshore cost factor [34].

Table 8: CAPEX overview per configuration

Component	DOFF-P	COFF-P	CON-P	CON-A	Ref
System (total cost)					
Wind turbines	933.3 M€	933.3 M€	933.3 M€	933.3 M€	[81]
Turbine substructures	666.7 M€	666.7 M€	666.7 M€	666.7 M€	[81]
Wind project development	100 M€	100 M€	100 M€	100 M€	[81]
Larger transition piece	100 M€	–	–	–	[82]
Inter-array cables	–	22.4 M€	22.4 M€	22.4 M€	[81]
Subsea HVAC cables	–	–	92 M€	92 M€	[22]
Offshore substation	–	–	74.8 M€	74.8 M€	[82]
Offshore substation platform	–	–	69 M€	69 M€	[78]
Onshore substation	–	–	34.5 M€	34.5 M€	[82]
Inter-array H_2 pipeline	44.2 M€	–	–	–	[22]
Subsea H_2 pipeline	44.2 M€	44.2 M€	–	–	[22]
H_2 compressor	–	–	–	9.3 M€	[83]
Electrolyser (cost per kW installed)					
Electrolyser system	1 800 €/kW	1 800 €/kW	1 800 €/kW	1 400 €/kW	[27]
Stack replacement	145.8 €/kW	145.8 €/kW	145.8 €/kW	45.5 €/kW	[27][84]
Desalination unit	3.6 €/kW	3.6 €/kW	–	–	[83]
Offshore cost factor	1.33	1.33	–	–	[34]
Offshore electrolyser platform	–	300 €/kW	–	–	[83]
Onshore electrolyser facility	–	–	60 €/kW	78 €/kW	[27]

The OPEX costs of the wind farm are estimated assuming an average wave height lower than 1.4 m [81]. Meanwhile, for the submarine cables, for both the inter-array and transmission to shore, these costs correspond to 0.5% of their CAPEX per year [22]. Similarly, the costs of the operation and maintenance of the substations are assumed to be the same, in percentage of their respective CAPEX. Additionally, the OPEX of the H_2 pipelines refer to the estimated costs of 2% of its CAPEX, while for the compressor, 4% of CAPEX is expected [34].

For the electrolyser system, the OPEX costs correspond to 2% of CAPEX [30], whereas for the desalination unit, 0.5% of CAPEX is assumed. For the offshore configurations, these values are multiplied by a cost factor reflecting the higher costs of offshore operation and maintenance [34]. Further, it is assumed that potential costs for freshwater and the operation and maintenance of facilities are negligible.

Table 9: OPEX overview per configuration

Component	DOFF-P	COFF-P	CON-P	CON-A	Ref
System (annual cost)					
Wind farm	45.3 M€	45.3 M€	45.3 M€	45.3 M€	[81]
Inter-array cables	–	0.11 M€	0.11 M€	0.11 M€	[22]
Subsea HVAC cables	–	–	0.46 M€	0.46 M€	[22]
Offshore substation	–	–	3.74 M€	3.74 M€	
Onshore substation	–	–	1.73 M€	1.73 M€	
Inter-array H_2 pipeline	0.88 M€		–	–	[34]
Subsea H_2 pipeline	0.88 M€	0.88 M€	–	–	[34]
H_2 compressor	–	–	–	0.37 M€	[34]
Electrolyser (annual cost per kW installed)					
Electrolyser system	36 €/kW	36 €/kW	36 €/kW	36 €/kW	[30]
Desalination unit	0.018 €/kW	0.018 €/kW	–	–	[34]
Offshore cost factor	1.41	1.41	–	–	[34]

3.6 Limitations

By only evaluating setups with dedicated hydrogen production, the potential for the co-generation of hydrogen and electricity will not be investigated. Depending on the off-taker, this could be a preferred solution. However, this report does not consider a specific off-taker and instead aims to gain more general conclusions. Additionally, for some of the parameters, no projected values for 2030 are found. In those cases, currently available values are chosen, likely resulting in more conservative estimates when considering projects planned for the future.

Due to the large scope of the study, only the most important components of the system are considered in-depth, but it is acknowledged that many other components are vital for the performance of the studied systems. The pipeline itself is considered the only hydrogen buffer, whereas additional buffer in the form of hydrogen tanks could help limit transmission fluctuations. Similarly, apart from designing the system for enough excess electricity, not much detail is put into sizing and modelling the required backup power source. The costs required for these components might differ between the cases but are not investigated further in this report. Similarly, the material and construction of the offshore platforms are not studied in detail.

Due to the lack of available minute-by-minute wind data, interpolations of hourly wind data have been used as input. However, the interpolation of these values results in fewer fluctuations than if higher resolution data was used. Such fluctuations are likely to favour the more flexible PEM systems. Similarly, the study lacks an empirical way of obtaining the impact of wind speed differences between the turbines on the power generation dynamics. This adds additional uncertainties to the wind power output and subsequent comparisons between decentralised and centralised configurations. The general lack of empirical data for similar projects considering system configurations, scale and location, combined with a shortage of experimental opportunities, further limits the possibilities for the ideal evaluation and validation of the models.

4
Results

Here, the main findings from the investigation are synthesised and presented in detail, serving as a basis for the following interpretations and discussion. Key results from the sizing optimisations and model simulations, techno-economic assessments and qualitative literature review will be introduced.

4.1 Modelling

In this section, the key results obtained from the simulations of the Simulink models are presented in 1-year and 30-year graphs and values. The x tick labels in the graphs where x represents time indicate the start of each month or year respectively. The estimated minute-by-minute wind speeds are illustrated in Figure 8. A peak wind speed of 26.48 m/s and a minimum wind speed of 1.74 m/s is observed, with a mean wind speed of 8.95 m/s.

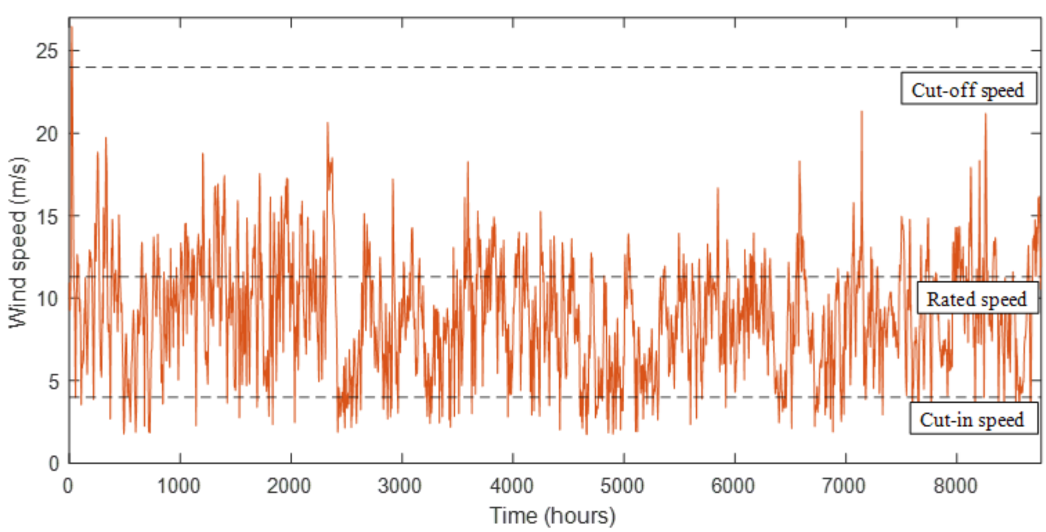

Figure 8: Annual wind speed at project site

The combined, smoothed-out power output from the OWF for any year is visualised in Figure 9. The output ranges between 0 and 1000 MW, with a mean value of 506.5 MW. Over the 30-year project period, an estimated total of 133.1 TWh (4.44 TWh/year) of electricity is generated, with a capacity factor of 50.6%.

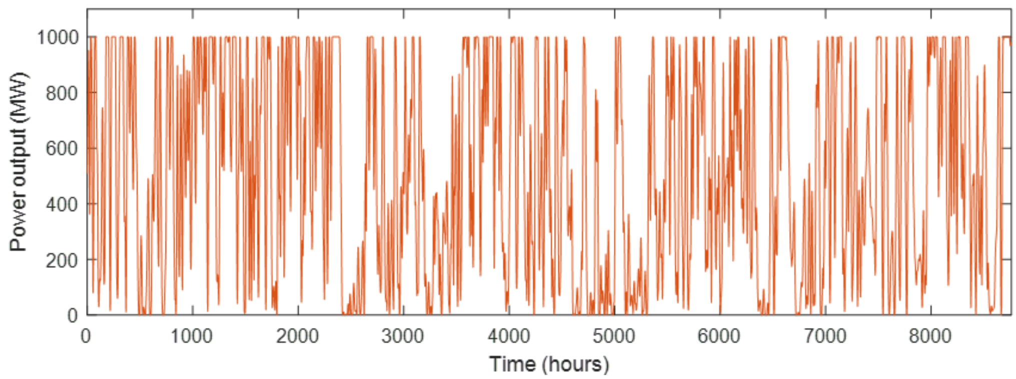

Figure 9: Annual OWF power output

The wind power coefficient is a measure of how much of the wind's energy is converted to electricity and is obtained by dividing the power output by the wind energy potential $c_p = \frac{P}{\frac{1}{2}\rho A V^3}$ with a theoretical maximum of 0.593, the Betz limit. In Figure 10, the minute-by-minute wind power coefficients are illustrated for any year during the project lifetime. The values range between 0 and 0.405, with a mean value of 0.298.

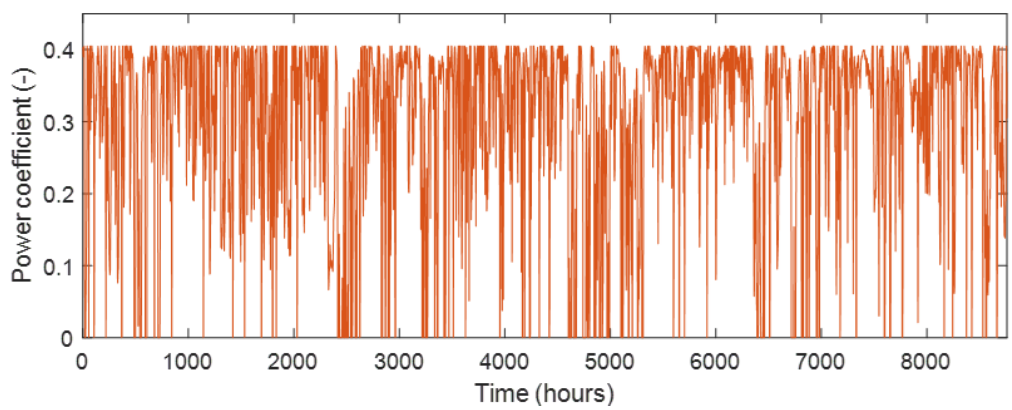

Figure 10: Annual wind turbine power coefficient

4.1.1 Centralised offshore – PEM (COFF-P)

The cost-optimal electrolyser capacity and key simulation results for the centralised offshore case, using offshore PEM electrolyser systems, are presented below.

Electrolyser power and sizing

As for the OWF power output, the quantity and distribution of power available to the electrolyser remain constant for all years during the project lifetime. The differences between the OWF output and the available supply are due to power conversion losses, auxiliary power demands, excess generation as well as transmission losses within the inter-array grid. Figure 11 illustrates the load duration curve of the supplied electricity, with a peak available power at 904.3 MW. The dashed line marks the installed capacity, indicating that during periods of larger input power, there will be excess electricity.

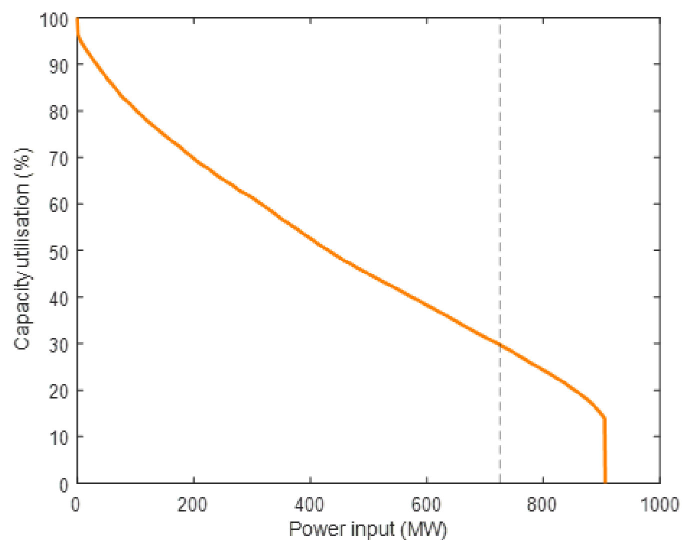

Figure 11: Electrolyser load duration (COFF-P)

Using the obtained curve, the cost-optimal capacity is calculated as 725 MW, as shown in Figure 12. Thus, the electrolyser system on the offshore platform contains 29 modules at 25 MW each, with a mean total power input of 417.3 MW, amounting to a total 30-year electricity input of 109.7 TWh. It should be noted that the relevant insights are drawn from the shape of the curve and not the values of the levelised costs themselves, as they are merely preliminary assessments. This consideration applies to all studied configurations.

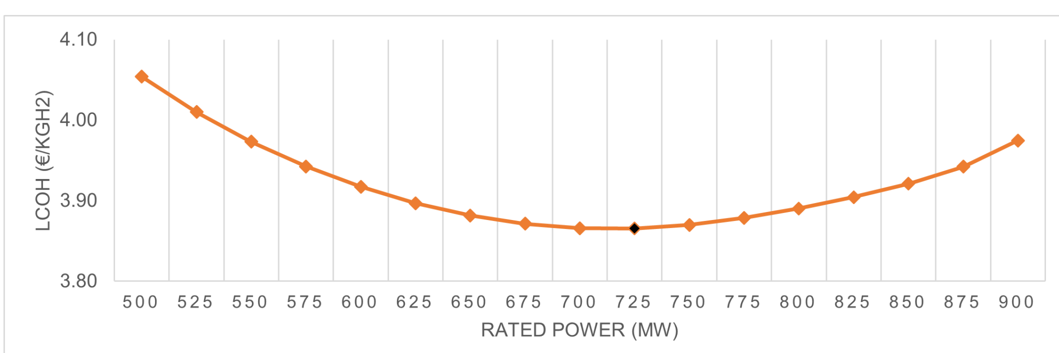

Figure 12: Electrolyser capacity optimisation (COFF-P)

Water demand

The water demands are divided into (i) seawater for electrolyser cooling and (ii) purified freshwater for the electrolysis process. There is a significantly larger need for cooling water to cover the considerable heat losses from the electrolyser. Further, an increase in cooling water demand through time can be observed as electrolyser stacks degrade, leading to increased heat losses. On the other hand, the degradation of the electrolyser decreases the water demand for the electrolysis process.

On a 30-year basis, the cooling water demand reaches a maximum of 49 470 m^3/h with a mean demand of 26 388 m^3/h, indicating a total required seawater volume of 6 935 Mm^3. Meanwhile, the electrolyser's demand for purified freshwater peaks at 302 m^3/h with a mean demand of 166 m^3/h, reaching a total volume of 43.7 Mm^3. Since a desalination unit is used to provide purified water for the offshore electrolyser, a higher-concentration brine will be produced as a by-product.

Hydrogen production

The hydrogen produced and subsequently transmitted to an off-taker fulfils the set outlet conditions with a minimum output pressure of 30.9 bar and a max pipeline velocity of 10.9 m/s. The mass output of hydrogen is shown to peak at 239.3 kg/min (2 664 Nm^3/min) with a mean production of 132.1 kg/min (1 471 Nm^3/min). Figure 13 illustrates the 30-year distribution of H_2 production amounts. It is estimated that in total, 2.08 Mton of H_2 would be produced, corresponding to a normal volume of 23.2 billion Nm^3 and an energy content of 69.4 TWh.

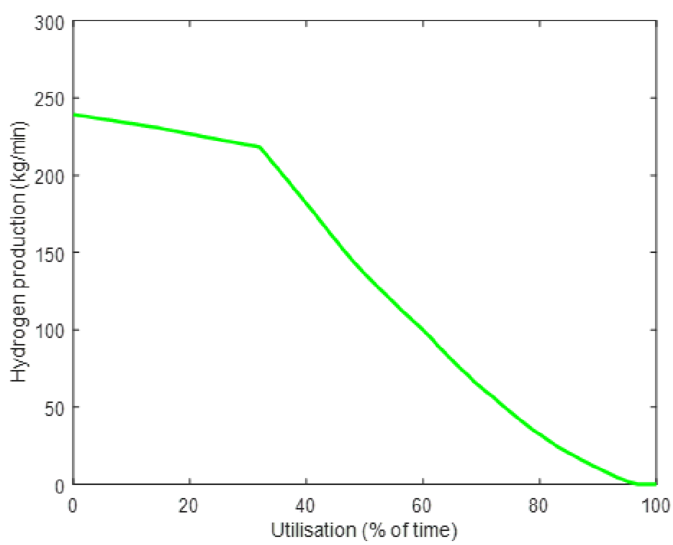

Figure 13: Distribution of H_2 production (COFF-P)

Energy losses

For the centralised offshore setup, the cooling and desalination units are two of the auxiliary systems that require input power. Due to the PEM electrolyser being pressurised, with a transmission pressure drop that is not large enough to fail the outlet requirements, no external compression is needed. The power demand for the cooling water pumps is significantly greater than for the desalination through the 30-year period. However, mostly due to the efficiency degradation of the electrolyser stacks, the exact values vary between the years. The cooling pump power demand reaches a peak of 5.30 MW with a 30-year mean of 2.66 MW, amounting to a total electricity demand of 698.3 GWh. Meanwhile, the power demand for desalination has a peak of 0.452 MW with a mean of 0.250 MW, adding up to a 30-year demand of 65.6 GWh.

Further, the inter-array power transmission that connects the wind turbines with the offshore platform sees energy losses of 732.0 GWh in total, while the conversion losses in the PSU amount to 11 133.7 GWh. The electrolyser losses reach a total of 40 260.1 GWh, indicating an average cooling duty of 153.2 MW. The excess electricity fulfils the requirements of exceeding the hot standby energy demands so that a backup power source, in theory, could fulfil the heating requirements of the electrolyser when in hot standby mode. Over the project lifetime, an excess of 10 707.6 GWh remains after supplying the standby energy demand of 93.1 GWh. Figure 14 illustrates the energy flows of the system, shown as percentages of the total energy input.

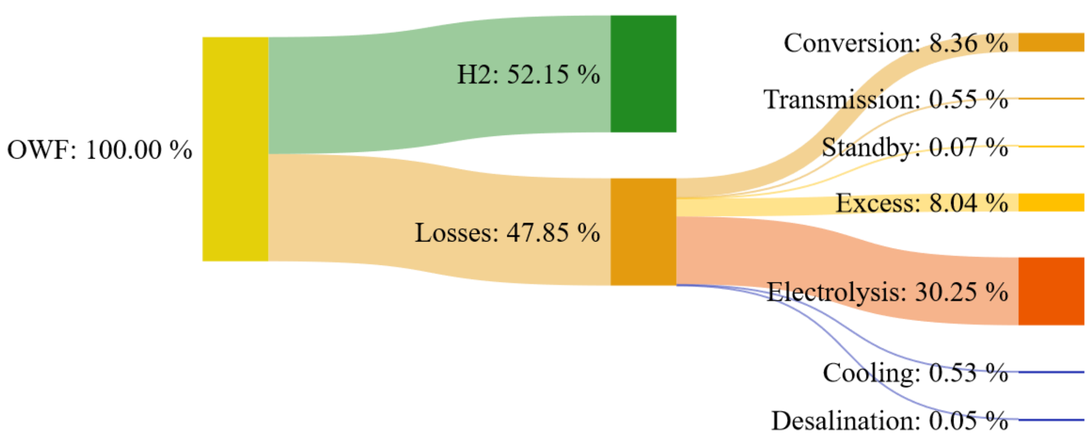

Figure 14: System energy flows (COFF-P)

Efficiencies

In Figure 15, the electrolyser efficiency and its degradation can be observed, together with temporary dips during periods of downtime or ramp-up, as well as stack replacements. The maximum lifetime efficiency equals the BOL electrolyser efficiency, 66%, while an end-of-life (EOL) efficiency cap is reached at 60.17 %. The PEM electrolyser stacks require replacement three times, at intervals of 8.8 years. A total downtime of 8 335 hours is observed, corresponding to 3.17% of the total hours. These values are directly applicable to the other PEM typologies, in sections 4.1.2 and 4.1.3.

The full system efficiency is defined as the total LHV of the hydrogen output of the system divided by the total power output from the OWF. After 30 years, the full system efficiency converges to a value of 52.15%.

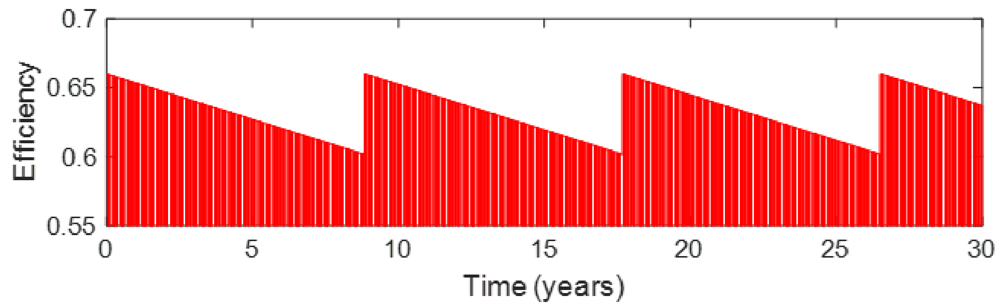

Figure 15: PEM efficiency

4.1.2 Decentralised offshore – PEM (DOFF-P)

The cost-optimal electrolyser capacity and key simulation results for the decentralised offshore case, using distributed offshore PEM electrolyser modules, are presented below.

Electrolyser power and sizing

Contrary to the centralised setup, the decentralised setup is assumed to have an electrolyser module connected to each turbine, where instead of varying the number of modules, the size of the modules is adapted. Figure 16 shows the load duration of the electricity supplied to the electrolyser, with available power reaching its high at 907.8 MW. The dashed line displays the installed capacity and input power cut-off limit.

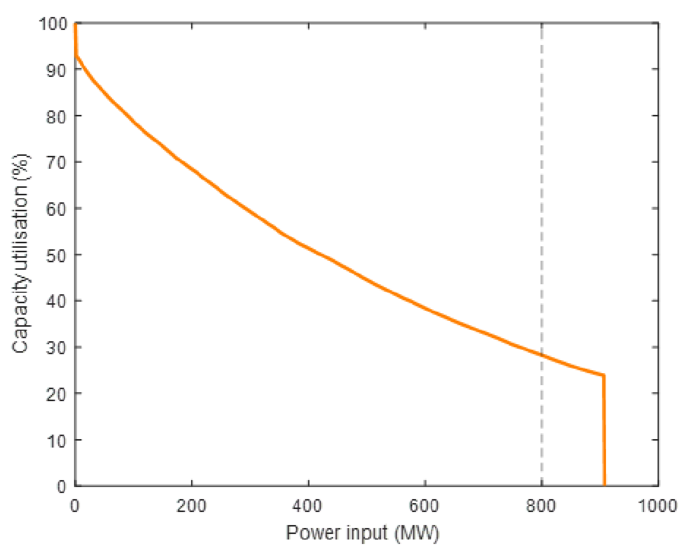

Figure 16: Electrolyser load duration (DOFF-P)

For this case, the cost-optimal combined electrolyser capacity is 800 MW, as demonstrated in Figure 17. This result indicates a module size of 21.25 MW connected to each of the 40 turbines, with a 30-year mean power of 433.3 MW and a total energy input to the combined electrolyser systems of 113.9 TWh.

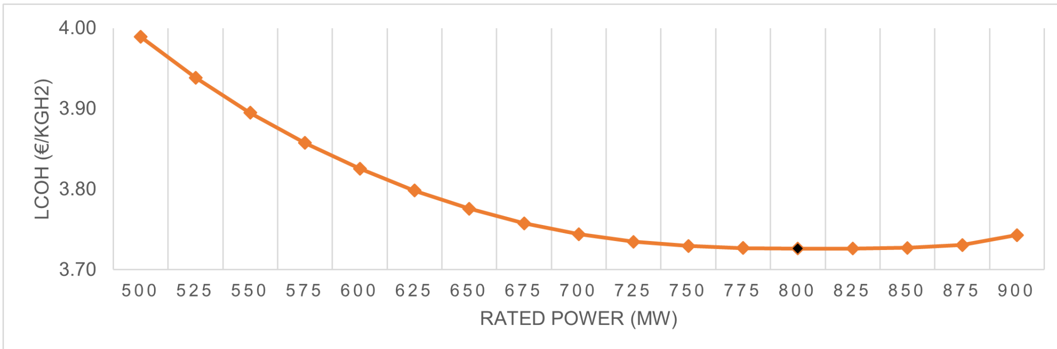

Figure 17: Electrolyser capacity optimisation (DOFF-P)

Water demand

As in the centralised offshore case, seawater is required for electrolyser cooling, while purified freshwater is needed for the electrolysis process. Similar trends are observed concerning their year-to-year changes and demand distributions.

Throughout the project lifetime, the cooling water demand reaches a maximum of 54 888 m^3/h with a mean demand of 27 402 m^3/h, adding up to a total seawater volume of 7 201 Mm^3. The electrolysis water demand peaks at 333 m^3/h with a mean demand of 173 m^3/h, reaching a 30-year demand of 45.4 Mm^3. The desalination process will produce brine as a by-product.

Hydrogen production

The generated H_2 fulfils the transmission conditions with a minimum output pressure of 29.9 bar and a max pipeline inlet velocity of 12.1 m/s. The mass output of hydrogen peaks at 264.0 kg/min (2 940 Nm^3/min) and has a 30-year mean production of 137.1 kg/min (1 527 Nm^3/min), with the full production distribution being demonstrated in Figure 18. During the project lifetime, it is estimated that 2.16 Mton of H_2 is produced, corresponding to a 24.1 billion Nm^3 normal volume and a total LHV content of 72.1 TWh.

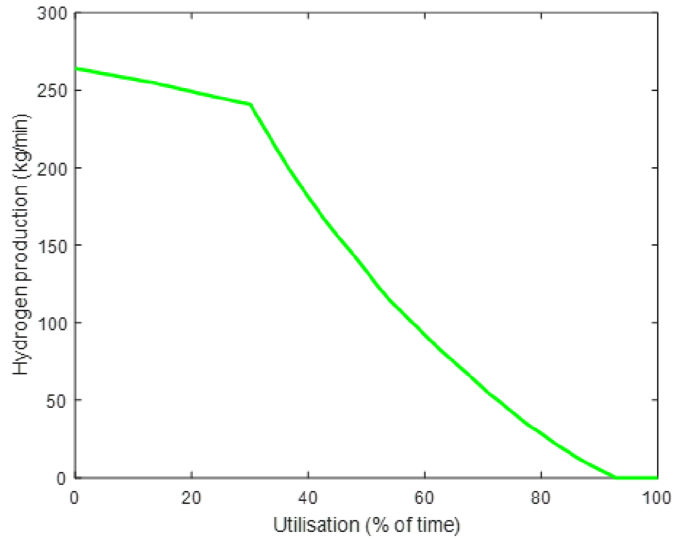

Figure 18: Distribution of H_2 production (DOFF-P)

Energy losses

Since no power transmission is involved in this setup, no significant transmission losses occur. However, the electrical conversions in the PSU provide losses of 11 198.8 GWh during the project lifetime. Similarly, energy losses from the electrolysis amount to 41 808.5 GWh, corresponding to an average cooling duty of 159.1 MW.

The cooling and desalination units are the two auxiliary systems that require input power during electrolyser uptime. Due to the PEM electrolyser having a higher output pressure than the required transmission pressure, with a small enough pressure drop in the to-shore pipeline, no external compression is needed. The cooling pump power demand has a peak of 4.99 MW with a 30-year mean of 2.49 MW, reaching a total electricity input of 654.1 GWh. The power demand for desalination reaches a peak of 0.499 MW with a mean of 0.259 MW, adding up to a demand of 68.1 GWh during the project lifetime.

As for the decentralised offshore case, the excess electricity should for the same reasons exceed the standby energy demands. Over the project lifetime, an excess of 7 209.2 GWh remains after supplying the 102.7 GWh required for keeping the electrolyser warm. Figure 19 gives an overview of the simulated energy flows and losses within the system, shown in percentages.

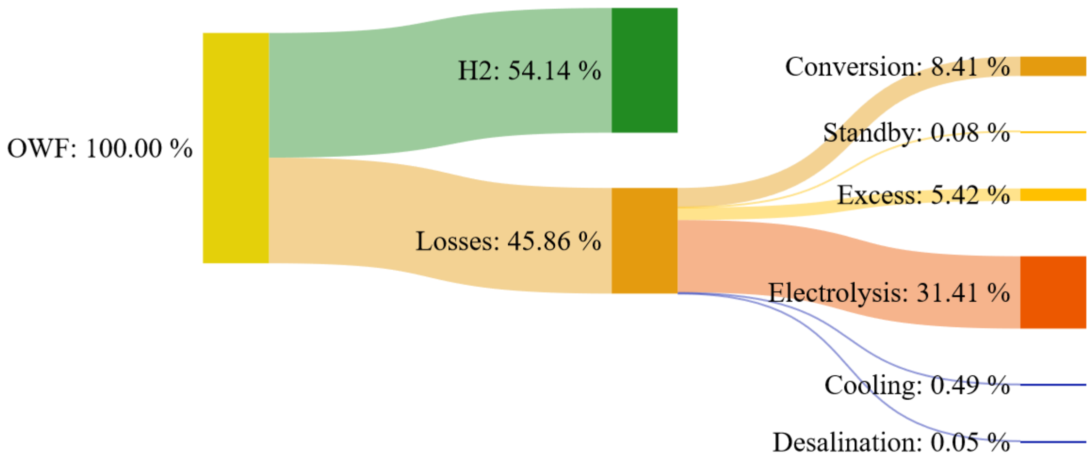

Figure 19: System energy flows (DOFF-P)

Efficiencies

As mentioned, the PEM efficiency follows the same pattern as in section 4.1.1. However, the full system efficiency converges to a value of 54.14% at the end of the 30 years.

4.1.3 Centralised onshore – PEM (CON-P)

This section presents the cost-optimal electrolyser capacity and key simulation results for the centralised onshore case, using a system of PEM electrolyser modules.

Electrolyser power and sizing

Figure 20 demonstrates the load duration of available input power with a peak at 871.4 MW supplied towards the onshore electrolyser system, with the cost-optimal size of the electrolyser system determined as 800 MW marked with a dashed line.

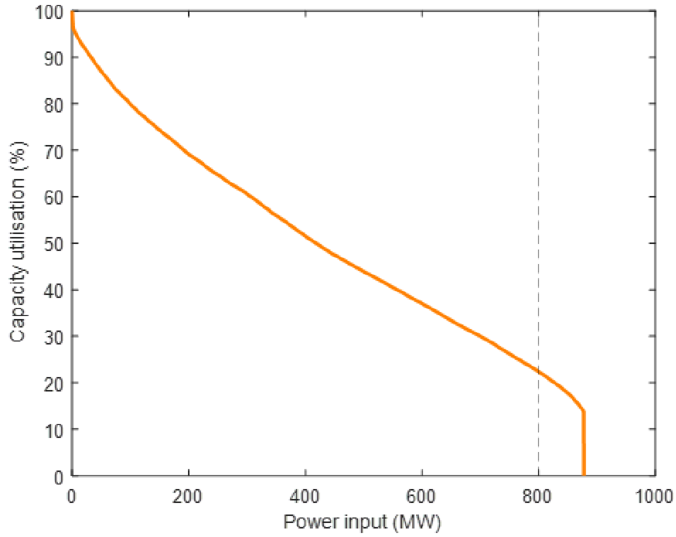

Figure 20: Electrolyser load duration (CON-P)

The cost-optimization indicates an installation of an 800 MW electrolyser system, as seen in Figure 21, divided into 32 modules of 25 MW each. From this, the 30-year mean power input is obtained as 430.0 MW, giving a total energy input of 113.0 TWh to the onshore electrolyser system. The relevant results are obtained values for the LCOH.

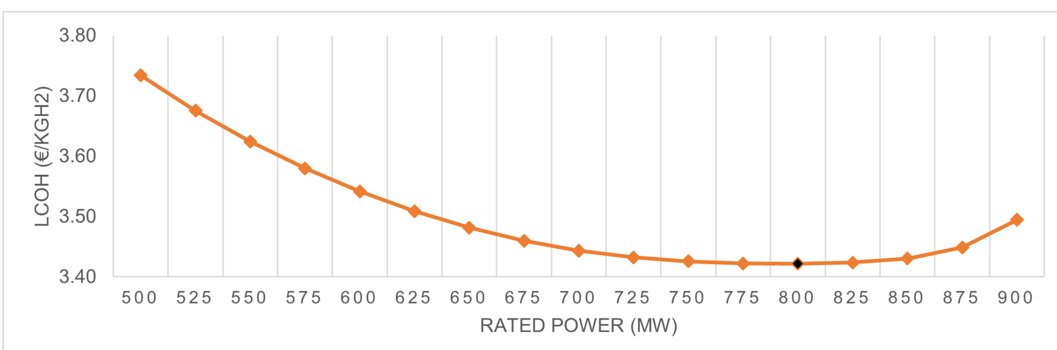

Figure 21: Electrolyser capacity optimisation (CON-P)

Water demand

In the onshore cases, seawater is used only for cooling, while a freshwater supply is assumed to fulfil the electrolysis water demands. Considering the 30-year lifetime, the cooling water demand peaks at 54 888 m^3/h with a mean of 27 192 m^3/h, adding up to a total volume of 7 146 Mm^3. Meanwhile, the electrolyser water usage is lower than for the offshore cases due to the use of freshwater as a resource. The flow peaks at 214 m^3/h with a mean of 110 m^3/h, amounting to a 29.0 Mm^3 total freshwater demand.

Hydrogen production

The hydrogen produced and transmitted fulfils the conditions with an electrolyser output pressure of 35 bar and a max inlet transmission velocity of 12.1 m/s. The H_2 generation reaches a high at 264.0 kg/min (2 940 Nm^3/min) with a mean production of 136.1 kg/min (1 516 Nm^3/min), with a lifetime distribution as shown in Figure 22. The total production adds up to 2.15 Mton, equalling a normal volume of 23.9 billion Nm^3 and a LHV energy content of 71.9 TWh.

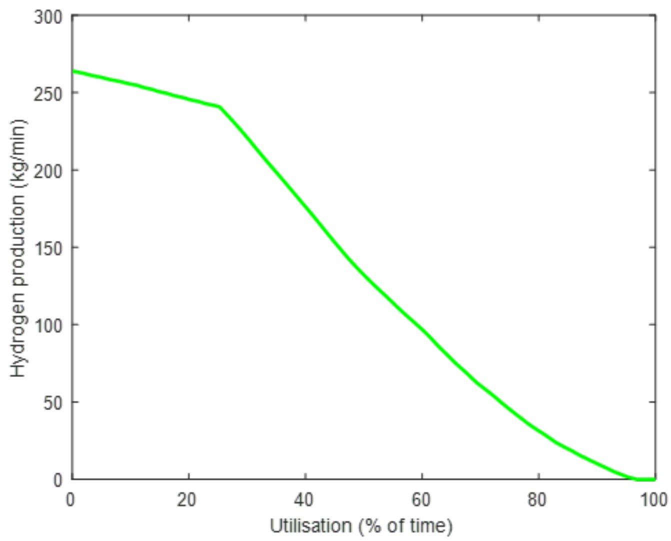

Figure 22: Distribution of H_2 production (CON-P)

Energy losses

For the onshore cases, power transmission losses will be significantly larger due to the need for both inter-array and to-shore transmission. During the project lifetime, these losses add up to 4 858.5 GWh. Meanwhile, the PSU conversion losses and the energy losses from the electrolysis are determined as 10 791.6 GWh and 41 482.4 GWh, respectively. The electrolyser losses indicate an average cooling duty of 157.8 MW. No external compression is needed due to the use of pressurised PEM electrolysers where the output pressure is greater than the required minimum transmission pressure. Additionally, no desalination is included, although there is still a need to pump the water to the electrolyser system. This is instead included as a minor part of the cooling power demand, which reaches a peak at 6.10 MW with a mean of 2.60 MW, adding up to a 30-year total of 682.5 GWh.

For the onshore cases, excess electricity is not considered vital for the supply of standby power to the electrolyser during downtime. However, throughout the project lifetime, 3 664.1 GWh of excess power remain after supplying the 102.7 GWh necessary to keep the electrolyser system on hot standby. In Figure 23, the system energy flows are presented.

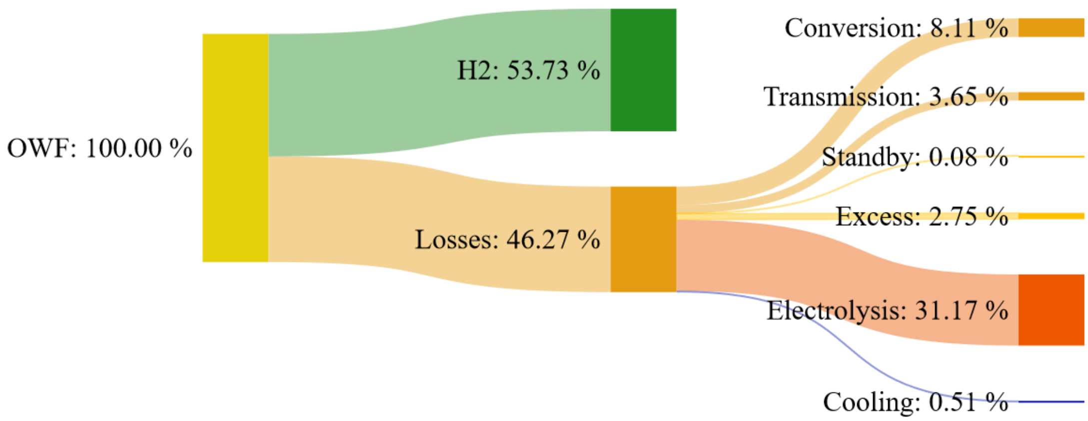

Figure 23: System energy flows (CON-P)

Efficiencies

The electrolyser efficiency follows the same patterns as the previous cases. Meanwhile, the full system efficiency after 30 years is determined as 53.73%.

4.1.4 Centralised onshore – ALK (CON-A)

This section presents additional results for the centralised onshore case, though instead using a system of ALK electrolyser modules.

Electrolyser power and sizing

The load duration of maximum power supplied to the electrolyser system is shown in Figure 24, together with the peak combined available power at 877 MW. The cost-optimal size of the electrolyser system, 825 MW, is marked with a dashed line.

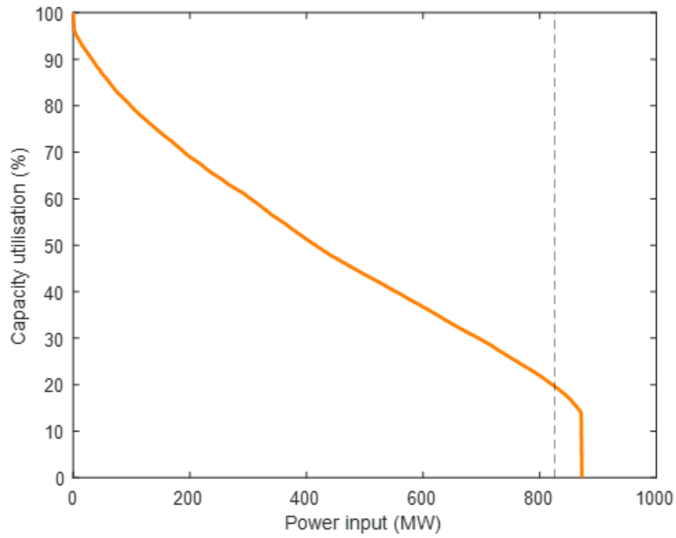

Figure 24: Electrolyser load duration (CON-A)

Based on Figure 25, the cost-optimisation results suggest the installation of an electrolyser system with an 825 MW capacity. This system is divided into 33 modules, each with a capacity of 25 MW. Meanwhile, the mean power input is determined to be 433.6 MW, resulting in a total energy input of 114.0 TWh to the onshore electrolyser system.

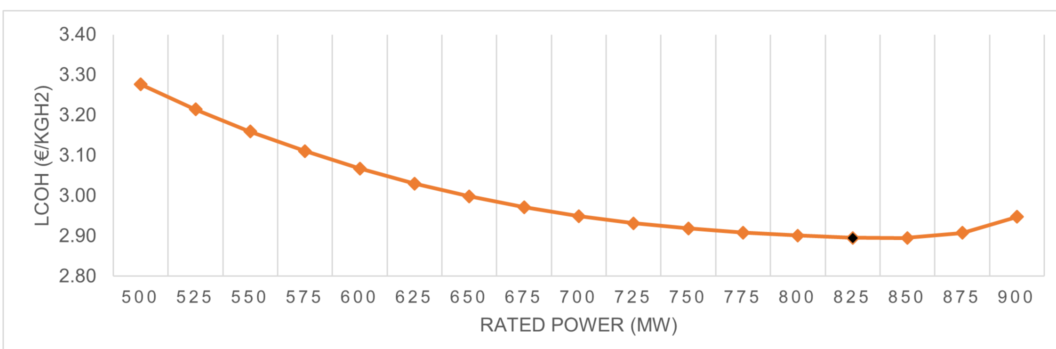

Figure 25: Electrolyser capacity optimisation (CON-A)

Water demand

The demand for cooling water peaks at 51 756 m^3/h with a mean of 25 902 m^3/h, amounting to a total of 6 807 Mm^3. As in the other onshore case, the electrolyser water requirement is fulfilled by a freshwater supply, with a maximum at 227 m^3/h and a mean flow of 115 m^3/h, leading to a total freshwater volume of 30.2 Mm^3.

Hydrogen production

The hydrogen transmission fulfils the set requirements with a compressor output pressure of 24 bar and a max pipeline velocity of 18.6 m/s. The requirements are met by the installation of a compressor to increase the pressure from 15 to 24 bar following the H_2 production due to the lower output pressures of the ALK system. The production reaches a peak at 280.5 kg/min (3 124 Nm^3/min) and has a mean at 141.6 kg/min (1 577 Nm^3/min), with a 30-year distribution as shown in Figure 26. The shutdown of H_2 production during loads below 10% does not impact the peak productions but has a limiting effect on the total production, which during the project lifetime adds up to 2.23 Mton, corresponding to 24.9 billion Nm^3 and 74.4 TWh.

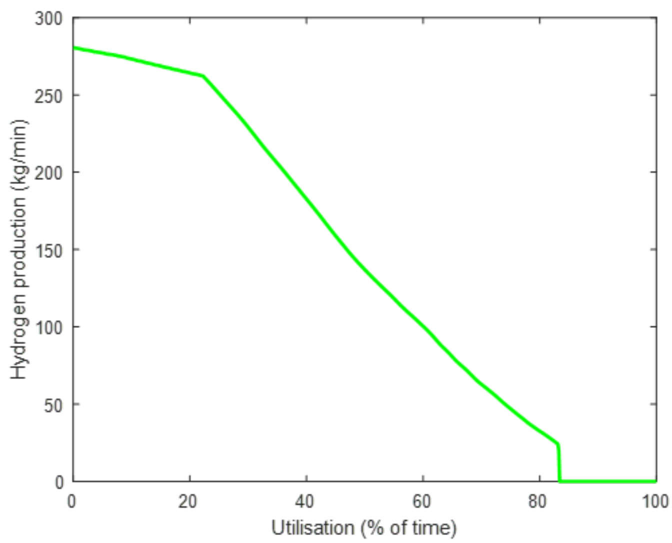

Figure 26: Distribution of H_2 production (CON-A)

Energy losses

The power transmission losses are the same as for the onshore PEM case, with a total of 4 858.5 GWh. The PSU conversion losses add up to 10 725.6 GWh, while the electrolyser energy losses reach a total of 39 519.8 GWh. An average cooling duty of 150.4 MW is determined. Like in the onshore PEM case, no desalination is needed. However, compression is necessary to raise the electrolyser output pressures to the required transmission pressures. Considering these pressures, the power required for the compressor peaks at 6.26 MW with a mean of 3.16 MW, adding up to a total of 831.0 GWh over the 30 years. The cooling power demand has a maximum of 5.54 MW with a mean of 2.40 MW, totalling 630.7 GWh.

105.9 GWh is required to support the standby power demands of the electrolyser system, and an excess of 1 995.2 GWh remains unused. Figure 27 gives a full overview of the energy flows used in the simulations, illustrated in percentages.

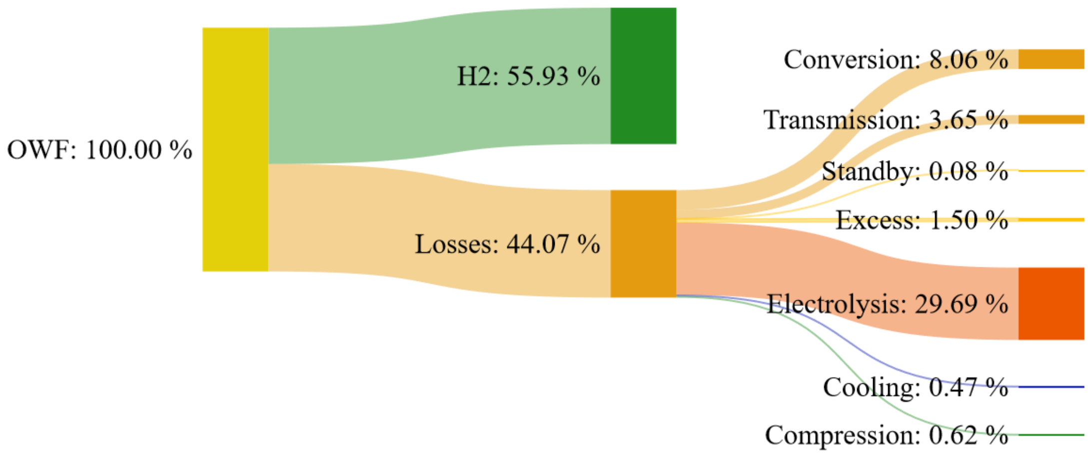

Figure 27: System energy flows (CON-A)

Efficiencies

Figure 28 shows the electrolyser efficiency and its degradation, along with dips during periods of downtime or ramp-up. The downtime adds up to 45 304 hours, totalling 17.24% of all hours, due to the minimum load limit. Additionally, the ramp-up period is longer than for the PEM electrolyser, further limiting the hours of running at high capacity. However, the electrolyser efficiency surpasses that of PEM, with maximum efficiency at 68%, and an end-of-life (EOL) efficiency at 63.58%. The ALK electrolyser is replaced two times, at intervals of 13.0 years. Further, the full system efficiency converges to a value of 55.93% after 30 years.

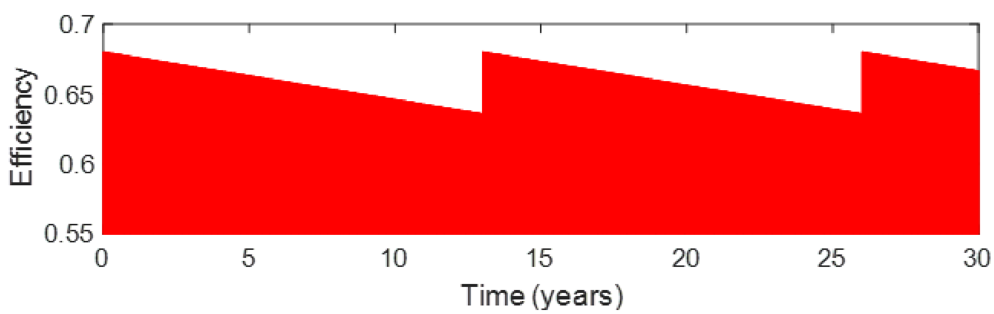

Figure 28: ALK efficiency

4.1.5 Comparison of simulation results

Table 10 below compares some of the key results obtained from the cost optimisations and model simulations. All results refer to a 30-year period.

Table 10: Key technical results

	Unit	COFF-P	DOFF-P	CON-P	CON-A
Electrolyser capacity	MW	725	800	800	825
H_2 production	Mton	2.08	2.16	2.15	2.23
Full system efficiency	–	52.15%	54.14%	53.74%	55.93%
Electrolyser input	TWh	109.7	113.9	113.0	114.0
Average cooling duty	MW	153.2	164.1	157.8	150.4
Electrolyser replacements	–	3	3	3	2
Downtime	–	3.17%	3.17%	3.17%	17.24%

Table 11 below compares the energy losses obtained from the simulations, considering the full project lifetime.

Table 11: System energy losses (in GWh)

	COFF-P	DOFF-P	CON-P	CON-A
Power transmission	732	–	4 859	4 859
PSU	11 134	11 199	10 792	10 725
Hot standby	93	103	103	106
Excess	10 707	7 209	3 664	1 995
Electrolysis	40 260	41 808	41 482	39 520
Cooling pump	698	654	682	631
Desalination	66	68	–	–
Compression	–	–	–	831
Total	63 690	61 041	61 582	58 667

4.2 Techno-economic assessment

By applying the economic assumptions and the simulation results, the LCOH for the different configurations are obtained by dividing the total discounted costs by the discounted H_2 production. Figure 29 shows a comparison of the levelised costs, further divided into costs for (i) the electrolyser system and (ii) all adjacent system components.

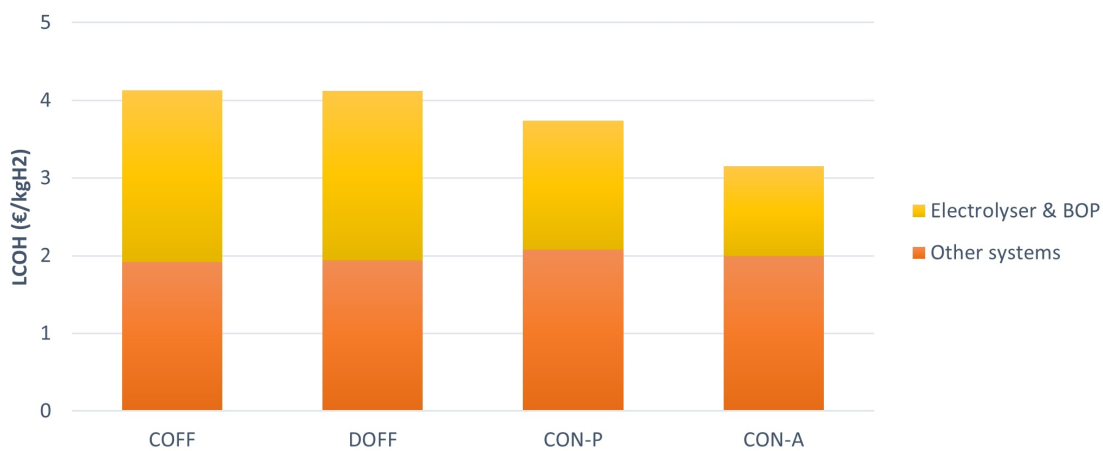

Figure 29: Levelised cost of hydrogen per configuration

As illustrated, the offshore cases offer the most expensive hydrogen. For the centralised offshore (COFF-P) configuration a cost of 4.13 €/kgH_2 is estimated, with the electrolyser system constituting 2.21 €/kgH_2. The decentralised offshore (DOFF-P) configuration cost is determined as 4.12 €/kgH_2, with 2.19 €/kgH_2 due to electrolyser system costs. The expensiveness of offshore installation and operation, as well as the PEM systems, are observed as major cost factors.

Meanwhile, the onshore cases offer the cheapest hydrogen. The use of PEM systems (CON-P) indicates a cost of 3.73 €/kgH_2, of which 1.66 €/kgH_2 come from the electrolyser system. For the ALK (CON-A) configuration, the LCOH stands at 3.15 €/kgH_2, with an electrolyser system cost at 1.15 €/kgH_2. While the other system components combined are more expensive for the onshore cases, the significantly lower electrolyser costs outweigh that downside.

The obtained LCOH values are observed to be higher compared to much of the literature where costs in the range of 2-3 €/kgH_2 are considered possible, if not probable, for projects with similar characteristics around 2030 [15][21][34]. However, it is also suggested that the levelised costs are likely to be higher, well above 4 €/kgH_2 [85]. Compared to current costs for green hydrogen, all four studied scenarios offer a cheaper solution while also being within the suggested reasonable range (2.84–4.63 €/kgH_2) to match future green hydrogen prices [86].

4.3 Qualitative assessment

In this section, each of the electrolyser placement configurations is analysed and compared based on qualitative conclusions from available literature using similar specifications, considering key aspects not already investigated in the previous sections.

4.3.1 Centralised offshore

Technological readiness

Although the key components themselves are technologically mature, the PEM electrolyser response is not validated for offshore operational conditions [18]. The lack of complete and active offshore hydrogen production projects increases the technological and regulatory complexities that need to be solved to make the system function properly [78]. Additionally, hydrogen compressors placed in connection to offshore hydrogen production systems have higher technical requirements than their onshore counterparts, while not being widely tested and implemented as of today, further increasing the uncertainties. These uncertainties refer not only to operational success but also to the lack of maturity of the supply chain. However, no other significant obstacles have yet been identified for the hydrogen pipelines with regard to function or resource availability. Overall, it is still possible that the offshore setups offer a faster system implementation [32]. In other geographical contexts, repurposing existing natural gas pipelines for hydrogen transmission could offer significant transmission cost reductions [22], although in this study, it is considered unlikely due to a lack of such networks in eastern Sweden [87].

Safety and regulations

Several challenges are highlighted concerning system and environmental safety. Being placed in harsh and remote offshore environments, failure events for the electrolyser system can be more difficult to manage than its onshore counterpart. Similarly, since all modules are placed in the same exposed location, the asset risk is higher [18].

As for environmental considerations, the discharge of large amounts of brine from the offshore electrolyser platform may have adverse effects on marine life [18]. However, the offshore configurations are generally preferable to the onshore one, both from the viewpoints of environmental concerns and permittance [32]. Considering the Baltic Sea specifically, the utilisation of the oxygen produced as a by-product from the electrolysis could offer benefits for the marine environment, limiting eutrophication while improving seabed habitability [88].

Further, offshore hydrogen production may have additional implications for standards and regulations for the produced hydrogen together with its necessary subsystems and -components. Although not necessarily a problem, the current lack of such standards and regulations adds to uncertainties when evaluating offshore configurations. Gas quality, flow conditions, pressures and corrosion are aspects where new regulations might be required before offshore hydrogen systems are considered mature [78].

Installation, operation and maintenance

Compared to the decentralised setup, this setup offers a more easily manageable and maintainable setup. The maintenance requirements for each turbine are lower, as are the repair times due to the more compact placement of the major components [18]. It is further considered that the offshore pipeline can act as a hydrogen buffer, reducing the need for dedicated storage tanks to fulfil that purpose. Such buffer capacity would indicate a more stable supply of hydrogen to the off-taker [29].

However, such as setup could require a crew to be permanently manned on the offshore platform, adding to the requirements for operating the offshore system. Several platforms and/or decks may be necessary to accommodate both the systems and the people [18]. Minimizing risks for the implementation of those is crucial and can be achieved through early supplier engagement and by ensuring adequate capacity for manufacturing and installation [32]. Further, as an offshore setup, a battery system is required to fulfil minimum energy requirements for the operating conditions of the electrolyser [18], contributing to additional costs and complexity.

4.3.2 Decentralised offshore

Technological readiness

As an offshore configuration, a shorter implementation time is suggested compared to onshore electrolysis when considering permitting and planning processes [32]. However, a successful PEM electrolyser response is not validated for offshore operations [18]. Other complexities with regard to regulations as well as adjacent technologies and systems also exist in this case, as offshore hydrogen systems are currently not mature enough in these matters [78]. The repurposing of natural gas pipelines for hydrogen transmission may be a general consideration, as for its centralised counterpart [22].

Safety and regulations

As a decentralised, modular system, failure events for this setup are somewhat easier to handle. Even when individual electrolysers stop functioning, hydrogen can be continuously produced from the other electrolysers, increasing the resiliency of the whole system [18].

The decentralised desalination also means that the brine discharge is spread out, reducing the adverse impacts on marine environments by increased diffusion [18]. As in the centralised configuration, artificial oxygenation using the oxygen produced by the electrolyser could offer additional environmental benefits [88]. The overall environmental impact is lower than with onshore electrolysis, and obtaining permits may be easier [32].

Installation, operation and maintenance

The use of wind turbines with a large nominal power is beneficial for this setup, as electrolyser systems are implemented individually, adding economies of scale advantages [21]. Additionally, there is no need for a large offshore platform, assuming that there is no need for a stationed crew [18]. Similar to the centralised offshore setup, the offshore pipelines can offer important buffer capabilities [29]. On the other hand, battery systems are also here required to supply backup power to the electrolysers [18].

However, the operation and maintenance procedures are more difficult. The decentralised systems add more complexity, and there is a challenge in having to manage both the electrolyser and turbine systems on the same platform, the extended transition piece [18]. Like in the centralised case, the construction of the electrolyser platforms needs to be coordinated and planned to avoid the significant implementation risks [32].

4.3.3 Centralised onshore

Technological readiness

Contrary to the offshore configurations, the onshore electrolyser function does not need validation since such setups are more widely implemented as of today. Further, weight and volume requirements for the onshore electrolyser facility do not necessarily pose any insurmountable challenges as they could at sea. This allows for the serious consideration of ALK electrolyser systems, offering a larger flexibility of choice [18].

Safety and regulations

The implementation of onshore electrolysis may be hindered by conflicts with local land use interests, with a higher risk of potential delays and lawsuits jeopardising the project. There are also larger environmental risks assigned to the power cable supply chains. Meanwhile, although freshwater access is assumed in this report, there is no guarantee. In case desalination is needed, there are challenges relating to getting approval for brine discharge, which would provide larger environmental risks for onshore environments [32].

However, the onshore environment increases the prospects of successfully sheltering sensitive equipment while offering an improved work environment for the required personnel. Even though ALK require more maintenance than PEM electrolysers, the easier access makes it less of an obstacle compared to offshore environments [21].

Installation, operation and maintenance

Installations and maintenance are significantly easier in onshore environments, though there are challenges of upscaling as well as losses during the extra steps of power conversion and transmission [18]. Meanwhile, compared to the offshore setups, a larger buffer capacity is likely required in the form of external storage systems since no significant pipeline volume is considered.

Excess energy to supply a battery is not considered as vital as in offshore cases due to the possibility of the grid acting as the backup power source for heating the electrolysers. This further highlights a main advantage of this configuration: the potential to choose when to buy and sell electricity from the grid based on market conditions. That way, the production of hydrogen can be designed to occur during periods of low electricity prices [21]. However, as the scope of this report only considers setups for dedicated hydrogen production, that remains a side note.

5 Discussion

In this chapter, the findings presented in the previous chapters are interpreted to provide a deeper understanding of the results. Additionally, the implications of the study are investigated, with recommendations for future research as well as practical suggestions.

5.1 Electrolyser sizing

The optimal size of the electrolyser system is considered to be the one with the lowest LCOH. However, as shown in the resulting optimisation graphs, there is a wide range of sizes that seem suitable from an economic perspective, especially for the DOFF-P and CON-P configurations. It is thus reasonable to consider that cost uncertainties and curve fitting inaccuracies are significant enough to impact sizing decisions. Such uncertainties will remain, at least to some degree, and an interpretation of the result is that the levelised costs do not seem to be heavily affected by sizing decisions within certain ranges.

Two main reasons can be given to explain the optimal sizes being different between the configurations. First, the share of electrolyser system costs to the other system costs is highlighted, a major factor as to why the CON-A scenario has the highest and the COFF-P scenario the lowest optimums. By reducing electrolyser-related costs compared to the rest of the system, the optimum would move closer to a ratio of 1:1 between the maximum electrolyser input power and electrolyser capacity. This is due to the cost increases per installed MW no longer being large enough for the electrolyser load factors, which decrease when capacities increase, to have a limiting impact on the LCOH. Additionally, the costs for the components required for the adjacent systems, such as cables, wind turbines, substations and pipelines, have not been considered to vary notably depending on the electrolyser capacity. Taking into account the suggested significant decreases in future electrolyser costs, while cost developments for other components are seemingly less radical, a sizing ratio of 1:1 is thus likely to be ideal in the longer run.

The second reason considers the difference between centralised and decentralised configurations, where the load distribution of the former is impacted by the balancing effects of geographical wind speed differences. The load duration curve is smoother for the centralised setups, especially at the maximum and minimum power inputs. Further, it is reasonable to consider that the reduced variations in input loads make a rapid electrolyser response less important. It is suggested that a method for quantifying the impacts of geographical wind speed differences on power outputs and electrolyser function should be developed to enable more accurate conclusions from the comparison of centralised and decentralised setups.

Further, there are several other areas relating to the electrolyser sizing in which a more detailed investigation could prove useful. In this report, allowing load ranges above 100% is not considered, although it could well add another level of complexity to the sizing decisions. Allowing higher load ranges would imply a decrease in optimal electrolyser capacities. Another suggestion for a study is to consider the impact of a hybrid system, where the system can deliver both hydrogen and electricity, on size optimisation. A hypothesis is that such a setup could benefit a smaller electrolyser system since it would be possible to obtain a high utilisation rate without losing large amounts of electricity. Additionally, purchasing electricity from the grid to increase utilisation may be unlikely to benefit the viability of larger capacities due to the electricity being bought during periods of low wind and, thus, when prices are likely high.

5.2 Simulation results

Comparing the simulation results, it is clear that some characteristics remain similar between the scenarios. The lifetime hydrogen production exceeds 2 Mton in all of the scenarios, although it is greater when using the more efficient ALK electrolyser, as well as in cases with a larger installed electrolyser capacity. Moreover, a comparison of the full system efficiencies and electrolyser input power shows similar trends, ranging between 52.15%–55.93% and 109.7–114.0 TWh, respectively.

The required cooling demands also differ slightly depending on electrolyser efficiency and installed capacity, with the largest demands being identified in the DOFF-P and CON-P scenarios. The average cooling demand for all of the cases ranges between 150.4–164.1 MW. The consumption of water for electrolysis is neither considered to have any impact on water levels due to the sheer size of the Baltic Sea. Meanwhile, further comparisons between obtaining it directly from a freshwater source and through desalination could provide additional technical and economic insights for practical cases.

The main difference in electrolyser function is between the two onshore cases, where ALK and PEM electrolysers are utilised, respectively. The higher degradation rate of the PEM electrolyser stacks indicates more frequent replacements during the project lifetime, leading to additional costs. The stack degradation rates and long-term electrolyser function are suggested to be subjected to further studies using empirical data where available. Another consideration regards electrolyser downtime, where the ALK electrolyser is down 17.2% of the time, while the PEM electrolyser downtime is 3.2%. Considering the CON-A case, the impact on hydrogen output is not too significant since the downtime occurs only during periods when the power load is below 10%, but it is worth noting that this study considers the equal distribution of loads to all electrolyser modules. Another reasonable approach could be to allow for specific ALK modules to be prioritised in the distribution of lower loads. Thus, significantly lower loads can be utilised, increasing the full system efficiency. It is also suggested to further investigate the load ranges for other components, such as the compressor, and not just for the electrolysers.

When looking at the losses, it is clear that for all cases, the main portion consists of the heat losses from the electrolyser process. These constitute between 63.2–68.5% of the total losses within the studied scenarios, and it can be deduced that increases in electrolyser efficiencies have, by a large margin, the highest potential impact on the full system efficiencies. PSU conversion losses from transformers and rectifiers remain similar across the studied cases and represent a considerably large share of total energy losses. Similarly, cooling pump and electrolyser standby power demands do not differ notably between the cases while having a relatively small impact on total system losses. Further investigations into the implementation and transient response of a dynamic backup power source and its ability to supply standby heat to the electrolysers are suggested since these aspects are merely touched upon in this study.

Meanwhile, power transmission losses occur mainly in the onshore scenarios, although some inter-array losses can be observed in the COFF-P scenario. This is one of the main divergences between the cases and offers an argument for offshore hydrogen production, where transmission losses are negligible. For the CON-P scenario, transmission losses amount to 7.9% of total losses, while for the CON-A scenario, the share is 8.3%. It should be pointed out that the transmission distance is a key variable since longer distances indicate larger power losses and a stronger case for offshore configurations from a techno-economic point of view. This is due to the negligible pipeline transmission losses, even though extra compression is required to compensate for the increased pressure losses. This remains an important consideration even when employing HVDC transmission, which would offer a higher transmission efficiency for longer distances. However, additional analyses comparing transmission distances while also including different HVDC transmission technologies are proposed since they would be able to provide more detailed conclusions in this regard.

It can further be concluded that the power required for seawater desalination in offshore scenarios barely contributes to the energy losses of the whole system. In some cases, reverse osmosis desalination could therefore offer a reasonable method for obtaining freshwater, even in onshore scenarios where the possibility to obtain it directly from freshwater sources exists. Thermal desalination has not been considered in this study but shows potential for future research into offshore freshwater access. The power demand for compression in the centralised offshore case using ALK systems is neither too remarkable, though it is important to remember that the ALK electrolyser is pressurised. In other cases where electrolyser outputs would not be pressurised, the power demand is likely to be much higher.

It is also observed that the variation of electrolyser sizes between the scenarios has an important impact on energy losses. As the electrolyser capacity increases towards a 1:1 ratio to the input power, the surplus electricity production decreases. If no such surplus is produced for the offshore cases, some of the electrolyser power input would need to be redirected to charge the UPS. However, as the electrolyser capacity decreases, an increasingly large portion of the electricity will remain unutilised. This can be observed especially in the COFF-P scenario where 16.8%, or 10.7 TWh, of all energy losses, are due to excess electricity. Further studies are suggested to investigate the possibility of utilising this resource, where a hybrid system with separate power and hydrogen transmission capabilities could be a solution. However, this is likely to add significant costs, and an assessment should be performed accordingly. Additionally, the necessity of a hydrogen buffer needs further examination from technical and economic perspectives, considering not only pipeline buffer capabilities but also dedicated hydrogen storage.

5.3 Techno-economic assessment

As shown, the onshore cases offer the lowest LCOH using the obtained costs and chosen discount rate, with the lowest value of 3.15 €/kgH_2 being reached for the onshore scenario using an ALK electrolyser system and the second lowest being the onshore PEM configuration at 3.73 €/kgH_2. Meanwhile, the cost for the offshore cases is higher, with 4.13 €/kgH_2 for the centralised and 4.12 €/kgH_2 for the decentralised setup. It is noteworthy that the DOFF-P scenario offers close to the highest LCOH while simultaneously being close to having the highest system efficiency and hydrogen production. This highlights the importance of not drawing substantial conclusions from looking at the costs or technical results separately. Comparing it to current costs for electrolytic hydrogen, the obtained values are all in the lower part of the 2.76–11 €/kgH_2 span while still not meeting the 2 €/kgH_2 target for 2030.

An explanation for the obtained LCOH is the consideration that no significant cost developments are likely to occur until 2030. PEM electrolyser systems are assumed to remain expensive, both compared to ALK systems but also considering its share of the full system costs, CAPEX and OPEX combined. Although electrolyser learning rates are likely to remain high in the foreseeable future, rapidly reducing production costs, it is uncertain to what degree the manufacturing capacity can keep up with the increased electrolyser demands on a global scale. The wide range of cost prognoses that has been identified indicates a large uncertainty, although it offers an important insight. Considering electrolyser costs to be subjected to larger potential price reductions than the other system components, the offshore cases grow increasingly relevant as electrolysers become cheaper. This is further supported by the consideration that the adjacent system costs are observed to be larger for the onshore cases, mainly because of costs related to power cables and substations. When prices decrease, the cost differences between ALK and PEM electrolysers similarly become less important as they constitute a smaller share of the total system costs. It is proposed that further efforts are made to develop price forecasts for electrolysers, including SOEC and AEM systems, where supply chains, demands and learning rates are considered.

The economic analysis is further impacted by several other factors, among which the choice of the discount rate, which is likely to impact LCOH values. A higher discount rate would result in a higher levelised cost for all the studied cases due to the assumption that all CAPEX investments are made at the beginning of the project. Meanwhile, OPEX and hydrogen production are spread out across the 30-year lifetime, subjecting them to time value effects. It should be noted that the choice of discount rate depends on a wide range of variables, many of them external. Additionally, the choice of the base year of the project similarly impacts the time value of the cash flows.

For future investigations into the subject, including the costs of more auxiliary components and services could improve the quality of the assessment. That might include costs for freshwater, water purification components, backup power sources and others. Including the possibility of hybrid setups, by selling surplus electricity to the grid or adapting the system to deliver hydrogen or power according to current market demands, might show additional economic benefits. Other studies might look at the delivery of hydrogen, where the steady flow and availability of hydrogen through implementing a buffer could improve the business case. Profitability analyses might be useful for such inquiries.

5.4 Additional considerations

From the qualitative study, several insights can be obtained. Offshore electrolysis is still less tried and implemented than onshore setups, indicating additional uncertainties for practical offshore implementations concerning operability, resource availability and the costs for offshore platforms. Meanwhile, weight and volume requirements are considered limiting factors in offshore environments, strengthening the case for PEM electrolysis. However, for centralised offshore setups, ALK electrolysis may not be fully disregarded, and an investigation into such a setup is encouraged, taking into account increased maintenance, lye management, as well as space and load requirements. Hybrids using a combination of PEM and ALK systems, or a setup including both pressurised and unpressurised ALK systems, could prove viable. Future studies might also consider the utilisation of SOEC or AEM electrolyser systems.

Environmental concerns are observed to be larger for the onshore cases, as are the regulatory challenges. Onshore desalination is not highlighted in this report, but in areas of limited or expensive freshwater access, desalination would be required, with the brine discharge having a higher risk of adverse environmental impacts than its offshore counterparts. The brine release effects remain the most moderate for the decentralised offshore setup. However, the main environmental and regulatory obstacle is observed to be conflicts of interest regarding land use, making meticulous planning efforts in these matters especially important for onshore electrolyser setups. Apart from the permits required for projects with environmental and water impacts, additional permits will be required due to the project being located in the Swedish economic zone outside of the territorial waters.

The centralised and the decentralised setups can generally be differentiated by their complexity and resilience. The centralised setups keep most of their components in the same location, increasing the asset risks while reducing operational complexities, especially in the harsher offshore environments. Meanwhile, the decentralised setup allows for continuous operation even when individual systems are down, offering high resilience but also high complexity, adding to maintenance difficulties. Deciding what setup is the most ideal will thus depend on the project owner's objectives and capabilities.

Apart from the explored aspects, additional safety concerns might include pipelines, where hostile interventions could endanger full transmission operability. Similarly, large-scale offshore electrolyser systems could come with higher risks connected to external events. Further, it is suggested that the possibility of weather anomalies is taken into consideration for future investigations. An UPS might have difficulties supporting the required backup power during long periods of cold temperatures and low wind speeds. In such cases, electrolyser stack safety and cold starts should be investigated. Meanwhile, investigating the oxygenation of the Baltic Sea using the produced oxygen could prove useful.

6 Conclusions

As an extensive study encompassing many systems and considerations, the main conclusions are not found in the specifics but instead in the insights obtained from the combined calculations, simulations and qualitative investigations. The optimal sizing of the electrolyser systems depends in large part on the assumed electrolyser costs, with higher costs corresponding to lower optimal capacities. Meanwhile, the capacity optimisation shows that a range of electrolyser sizes are likely to be viable, with marginal impacts on the LCOH. A 1:1 ratio between electrolyser capacity and input power is therefore not assumed to be the obvious choice. The distribution of energy losses further highlights the importance of certain subsystems. The power demands for hot standby, cooling and desalination subsystems remain relatively inconsequential, while small changes in efficiencies relating to the electrolyser or electric conversion have remarkably larger impacts.

Although the centralised onshore setup using an ALK system requires additional compression and has notable transmission losses, it currently offers the largest production, highest efficiency and lowest LCOH of the studied configurations, making it the suggested choice from both an economic and technical perspective. However, such a statement comes with important caveats. First, social and environmental regulations and concerns might be significant obstacles to onshore implementations and need to be considered. Second, as electrolyser costs eventually go through a rapid decline, offshore and PEM configurations become increasingly viable regarding costs and technical performance. By considering alternative cost developments or changing the active years of the project, new conclusions in favour of offshore configurations might be extracted. Third, though onshore setups are observed to be more feasible, offshore ALK systems not investigated in this report can not be discarded. Meanwhile, several knowledge gaps are identified, and the lack of empirical data increases the uncertainties. The simulation results and LCOH calculations, however, indicate opportunities in dedicating large-scale Baltic Sea offshore wind power to H_2 production.

Bibliography

[1] International Energy Agency (IEA), "World energy outlook 2022," 2022. [Online]. Available: https://iea.blob.core.windows.net/assets/830fe099-5530-48f2-a7c1-11f35d510983/WorldEnergyOutlook2022.pdf (visited on Feb. 17, 2023).

[2] World Energy Council and Oliver Wyman, "World energy trilemma index 2022," 2022. [Online]. Available: https://www.marshmclennan.com/content/dam/mmc-web/insights/publications/2022/december/World_Energy_Trilemma_Index_2022.pdf (visited on Feb. 17, 2023).

[3] Energy Transitions Commission (ETC), "Making clean electrification possible: 30 years to electrify the global economy," 2021. [Online]. Available: https://www.energy-transitions.org/wp-content/uploads/2022/07/ETC-Global-Power-Report-Final.pdf (visited on Feb. 15, 2023).

[4] Energy Transitions Commission (ETC), "Making the hydrogen economy possible: Accelerating clean hydrogen in an electrified economy," 2021. [Online]. Available: https://www.energy-transitions.org/publications/making-clean-hydrogen-possible/ (visited on Feb. 15, 2023).

[5] International Energy Agency (IEA), "The future of hydrogen," 2019. [Online]. Available: https://iea.blob.core.windows.net/assets/9e3a3493-b9a6-4b7d-b499-7ca48e357561/The_Future_of_Hydrogen.pdf (visited on Feb. 15, 2023).

[6] M. Klell, "Storage of hydrogen in the pure form," in *Handbook of Hydrogen Storage*, M. Hirscher, Ed., 1st ed., WILEY-VCH Verlag GmbH & Co. KGaA, 2010, pp. 1–38, ISBN: 978-3-527-32273-2.

[7] M. Ball and M. Weeda, "The hydrogen economy – vision or reality?" *International Journal of Hydrogen Energy*, vol. 40, pp. 7903–7919, 25 Jul. 2015, ISSN: 03603199. DOI: 10.1016/j.ijhydene.2015.04.032.

[8] M. Salimi, M. Hosseinpour, and T. N.Borhani, "The role of clean hydrogen value chain in a successful energy transition of japan," *Energies*, vol. 15, 16 Aug. 2022, ISSN: 19961073. DOI: 10.3390/en15166064.

[9] A. Ajanovic, M. Sayer, and R. Haas, "The economics and the environmental benignity of different colors of hydrogen," *International Journal of Hydrogen Energy*, vol. 47, pp. 24 136–24 154, 57 Jul. 2022, ISSN: 03603199. DOI: 10.1016/j.ijhydene.2022.02.094.

[10] I. Dincer and C. Acar, "Innovation in hydrogen production," *International Journal of Hydrogen Energy*, vol. 42, pp. 14 843–14 864, 22 Jun. 2017, ISSN: 03603199. DOI: 10.1016/j.ijhydene.2017.04.107.

[11] N. M. Dowell, N. Sunny, N. Brandon, *et al.*, "The hydrogen economy: A pragmatic path forward," *Joule*, vol. 5, pp. 2524–2529, 10 Oct. 2021, ISSN: 25424351. DOI: 10.1016/j.joule.2021.09.014.

[12] M. Katebah, M. Al-Rawashdeh, and P. Linke, "Analysis of hydrogen production costs in steam-methane reforming considering integration with electrolysis and co2 capture," *Cleaner Engineering and Technology*, vol. 10, p. 100 552, Oct. 2022, ISSN: 26667908. DOI: 10.1016/j.clet.2022.100552.

[13] International Energy Agency (IEA), *About ccus*, 2021. [Online]. Available: https://www.iea.org/reports/about-ccus (visited on Jul. 4, 2023).

[14] International Energy Agency (IEA), "Electrolysers," 2022. [Online]. Available: https://www.iea.org/reports/electrolysers (visited on Feb. 21, 2023).

[15] IRENA, "Green hydrogen cost reduction: Scaling up electrolysers to meet the 1.5c climate goal," 2020. [Online]. Available: https://www.irena.org/-/media/Files/IRENA/Agency/Publication/2020/Dec/IRENA_Green_hydrogen_cost_2020.pdf?rev=4ce868aa69b54674a789f990e85a3f00 (visited on Mar. 1, 2023).

[16] B. E. Logan, L. Shi, and R. Rossi, "Enabling the use of seawater for hydrogen gas production in water electrolyzers," *Joule*, vol. 5, pp. 760–762, 4 Apr. 2021, ISSN: 25424351. DOI: 10.1016/j.joule.2021.03.018.

[17] Hydrogen TCP, "Task 38 final report - power-to-hydrogen and hydrogen-to-x: System analysis of the techno-economic, legal and regulatory conditions," Sep. 2020. [Online]. Available: https://www.ieahydrogen.org/tasks-reports/ (visited on Mar. 3, 2023).

[18] O. S. Ibrahim, A. Singlitico, R. Proskovics, S. McDonagh, C. Desmond, and J. D. Murphy, "Dedicated large-scale floating offshore wind to hydrogen: Assessing design variables in proposed typologies," *Renewable and Sustainable Energy Reviews*, vol. 160, p. 112 310, May 2022, ISSN: 13640321. DOI: 10.1016/j.rser.2022.112310.

[19] C. Bernuy-Lopez, "Electrolysis technologies and lcoh: Current state and prospects for 2030," *Hydrogen Tech World*, pp. 30–36, Apr. 2023. [Online]. Available: https://viewer.joomag.com/hydrogen-tech-world-april-2023/0839460001679914049?fbclid=IwAR1IinNFAK2ruNDhJ-prpF2DD8PKK4Me2igJmnWCn4tyjMSc0Qt9eXm7Z8s (visited on May 27, 2023).

[20] F. Zhang, P. Zhao, M. Niu, and J. Maddy, "The survey of key technologies in hydrogen energy storage," *International Journal of Hydrogen Energy*, vol. 41, pp. 14 535–14 552, 33 Sep. 2016, ISSN: 03603199. DOI: 10.1016/j.ijhydene.2016.05.293.

[21] G. Calado and R. Castro, "Hydrogen production from offshore wind parks: Current situation and future perspectives," *Applied Sciences*, vol. 11, p. 5561, 12 Jun. 2021, ISSN: 2076-3417. DOI: 10.3390/app11125561.

[22] B. Miao, L. Giordano, and S. H. Chan, "Long-distance renewable hydrogen transmission via cables and pipelines," *International Journal of Hydrogen Energy*, vol. 46, pp. 18 699–18 718, 36 May 2021, ISSN: 03603199. DOI: 10.1016/j.ijhydene.2021.03.067.

[23] M. Hirscher, *Handbook of Hydrogen Storage*, 1st ed. WILEY-VCH Verlag GmbH & Co. KGaA, 2010, pp. XV–XVII, ISBN: 978-3-527-32273-2.

[24] G. He, D. S. Mallapragada, A. Bose, C. F. Heuberger, and E. Gençer, "Hydrogen supply chain planning with flexible transmission and storage scheduling," Aug. 2020. DOI: 10.1109/TSTE.2021.3064015. [Online]. Available: https://arxiv.org/pdf/2008.07611.pdf (visited on Mar. 6, 2023).

[25] J. Huot, "Metal hydrides," in *Handbook of Hydrogen Storage*, M. Hirscher, Ed., 1st ed., WILEY-VCH Verlag GmbH & Co. KGaA, 2010, pp. 81–116, ISBN: 978-3-527-32273-2.

[26] U.S. Department of Energy, "U.s. national clean hydrogen strategy and roadmap," Jun. 2023. [Online]. Available: https://www.hydrogen.energy.gov/clean-hydrogen-strategy-roadmap.html (visited on Jun. 29, 2023).

[27] ISPT, "Gigawatt green hydrogen plant," 2020. [Online]. Available: https://ispt.eu/media/ISPT-public-report-gigawatt-green-hydrogen-plant.pdf (visited on May 11, 2023).

[28] Hydrogen Council, "Path to hydrogen competitiveness – a cost perspective," Jan. 2020. [Online]. Available: https://hydrogencouncil.com/wp-content/uploads/2020/01/Path-to-Hydrogen-Competitiveness_Full-Study-1.pdf (visited on May 30, 2023).

[29] P. Raposo, AFRY, Global Director Power-to-X, *Personal communication*, May 2023.

[30] IRENA, "Hydrogen from renewable power: Technology outlook for the energy transition," International Renewable Energy Agency, 2018. [Online]. Available: https://www.irena.org/-/media/Files/IRENA/Agency/Publication/2018/Sep/IRENA_Hydrogen_from_renewable_power_2018.pdf?rev=817ffa3e16dd4aebb89098bdf69be6a8 (visited on Mar. 6, 2023).

[31] Y. Guo, G. Li, J. Zhou, and Y. Liu, "Comparison between hydrogen production by alkaline water electrolysis and hydrogen production by pem electrolysis," *IOP Conference Series: Earth and Environmental Science*, vol. 371, p. 042 022, 4 Dec. 2019, ISSN: 1755-1307. DOI: 10.1088/1755-1315/371/4/042022.

[32] AFRY, "Comparison of system variants for hydrogen production from offshore wind power," Mar. 2022. [Online]. Available: https://aquaventus.org/wp-content/uploads/2022/05/AquaDuctusShortStudy_OffshoreHydrogenProduction_v120_EN.pdf (visited on Feb. 21, 2023).

[33] R. Hancke, T. Holm, and Ø. Ulleberg, "The case for high-pressure pem water electrolysis," *Energy Conversion and Management*, vol. 261, p. 115 642, Jun. 2022, ISSN: 01968904. DOI: 10.1016/j.enconman.2022.115642.

[34] A. Singlitico, J. Østergaard, and S. Chatzivasileiadis, "Onshore, offshore or in-turbine electrolysis? techno-economic overview of alternative integration designs for green hydrogen production into offshore wind power hubs," *Renewable and Sustainable Energy Transition*, vol. 1, p. 100 005, Aug. 2021, ISSN: 2667095X. DOI: 10.1016/j.rset.2021.100005.

[35] Sunfire, *World's largest high-temperature electrolyzer achieves record efficiency*, Apr. 2022. [Online]. Available: https://www.sunfire.de/en/news/detail/worlds-largest-high-temperature-electrolyzer-achieves-record-efficiency (visited on Mar. 3, 2023).

[36] M. Ozturk and I. Dincer, "A comprehensive review on power-to-gas with hydrogen options for cleaner applications," *International Journal of Hydrogen Energy*, vol. 46, pp. 31 511–31 522, 62 Sep. 2021, ISSN: 03603199. DOI: 10.1016/j.ijhydene.2021.07.066.

[37] I. Vincent, E.-C. Lee, and H.-M. Kim, "Comprehensive impedance investigation of low-cost anion exchange membrane electrolysis for large-scale hydrogen production," *Scientific Reports*, vol. 11, p. 293, 1 Jan. 2021, ISSN: 2045-2322. DOI: 10.1038/s41598-020-80683-6.

[38] Svensk Vindenergi, "Havsbaserad vindkraft – en nyckel till industrins omställning," Dec. 2021. [Online]. Available: https://svenskvindenergi.org/wp-content/uploads/2021/12/Policyrapport-Havsbaserad-vindkraft-en-nyckel-till-industrins-omstallning.pdf (visited on Feb. 27, 2023).

[39] A. Fernández-Guillamón, K. Das, N. A. Cutululis, and Á. Molina-García, "Offshore wind power integration into future power systems: Overview and trends," *Journal of Marine Science and Engineering*, vol. 7, p. 399, 11 Nov. 2019, ISSN: 2077-1312. DOI: 10.3390/jmse7110399.

[40] IRENA, "Future of wind: Deployment, investment, technology, grid integration and socio-economic aspects (a global energy transformation paper)," International Renewable Energy Agency, Oct. 2019. [Online]. Available: https://www.irena.org/-/media/files/irena/agency/publication/2019/oct/irena_future_of_wind_2019.pdf (visited on Mar. 16, 2023).

[41] C. Poynter, *Crossing the power threshold for offshore wind turbines*, Aug. 2021. [Online]. Available: https://www.windpowerengineering.com/crossing-the-power-threshold-for-offshore-wind-turbines/ (visited on May 22, 2023).

[42] A. Sedaghat, A. Hassanzadeh, J. Jamali, A. Mostafaeipour, and W. H. Chen, "Determination of rated wind speed for maximum annual energy production of variable speed wind turbines," *Applied Energy*, vol. 205, pp. 781–789, Nov. 2017, ISSN: 03062619. DOI: 10.1016/j.apenergy.2017.08.079.

[43] S. Lundberg, "Performance comparison of wind park configurations," Chalmers University of Technology, 2003. [Online]. Available: https://publications.lib.chalmers.se/records/fulltext/2691/local_2691.pdf (visited on May 3, 2023).

[44] M. Gaumond, P.-E. Réthoré, A. Bechmann, *et al.*, "Benchmarking of wind turbine wake models in large offshore windfarms," in Jan. 2012. [Online]. Available: https://www.eera-dtoc.eu/wp-content/uploads/files/Gaumond-et-al-Benchmarking-of-wind-turbine-wake-models-in-large-offshore-wind-farms.pdf (visited on May 11, 2023).

[45] Länsstyrelsen, *Vindbrukskollen*. [Online]. Available: https://vbk.lansstyrelsen.se/ (visited on Mar. 17, 2023).

[46] B. Yang, B. Liu, H. Zhou, *et al.*, "A critical survey of technologies of large offshore wind farm integration: Summary, advances, and perspectives," *Protection and Control of Modern Power Systems*, vol. 7, p. 17, 1 Dec. 2022, ISSN: 2367-2617. DOI: 10.1186/s41601-022-00239-w.

[47] U.S. Energy Information Administration (EIA), "Assessing hvdc transmission for impacts of non-dispatchable generation," EIA, Jun. 2018. [Online]. Available: https://www.eia.gov/analysis/studies/electricity/hvdctransmission/pdf/transmission.pdf (visited on Mar. 15, 2023).

[48] Svenska Kraftnät, *Elområden*, May 2022. [Online]. Available: https://www.svk.se/om-kraftsystemet/om-elmarknaden/elomraden/ (visited on Feb. 27, 2023).

[49] Svenska Kraftnät, "Commission regarding preparatory work for the expansion of the transmission grid into swedish territorial waters," Jun. 2022. [Online]. Available: https://www.svk.se/siteassets/2.utveckling-av-kraftsystemet/transmissionsnatet/utbyggnad-av-transmissionsnat-till-havs/report---commission-regarding-preparatory-work-for-the-expansion-of-the-transmission-grid-into-swedish-territorial-waters.pdf (visited on Mar. 2, 2023).

[50] Energimyndigheten, *Vindkraft i svenskt vatten*, 2022. [Online]. Available: https://www.energimyndigheten.se/fornybart/vindkraft/vindlov/planering-och-tillstand/svenskt-vatten/ (visited on Mar. 12, 2023).

[51] Vätgas Sverige, *Grön vätgas produceras till havs*, Feb. 2021. [Online]. Available: https://vatgas.se/2021/02/02/gron-vatgas-produceras-till-havs/ (visited on Jun. 25, 2023).

[52] Eolus, *Eolus planerar havsbaserad vindkraftspark med vätgasproduktion utanför robertsfors*, May 2023. [Online]. Available: https://www.eolusvind.com/nyheter/eolus-planerar-havsbaserad-vindkraftspark-utanfor-robertsfors/ (visited on Jun. 25, 2023).

[53] A. Wennberg, *Abb samarbetar med lhyfe och skyborn i vätgasprojekt*, May 2023. [Online]. Available: https://www.vindkraftsnyheter.se/20230508/7707/abb-samarbetar-med-lhyfe-och-skyborn-i-vatgasprojekt (visited on Jun. 25, 2023).

[54] K. Meier, "Hydrogen production with sea water electrolysis using norwegian offshore wind energy potentials: Techno-economic assessment for an offshore-based hydrogen production approach with state-of-the-art technology," *International Journal of Energy and Environmental Engineering*, vol. 5, pp. 1–12, 2-3 Jul. 2014, ISSN: 22516832. DOI: 10.1007/s40095-014-0104-6.

[55] H. T. Madsen, *Water treatment for green hydrogen: What you need to know*, Oct. 2022. [Online]. Available: https://hydrogentechworld.com/water-treatment-for-green-hydrogen-what-you-need-to-know (visited on Mar. 22, 2023).

[56] W. J. Tiktak, "Heat management of pem electrolysis," Oct. 2019. [Online]. Available: https://repository.tudelft.nl/islandora/object/uuid%5C%3Ac046820a-72bc-4f05-b72d-e60a3ecb8c89 (visited on Mar. 22, 2023).

[57] A. Panagopoulos and K.-J. Haralambous, "Environmental impacts of desalination and brine treatment - challenges and mitigation measures," *Marine Pollution Bulletin*, vol. 161, p. 111 773, Dec. 2020, ISSN: 0025326X. DOI: 10.1016/j.marpolbul.2020.111773.

[58] A. C. Weber and L. G. Papageorgiou, "Design of hydrogen transmission pipeline networks with hydraulics," *Chemical Engineering Research and Design*, vol. 131, pp. 266–278, Mar. 2018, ISSN: 02638762. DOI: 10.1016/j.cherd.2018.01.022.

[59] Baltic Sea Hydrographic Commission (BSHC), *Baltic sea bathymetry database*. [Online]. Available: http://data.bshc.pro (visited on May 7, 2023).

[60] Renewables.ninja, *Renewables.ninja*. [Online]. Available: https://www.renewables.ninja (visited on Mar. 12, 2023).

[61] T. Schlemmer and L. Greedy, "66 kv systems for offshore wind farms," DNV GL Energy, Mar. 2015. [Online]. Available: https://silo.tips/download/tennet-nl-offshore-wind-farm-transmission-systems (visited on May 3, 2023).

[62] CFI, *Levelized cost of energy (lcoe)*, May 2023. [Online]. Available: https://corporatefinanceinstitute.com/resources/valuation/levelized-cost-of-energy-lcoe/ (visited on Jun. 16, 2023).

[63] C. Qin, E. Loth, D. S. Zalkind, *et al.*, "Downwind coning concept rotor for a 25 mw offshore wind turbine," *Renewable Energy*, vol. 156, pp. 314–327, Aug. 2020, ISSN: 18790682. DOI: 10.1016/j.renene.2020.04.039.

[64] M. Albadi and E. El-Saadany, "Wind turbines capacity factor modeling—a novel approach," *IEEE Transactions on Power Systems*, vol. 24, pp. 1637–1638, 3 Aug. 2009, ISSN: 0885-8950. DOI: 10.1109/TPWRS.2009.2023274.

[65] D. Lim, B. Lee, H. Lee, *et al.*, "Impact of voltage degradation in water electrolyzers on sustainability of synthetic natural gas production: Energy, economic, and environmental analysis," *Energy Conversion and Management*, vol. 245, p. 114 516, Oct. 2021, ISSN: 01968904. DOI: 10.1016/j.enconman.2021.114516.

[66] North Sea Energy, "Technical assessment of hydrogen transport, compression, processing offshore," Jun. 2020. [Online]. Available: https://north-sea-energy.eu/static/7ffd23ec69b9d82a7a982b828be04c50/FINAL-NSE3-D3.1-Final-report-technical-assessment-of-Hydrogen-transport-compression-processing-offshore.pdf (visited on May 24, 2023).

[67] E. Frank, J. Gorre, F. Ruoss, and M. J. Friedl, "Calculation and analysis of efficiencies and annual performances of power-to-gas systems," *Applied Energy*, vol. 218, pp. 217–231, May 2018, ISSN: 03062619. DOI: 10.1016/j.apenergy.2018.02.105.

[68] E. Lillieblad, AFRY, Process Engineer Power-to-X, *Personal communication*, May 2023.

[69] Svenska Kraftnät, *Technology*, Mar. 2021. [Online]. Available: https://www.svk.se/en/grid-development/the-construction-process/technology/ (visited on May 3, 2023).

[70] A. Roderick, *Transformer losses and efficiency*, Jun. 2021. [Online]. Available: https://eepower.com/technical-articles/transformer-losses-and-efficiency/ (visited on May 3, 2023).

[71] C. F. Pedersen and R. R. Rønne, "An efficient ac-dc electrical power converting unit configuration," 2016. [Online]. Available: https://patentimages.storage.googleapis.com/43/15/5c/326b991d6d3575/EP2963761A1.pdf (visited on Mar. 29, 2023).

[72] N. B. Negra, J. Todorovic, and T. Ackermann, "Loss evaluation of hvac and hvdc transmission solutions for large offshore wind farms," *Electric Power Systems Research*, vol. 76, pp. 916–927, 11 Jul. 2006, ISSN: 03787796. DOI: 10.1016/j.epsr.2005.11.004.

[73] A. Martin-Candilejo, D. Santillán, and L. Garrote, "Pump efficiency analysis for proper energy assessment in optimization of water supply systems," *Water*, vol. 12, p. 132, 1 Dec. 2019, ISSN: 2073-4441. DOI: 10.3390/w12010132.

[74] Iplex, *Flowtite grp pipe and fittings*, 2019. [Online]. Available: https://www.iplex.com.au/assets/Uploads/5188d1e29b/FLOWTITE-Pipeline-Design-Hydraulic.pdf (visited on May 3, 2023).

[75] Topfibra, *Do you know how much the maximum flow velocity in a grp pipe is?* May 2019. [Online]. Available: https://topfibra.eu/do-you-know-how-much-is-the-maximum-flow-velocity-in-a-grp-pipe/ (visited on May 3, 2023).

[76] E. S. Menon, *Pipeline Planning and Construction Field Manual*, 1st ed. Elsevier Inc., 2011, p. 270, ISBN: 978-0-12-383867-4.

[77] S. Kuczynski, M. Łaciak, A. Olijnyk, A. Szurlej, and T. Włodek, "Thermodynamic and technical issues of hydrogen and methane-hydrogen mixtures pipeline transmission," *Energies*, vol. 12, 3 Feb. 2019, ISSN: 19961073. DOI: 10.3390/en12030569.

[78] North Sea Energy, "A vision on hydrogen potential from the north sea," Jun. 2020. [Online]. Available: https://north-sea-energy.eu/static/29bef9235ee0548a2425dea4356a2f1e/NSE3-D1.6-D1.7-D1.8-Offshore-Hydrogen-Roadmap-linked-to-national-hydrogen-grid.pdf (visited on Mar. 15, 2023).

[79] E. S. Menon, *Gas Pipeline Hydraulics*, 1st ed. Taylor & Francis Group, 2005, ISBN: 0-8493-2785-7.

[80] S. S. Makridis, "Hydrogen storage and compression," in *Methane and Hydrogen for Energy Storage*, R. Carriveau and D. S.-K. Ting, Eds., 1st ed., IET, 2016, pp. 1–22, ISBN: 978-1-785-61193-3.

[81] E. C. M. Ruijgrok, E. J. V. Druten, and B. H. Bulder, "Cost evaluation of north sea offshore wind post 2030," Witteveen+Bos, Feb. 2019. [Online]. Available: https://northseawindpowerhub.eu/sites/northseawindpowerhub.eu/files/media/document/Cost-Evaluation-of-North-Sea-Offshore-Wind-1.pdf (visited on May 10, 2023).

[82] BVG Associates, *Wind farm costs*. [Online]. Available: https://guidetoanoffshorewindfarm.com/wind-farm-costs (visited on May 11, 2023).

[83] North Sea Energy, "Energy transport and energy carriers," Jun. 2020. [Online]. Available: https://north-sea-energy.eu/static/afcbb8ede73e006a185c2499f2735f34/FINAL-NSE3-D3.2-D3.3-D3.4-D3.4-D3.5-D3.6-Inventory-of-power-to-X-integration-options.pdf (visited on May 11, 2023).

[84] S. Brynolf, M. Taljegard, M. Grahn, and J. Hansson, "Electrofuels for the transport sector: A review of production costs," *Renewable and Sustainable Energy Reviews*, vol. 81, pp. 1887–1905, Jan. 2018, ISSN: 13640321. DOI: 10.1016/j.rser.2017.05.288.

[85] A. Giampieri, J. Ling-Chin, and A. P. Roskilly, "Techno-economic assessment of offshore wind-to-hydrogen scenarios: A uk case study," *International Journal of Hydrogen Energy*, Feb. 2023, ISSN: 03603199. DOI: 10.1016/j.ijhydene.2023.01.346.

[86] C. J. Jepma and M. van Schot, "On the economics of offshore energy conversion: Smart combinations," Energy Delta Institute, Feb. 2017.

[87] P. Lustenberger, F. Schumacher, M. Spada, P. Burgherr, and B. Stojadinovic, "Assessing the performance of the european natural gas network for selected supply disruption scenarios using open-source information," *Energies*, vol. 12, p. 4685, 24 Dec. 2019, ISSN: 1996-1073. DOI: 10.3390/en12244685.

[88] M. Nilsson, "Offshore wind power co-operated green hydrogen and sea-water oxygenation plant: A feasibility case study for sweden," Uppsala University, Nov. 2022. [Online]. Available: http://www.diva-portal.org/smash/get/diva2:1724877/FULLTEXT01.pdf (visited on Jun. 14, 2023).

[89] International Energy Agency (IEA), "Offshore wind outlook 2019," 2019. [Online]. Available: https://www.iea.org/reports/offshore-wind-outlook-2019 (visited on Jun. 17, 2023).

A

Appendix

A.1 MATLAB code

The MATLAB scripts and functions that are written and used in the Simulink simulations are introduced below.

A.1.1 Main script

```
clc;
clear all;
close all;

%%% PARAMETER INPUTS %%%
electrolyser = "PEM";          %   "ALK or PEM"
typology = "COFF";             %   "ON, DOFF or COFF"
elec_capacity = 725;           %   MW
lifetime = 30;                 %   years

%%% WIND SPEEDS %%%
min_wind_speed = 4;            %   m/s
max_wind_speed = 24;           %   m/s
rated_wind_speed = 11.3;       %   m/s
[minute_wind_speed] = getWind(lifetime);
[mins] = 1:length(minute_wind_speed);
minute_wind_speed_mat = [mins; minute_wind_speed]';

%%% OWF %%%
rated_power_turb = 25;         %   MW
turbines = 40;                 %   pcs
[power_turb, power_farm] = powerOWF(minute_wind_speed, min_wind_speed,...
    max_wind_speed, rated_wind_speed, rated_power_turb, turbines);
power_turb_mat = [mins; power_turb]';
power_farm_mat = [mins; power_farm]';
```

```

%%% ELECTROLYSER SETUP %%%
[elec_efficiency, operated_hrs, operating_pressure, elec_replace, downtime,...
    standby_power, density_inlet] = electrolyserSetup(electrolyser, power_farm,
    elec_capacity);
elec_efficiency_mat = [mins; elec_efficiency]';
standby_energy = sum(standby_power)*(1/60)*(1/1000);

%%% COMPRESSOR ENERGY %%%
min_outlet_pressure = 24;    %   bar
[compressor_energy, inlet_pressure] = compressorEnergy(operating_pressure,...
    min_outlet_pressure, typology); % (kWh/kgH2)

%%% WATER SETUP %%%
[pump_height, pipe_length, pipe_diameter] = waterSystem(typology);
```

A.1.2 Sizing and excess power script

```
clc;
close all;

% Create load duration curve from available input power
elec_input_power = out.elec_input_power;
elec_LDC = sort(elec_input_power, 'descend');
cap_utilisation = 0:(100/(length(elec_input_power)-1)):100;

figure;
plot(elec_LDC, cap_utilisation,'Color', [1, 0.5, 0], 'LineWidth',2);
hold on
xline(elec_capacity, "--", 'Color', 'k')
xlabel('Power input (MW)');
ylabel('Capacity utilisation (%)');

% Fit to 9th deg polynomial
p = polyfit(elec_LDC, cap_utilisation, 9);
q = polyint(p);
capacity = 25:25:900;
for i = 1:length(capacity)
    load(i) = (diff(polyval(q,[0 capacity(i)]))/capacity(i))/100;
end
load = load';

% Calculate excess power
excess_power = zeros(1,length(minute_wind_speed));

for i = 1:length(excess_power)
    if elec_input_power(i) > elec_capacity
        excess_power(i) = elec_input_power(i) - elec_capacity;
    end
```

```
end

% Calculate lifetime excess energy
excess_energy = (sum(excess_power)*(1/60)*(1/1000))-standby_energy;
```

A.1.3 Wind speed function

```
function [minute_wind_speed] = getWind(lifetime)

if nargin ~= 1
    error('Wrong number of input arguments.')
end

% Get wind velocities and time in hours (8760)
filename = 'windData.csv';
annual_hourly_wind_speed = readmatrix(filename,'Range','D5:D8764');

% Check input vector size
if size(annual_hourly_wind_speed,2) > 1
    annual_hourly_wind_speed = annual_hourly_wind_speed';
end

% Extend to project lifetime
hourly_wind_speed = repmat(annual_hourly_wind_speed, lifetime, 1);

% Linear interpolation to minute-by-minute wind
minute_wind_speed = interp1(0:60:(size(hourly_wind_speed,1))*60-60,...
    hourly_wind_speed, 0:(size(hourly_wind_speed,1)*60-60), 'linear');

end
```

A.1.4 Wind farm power function

```
function [power_turb, power_farm] = powerOWF(minute_wind_speed, min_wind_speed,...
    max_wind_speed, rated_wind_speed, rated_power_turb, turbines)

if nargin ~= 6
    error('Wrong number of input arguments.')
end

for i = 1:length(minute_wind_speed)
    if minute_wind_speed(i) < min_wind_speed
        power_turb(i) = 0;
    elseif minute_wind_speed(i) > max_wind_speed
        power_turb(i) = 0;
    elseif (minute_wind_speed(i) >= min_wind_speed) &&...
            (minute_wind_speed(i) < rated_wind_speed)
        power_turb(i) = rated_power_turb*((minute_wind_speed(i).^3-min_wind_speed
   ^3)...
            /(rated_wind_speed^3-min_wind_speed^3));
```

```
    else
        power_turb(i) = rated_power_turb;
    end
end

power_farm = smoothdata(power_turb,"sgolay");

for i = 1:length(power_farm)
    if power_farm(i) > rated_power_turb
        power_farm(i) = turbines*rated_power_turb;
    elseif power_farm(i) < 0
        power_farm(i) = 0;
    else
        power_farm(i) = turbines*power_farm(i);
    end
end
```

A.1.5 Electrolyser setup function

```
function [elec_efficiency, operated_hrs, operating_pressure, elec_replace,...
    downtime, standby_power, density_inlet] = electrolyserSetup(electrolyser...
    , power_farm, elec_capacity)

if nargin ~= 3
    error('Wrong number of input arguments.')
end

% Set electrolyser parameters
if electrolyser == "ALK"
    efficiency_BOL = 0.68;      %
    degr_rate = 9.5129e-09;     %   /min (0.5%/year)
    operating_hrs = 95000;      %   hours
    operating_pressure = 15;     %   bar
    min_load = 0.1;             %
    density_inlet = 1.997;      %   kg/m3 (24 bar post-compression)
elseif electrolyser == "PEM"
    efficiency_BOL = 0.66;      %
    degr_rate = 1.9026e-08;     %   /min (1%/year)
    operating_hrs = 75000;      %   hours
    operating_pressure = 35;    %   bar
    min_load = 0;               %
    density_inlet = 2.901;      %   kg/m3 (35 bar)
else
    error('String "electrolyser" has to be either "PEM" or "ALK".')
end

% Form efficiency matrix
elec_efficiency = efficiency_BOL*ones(1,length(power_farm));

```

```
% Define time steps
min = 60;
operated_mins = 0;
elec_replace = 0;

% Operation time and electrolyser efficiency loop
for i = 2:length(power_farm)
    % Operation lifetime and electrolyser replacement
    if power_farm(i) > min_load * elec_capacity
        operated_mins = operated_mins+1;
        if operated_mins > operating_hrs*min-1
            elec_replace = elec_replace + 1;
            operated_mins = 0;
            elec_efficiency(i) = efficiency_BOL;
            continue
        end
    end
    % Efficiency degradation
    elec_efficiency(i) = elec_efficiency(i-1) - efficiency_BOL*degr_rate;
end

operated_hrs = operated_mins/min;

% No load, standby, ramp-up efficiency
standby = zeros(1,length(power_farm));
downtime = 0;
if electrolyser == "ALK"
    for i = 2:length(power_farm)
        if power_farm(i) <= min_load * elec_capacity
            ramp_up = 0:0.1:0.9;
            elec_efficiency(i:i+9) = ramp_up * efficiency_BOL;
            downtime = downtime + 1;
            if power_farm(i) == 0
                standby(i) = true;
            else
                standby(i) = false;
            end
        else
            standby(i) = false;
        end
    end
elseif electrolyser == "PEM"
    for i = 2:length(power_farm)
        if power_farm(i) == 0
            ramp_up = 0:0.9:0.9;
            elec_efficiency(i:i+1) = ramp_up * efficiency_BOL;
            standby(i) = true;
            downtime = downtime + 1;
        else
```

```
            standby(i) = false;
        end
    end
end

% Define standby power demand
standby_consumption = 0.0154;           %   /MW_elec (25MW module)
standby_power = zeros(1,length(power_farm));
for i = 2:length(power_farm)
    if standby(i) == true
        standby_power(i) = standby_consumption * elec_capacity;
    end
end
```

A.1.6 Compressor energy function

```
function [compressor_energy, inlet_pressure] =...
    compressorEnergy(operating_pressure, min_outlet_pressure, typology)

if nargin ~= 3
    error('Wrong number of input arguments.')
end

% Inputs
Tmean = 285.15;     %   K
kappa = 1.4;        %   cp/cv
eff = 0.5;          %
G = 0.0696;         %

% Pipeline pressure drop
if typology == "ON"
    pressure_drop = 0;  %   bar
% Initial guess
elseif typology == "DOFF" || typology == "COFF"
    pressure_drop = 6;  %   bar
else
    error('String "typology" has to be either "ON", "DOFF" or "COFF".')
end

% Calculation of compressor energy
if operating_pressure > min_outlet_pressure + pressure_drop
    inlet_pressure = operating_pressure;
    compressor_energy = 0;
else
    inlet_pressure = min_outlet_pressure + pressure_drop;
    compressor_energy = (286.76/(G*eff*3.6*10^6))*Tmean*(kappa/(kappa-1))...
        *(((min_outlet_pressure/operating_pressure)^((kappa-1)/kappa))-1);
end
end
```

A.1.7 Water system function

```
function [pump_height, pipe_length, pipe_diameter] = waterSystem(typology)

if nargin ~= 1
    error('Wrong number of input arguments.')
end

if typology == "COFF"
    pump_height = 25; % m
    pipe_length = 100; % m
    pipe_diameter = 2.06; % m
elseif typology == "DOFF"
    pump_height = 25; % m
    pipe_length = 10; % m
    pipe_diameter = 0.325; % m
else
    pump_height = 20; % m
    pipe_length = 200; % m
    pipe_diameter = 2.06; % m
end
```

A.2 Capacity optimisation

Figure 30 shows the obtained estimations of load factors for each investigated capacity and configuration, using the fitted curves.

MW	DOFF	COFF	CON-P	CON-A
25	0.9196	0.9426	0.9417	0.9415
50	0.8917	0.9161	0.9147	0.9143
75	0.8710	0.8947	0.8928	0.8924
100	0.8540	0.8760	0.8738	0.8733
125	0.8386	0.8588	0.8563	0.8557
150	0.8239	0.8426	0.8397	0.8390
175	0.8094	0.8272	0.8239	0.8232
200	0.7952	0.8124	0.8088	0.8080
225	0.7813	0.7982	0.7944	0.7936
250	0.7677	0.7847	0.7807	0.7798
275	0.7547	0.7718	0.7675	0.7666
300	0.7421	0.7593	0.7549	0.7538
325	0.7300	0.7473	0.7425	0.7414
350	0.7182	0.7354	0.7304	0.7293
375	0.7067	0.7237	0.7184	0.7172
400	0.6955	0.7122	0.7065	0.7052
425	0.6844	0.7007	0.6947	0.6933
450	0.6735	0.6892	0.6830	0.6816
475	0.6627	0.6779	0.6714	0.6699
500	0.6521	0.6668	0.6600	0.6585
525	0.6418	0.6559	0.6489	0.6474
550	0.6318	0.6452	0.6382	0.6366
575	0.6221	0.6348	0.6277	0.6261
600	0.6126	0.6247	0.6174	0.6158
625	0.6035	0.6149	0.6073	0.6057
650	0.5945	0.6051	0.5974	0.5956
675	0.5856	0.5955	0.5874	0.5856
700	0.5768	0.5858	0.5773	0.5755
725	0.5680	0.5760	0.5672	0.5653
750	0.5593	0.5663	0.5572	0.5552
775	0.5508	0.5565	0.5472	0.5452
800	0.5425	0.5469	0.5375	0.5355
825	0.5346	0.5374	0.5280	0.5259
850	0.5271	0.5282	0.5183	0.5160
875	0.5197	0.5188	0.5074	0.5046
900	0.5114	0.5085	0.4932	0.4891

Figure 30: Capacity optimisation – load factor per size and configuration

A.3 Evaluating model performance

Considering electrolyser systems in the configurations, scales and locations studied in this report, significant limitations exist with regard to the availability of empirical data and possibilities of obtaining experimental data. However, key simulation outputs can be compared to theoretical results and calculations in order to substantiate the validity of the models. In this section, such comparisons are done for the wind power outputs as well as full system and electrolyser efficiencies.

The wind power capacity factor is simulated as 50.6% throughout the project lifetime. Estimated capacity factors for new offshore wind power currently lie between 40–50%, with larger turbines and technological improvements helping to increase that value for the future [89], indicating a reasonable simulation result.

The lifetime H_2 production (m_{H_2}) ranges between 2.08–2.23 Mton as obtained from the simulations. With a *LHV* of 33.33 kWh/kgH_2, the energy content of the produced hydrogen can be obtained. The theoretical full system efficiencies ($\eta_{tot,th}$) are calculated by dividing the hydrogen energy by the total wind energy output (E_{OWF}), 133.1 TWh, as shown in Table 12 and Eq. 23. The values correspond to the simulated system efficiencies demonstrated in Table 10.

Table 12: Calculated system efficiencies

	COFF-P	DOFF-P	CON-P	CON-A
H_2 production [Mton]	2.08	2.16	2.15	2.23
H_2 energy content [TWh]	69.4	72.0	71.7	74.4
System efficiency [%]	52.1	54.1	53.8	55.9

$$\eta_{tot,th} = \frac{m_{H_2} \cdot LHV}{E_{OWF}} \tag{23}$$

The theoretical average electrolyser efficiencies ($\eta_{el,th}$) can then be obtained using Eq. 24 and the values in Table 13, E_{input} representing the total electrolyser input and E_{loss} the electrolyser losses. The theoretical values correspond to the efficiency simulations as seen in Figures 15 and 28.

Table 13: Calculated electrolyser efficiencies

	COFF-P	DOFF-P	CON-P	CON-A
Electrolyser input [TWh]	109.7	113.9	113.0	114.0
Electrolyser losses [TWh]	40.3	41.8	41.5	39.5
Electrolyser efficiency [%]	63.3	63.3	63.3	65.4

$$\eta_{el,th} = \frac{E_{input} - E_{loss}}{E_{input}} = \frac{m_{H_2} \cdot LHV}{E_{input}} \tag{24}$$

A.4 Example model setup

One of the Simulink models, the centralised offshore – PEM (COFF-P) setup, is demonstrated as an example in Figures 31–41. Its main setups as well as some of the nested subsystems are shown. The other models are constructed in a similar fashion, differing mainly in terms of connections and input values as defined in Chapter 3.

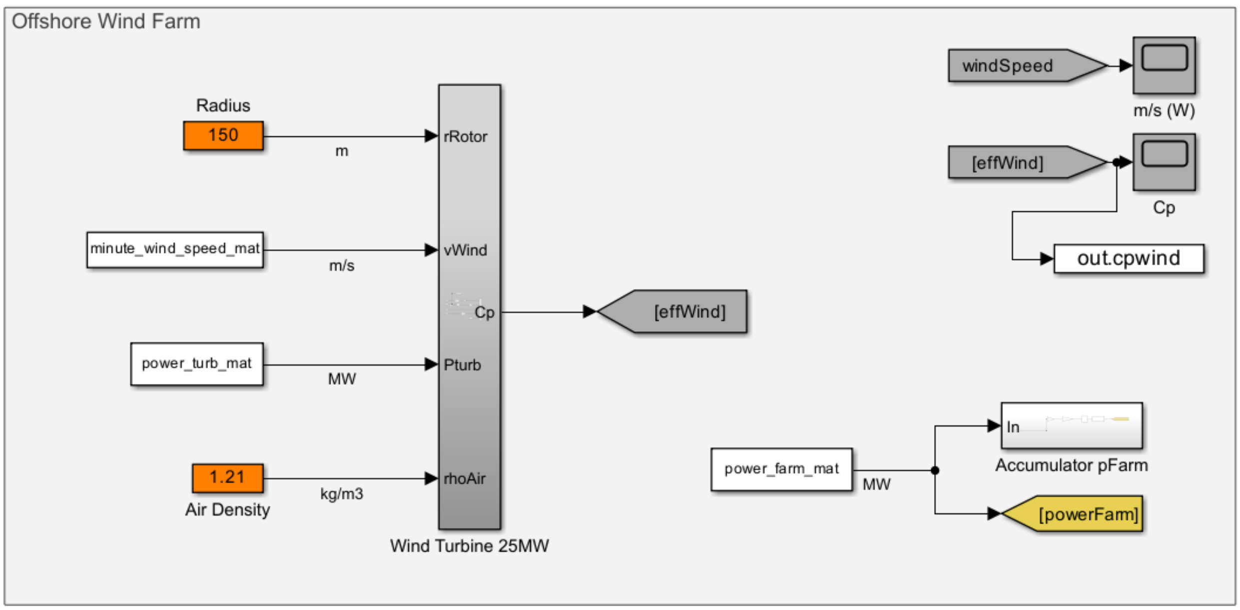

Figure 31: OWF setup

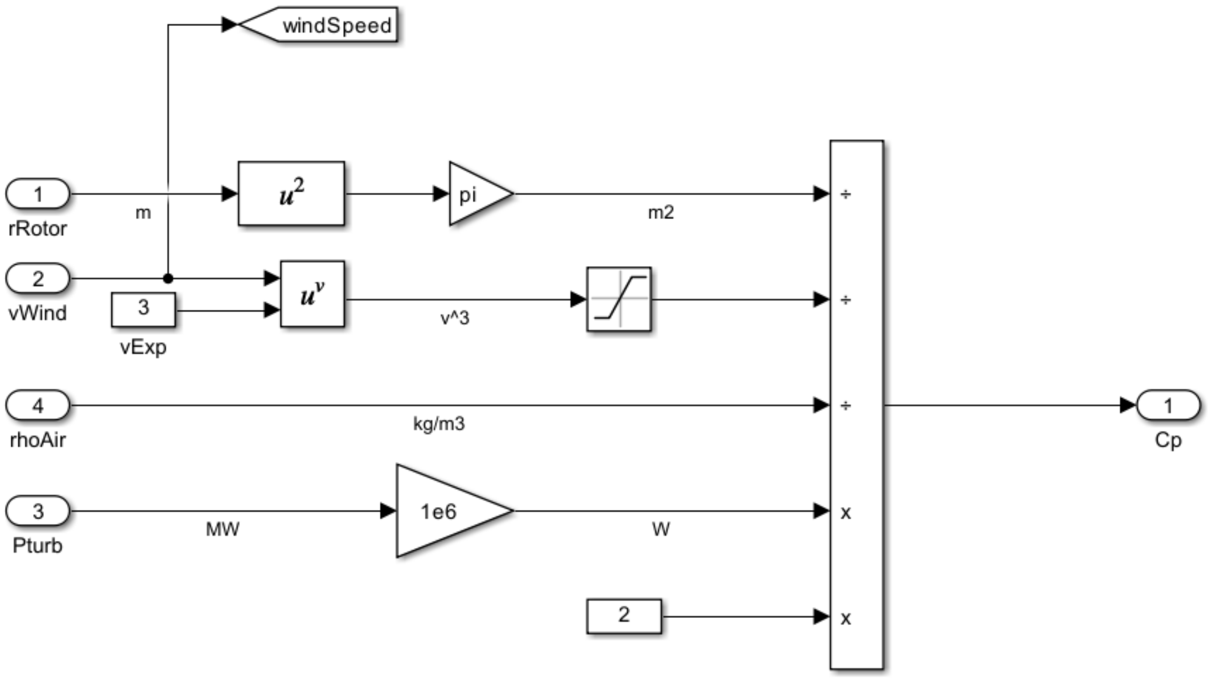

Figure 32: Wind turbine subsystem

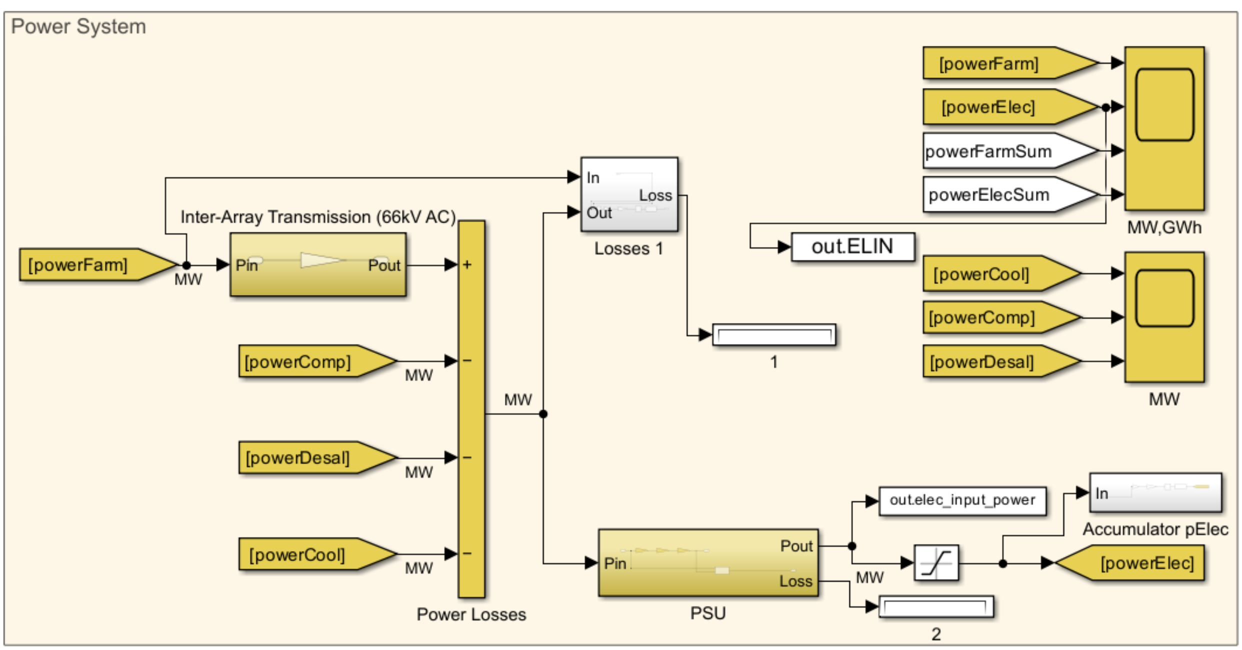

Figure 33: Power system setup

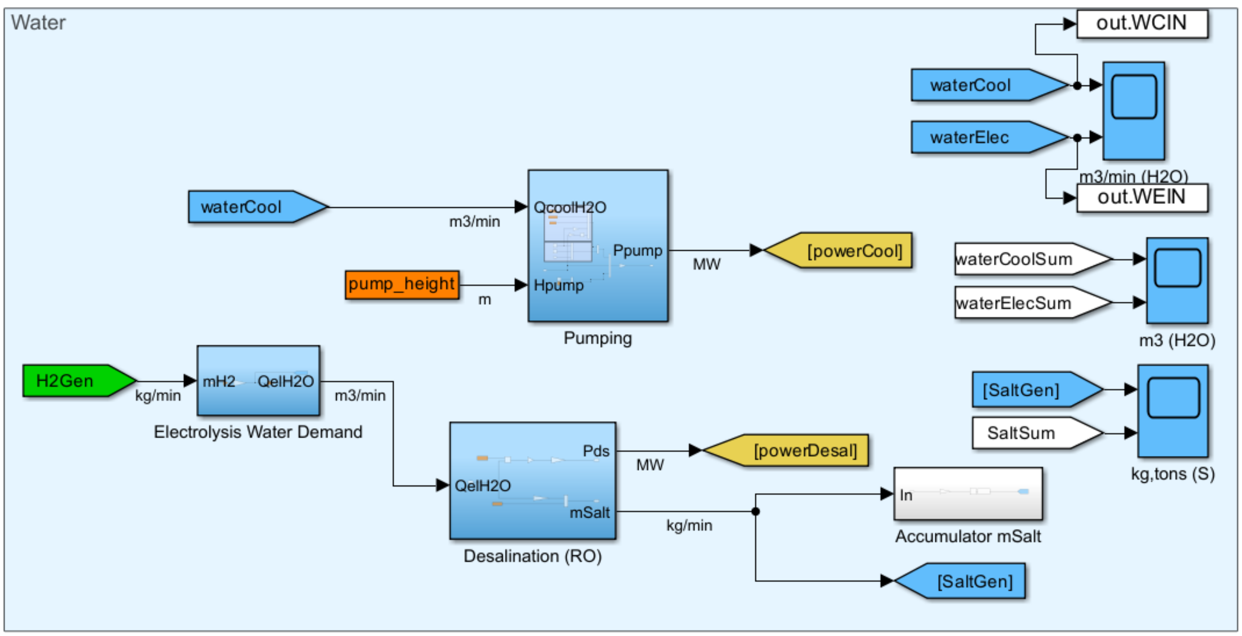

Figure 34: Water system setup

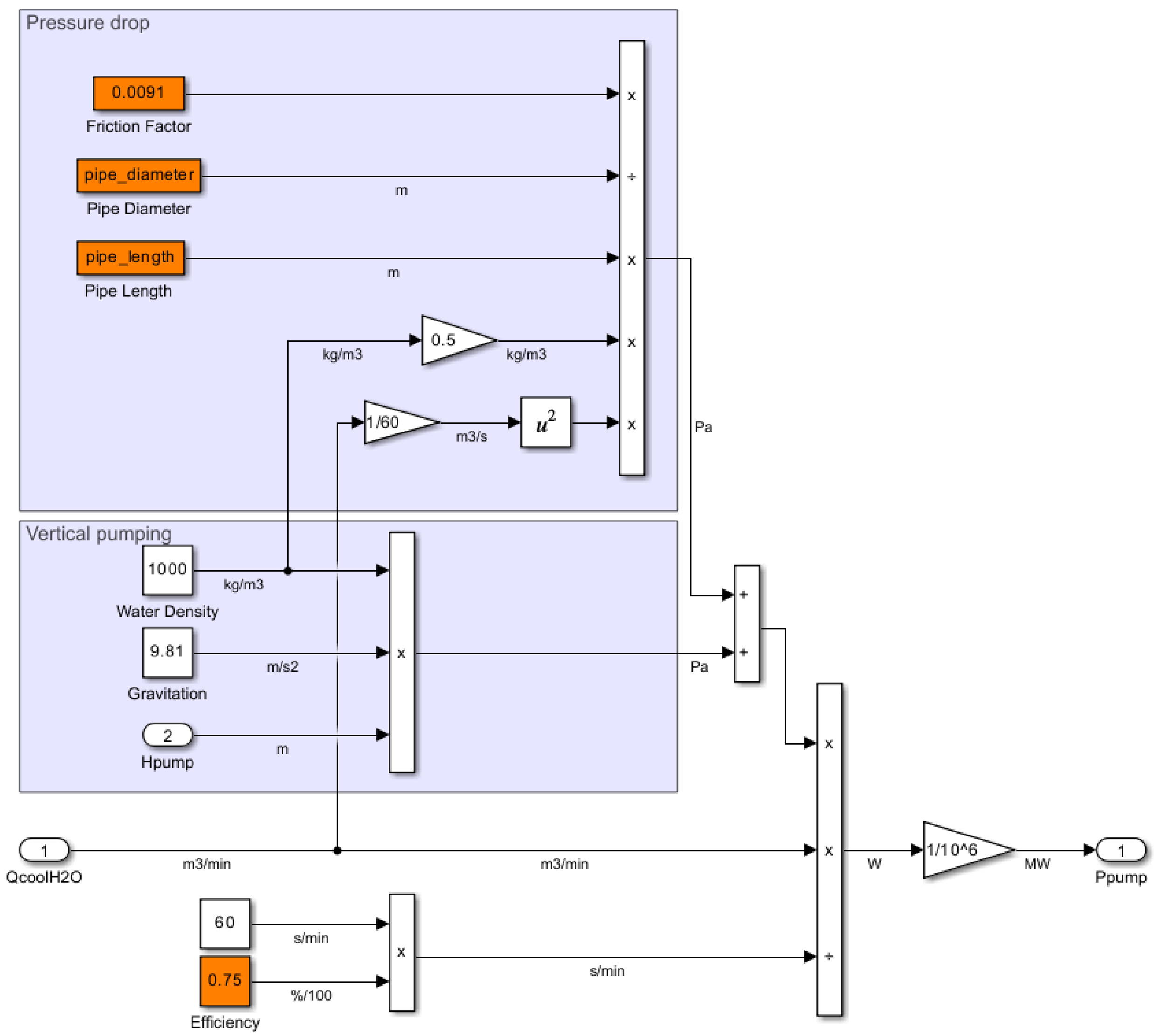

Figure 35: Water pumping subsystem

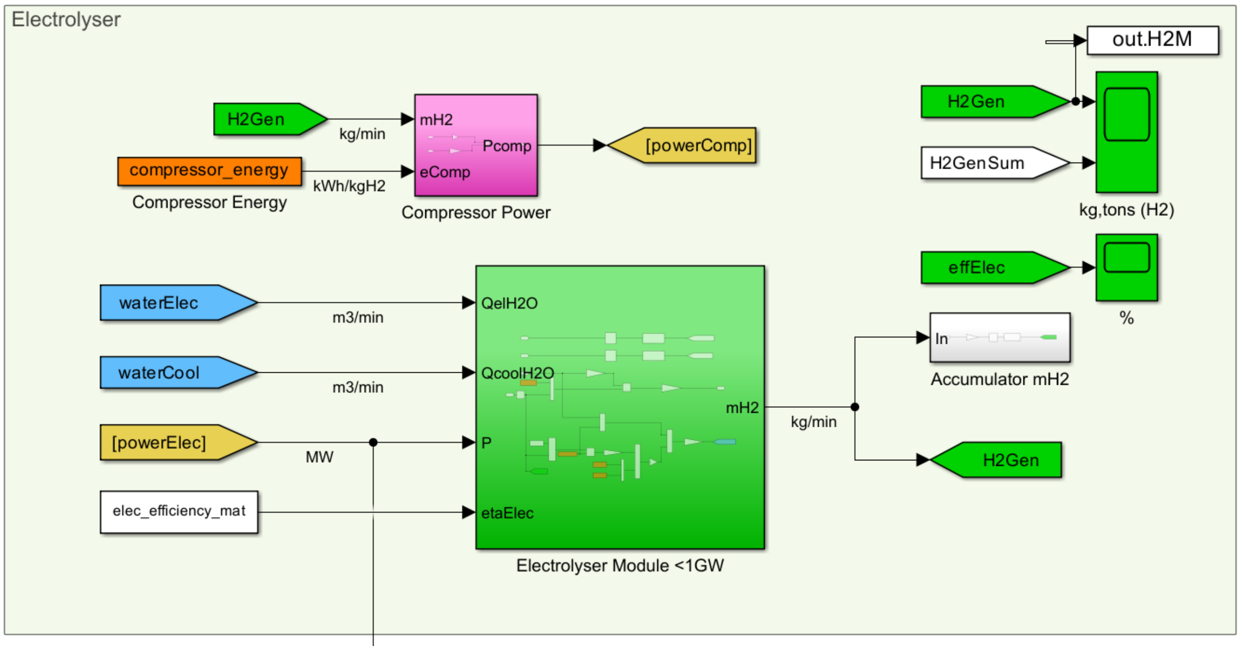

Figure 36: Electrolyser setup

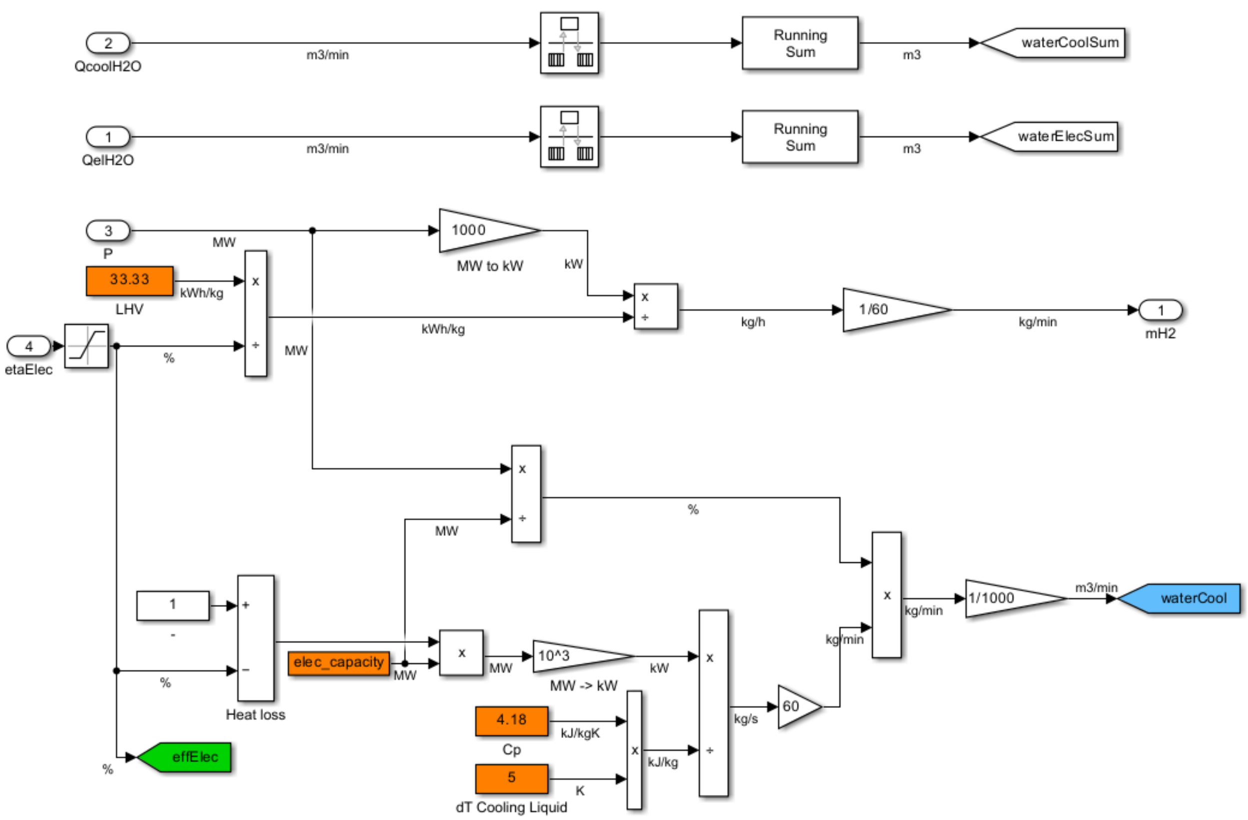

Figure 37: Electrolyser subsystem

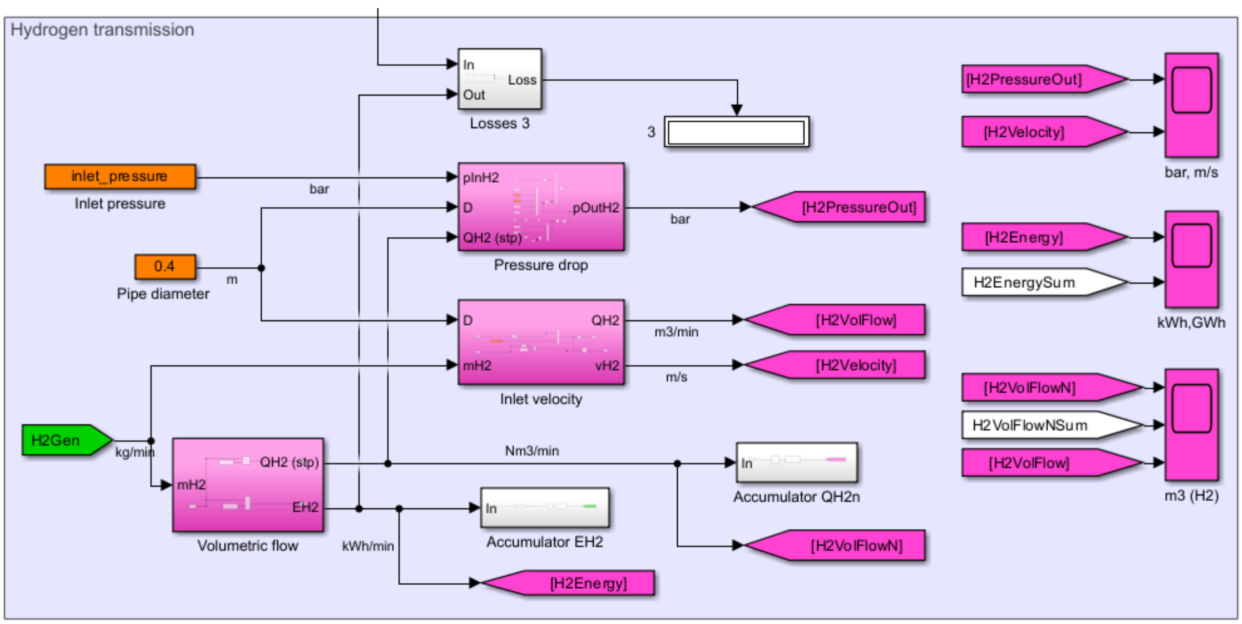

Figure 38: Hydrogen transmission setup

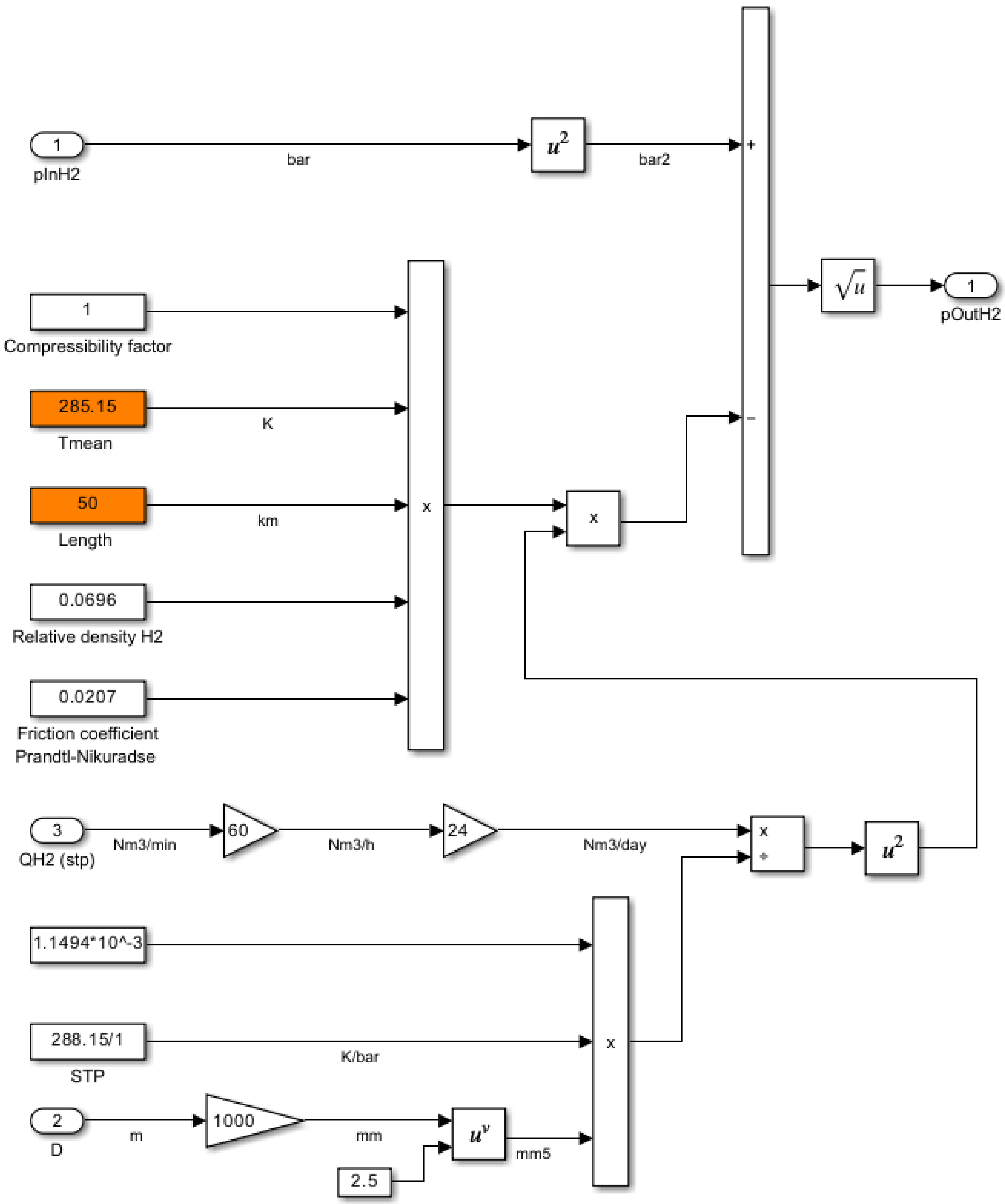

Figure 39: Pipeline pressure drop subsystem

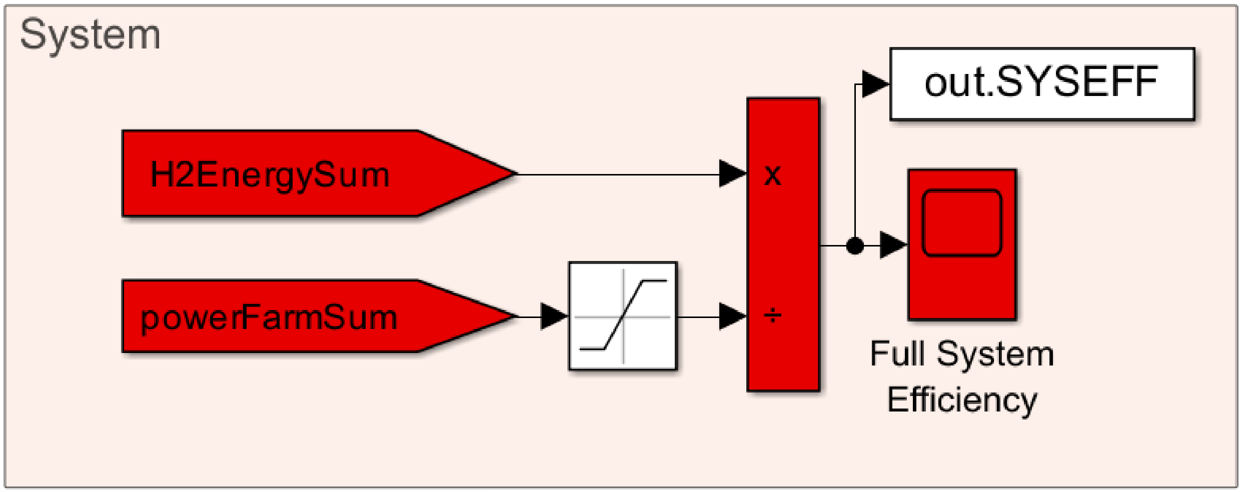

Figure 40: System efficiency setup

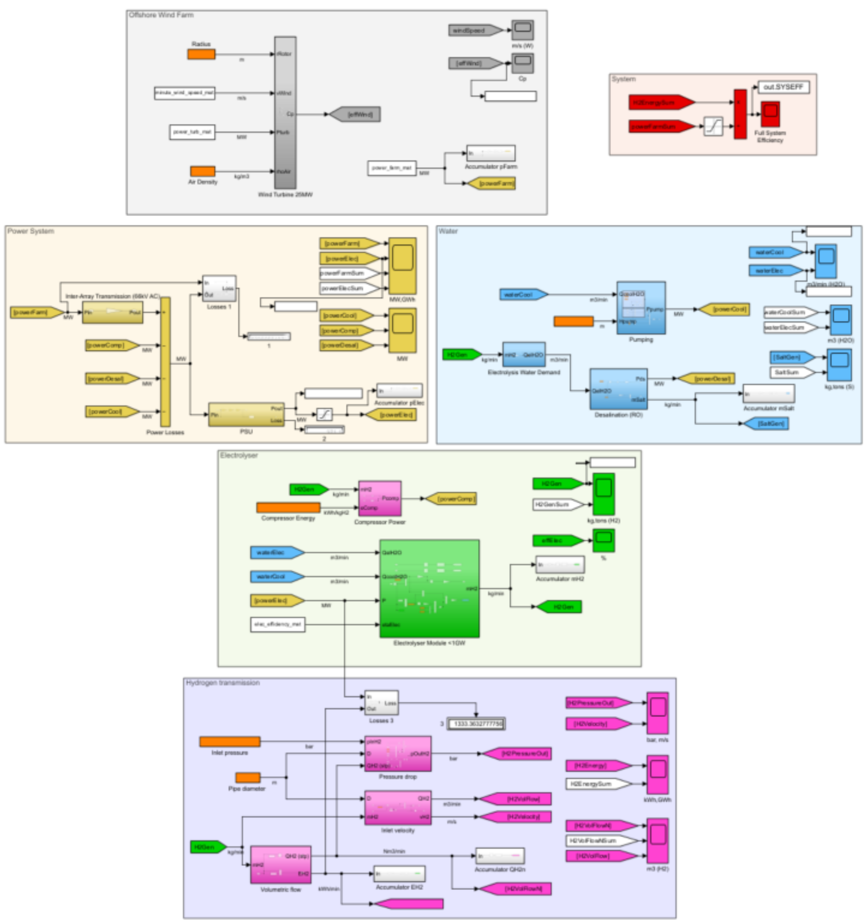

Figure 41: Full model overview